Monographs in Electrochemistry
Series Editor: F. Scholz

Peter Gründler

In-situ Thermoelectrochemistry

Working with Heated Electrodes

Springer

In-situ Thermoelectrochemistry

Monographs in Electrochemistry

Series Editor: Fritz Scholz, University of Greifswald, Germany

Surprisingly, a large number of important topics in electrochemistry is not covered by up-to-date monographs and series on the market, some topics are even not covered at all. The series Monographs in Electrochemistry fills this gap by publishing indepth monographs written by experienced and distinguished electrochemists, covering both theory and applications. The focus is set on existing as well as emerging methods for researchers, engineers, and practitioners active in the many and often interdisciplinary fields, where electrochemistry plays a key role. These fields will range – among others – from analytical and environmental sciences to sensors, materials sciences and biochemical research.

More information about this series at
http://www.springer.com/series/7386

Peter Gründler

In-situ Thermoelectrochemistry

Working with Heated Electrodes

Springer

Peter Gründler
Institute for Solid State Research
Leibniz Institute for Solid State and Materials Research Dresden (IFW)
Dresden
Germany

ISSN 1865-1836 ISSN 1865-1844 (electronic)
ISBN 978-3-662-45817-4 ISBN 978-3-662-45818-1 (eBook)
DOI 10.1007/978-3-662-45818-1
Springer Heidelberg New York Dordrecht London

Library of Congress Control Number: 2015932767

Printed on acid-free paper

Springer is part of Springer Science+Business Media (www.springer.com)

Preface of the Editor

I had the fortune to know the author of this book since about 45 years, when Peter Gründler was still a docent at the University of Leipzig and gave talks on conferences on coulometry and stripping voltammetric detection of the end point of titrations. I remember that his research always showed that he could take advantage of a profound ability to build up his own electronic measuring equipment. This was especially important at times when modern instrumentation from Western companies was very difficult, if not impossible, to purchase in East Germany. Then, after the reunification of Germany, when Peter Gründler already was full Professor at the University of Rostock, I have witnessed from the very beginning Peter Gründler's ingenious developments of what he has called at that time "hot-wire electrochemistry". During the following years of very hard work, he has, together with a number of dedicated co-workers, achieved the establishment of a completely new technique for electrochemical investigations, which he now describes in this book entitled "In situ Thermoelectrochemistry – Working with Heated Electrodes". I am very happy that Peter Gründler has decided to describe the background, the foundations and the experimental achievements of his technique in book form, because not only this will help to popularize this important new direction in electrochemistry, but it will also efficiently help to convince more electrochemists, analytical chemists and maybe also physicists and biologists to apply the technique for solving their own problems. The prospects for applications of heated electrodes are almost limitless, and we can expect an avalanche of new research work with this new experimental means.

Greifswald, Germany — Fritz Scholz
October 2014

Preface of the Author

The year 1989 was a time of great change and great opportunities in Germany and the whole of Europe. When the author of this book—then a freshly appointed professor at an old university in Eastern Germany (the GDR)—became aware of these great opportunities to conduct research freely, he remembered some older ideas which had not been viable to work on before the fall of the Berlin wall. One of these ideas was the question "what would happen if I dipped the filament of a light bulb into a solution, heated it, and used it as an electrode?" After some short experiments, it became clear that it was not a problem to make a heated electrode this way, even a microelectrode. When a suitable PhD student had been found and funding had been arranged, the first question to be answered was whether the high frequency alternating current necessary for the heating would allow sensitive signal measurement in the electrochemical cell. At this point, we suffered a catastrophic setback. It was nearly impossible to follow the tiny electrolysis current when, simultaneously, a very strong alternating current flowed through the electrode wire and generated massive distortions. Furthermore, it turned out that other groups had previously tried to use an identical arrangement for electrochemical purposes, obviously encountering the same problem. What next?

Fortunately, there was a solution—compensate the AC distortions by means of a symmetric electrode wire arrangement. This worked perfectly, and the result was a technique that enabled, with negligible effort, the heating of an electrode in situ, opening up many useful possibilities, such as efficient microstirring and the ability to work in overheated solvents, excite kinetically hindered substances to react, study volatile substances at high temperatures without any loss, etc. In the international scientific community, the term "hot-wire electrochemistry" became popular for this technique. Thus, the simple technique mentioned above marked the start of a fruitful, innovative development in electrochemistry. This has been very satisfying for the author of this book, who has been able to work on a subject of longstanding interest with a group of highly talented young people in a friendly atmosphere of political freedom.

After being used in many different regions of the world and discussed at many conferences, hot wire electrochemistry has become part of a larger field. It has therefore been decided to summarize all the effort made to apply temperature changes to the surface of an electrode as an intentionally varied external parameter. The history of all that is known as thermoelectrochemistry is also related, and these areas represent the main subjects covered in this book. Experimental experiences are also related, together with many useful "tricks".

The author hopes that this book leads to wider application of modern thermoelectrochemical methods.

Dresden, Germany Peter Gründler

Acknowledgements

I thank all my young friends who worked together with me during one of the most fruitful and happy periods of my life, when we worked out together the hot-wire electrochemistry. Thank you, Tadesse, Andreas, Torsten, André, Markus and Bello!

I am happy and grateful that there are, among my scientific friends, such outstanding people as Joe Wang, Richard Compton, Christopher Brett and Danny Mandler. Their interest, the discussions with them and their encouragement were of invaluable use for me.

I am very grateful to my late friend Lothar Dunsch who offered me the chance to continue to work with hot-wire electrochemistry after my retirement from the university, in the wonderful atmosphere of his group.

I have to thank also the editor of the series "Monographs in Electrochemistry", Fritz Scholz, for his invitation to publish this monograph and for his encouragement.

Contents

Chapter 1
Introduction

Properties of substances highly depend on temperature. As an extreme example, water can be considered. We know very well the behaviour of "normal" water, but it is less familiar that water heated up near to its critical temperature behaves like a completely different solvent. Subcritical water and supercritical water are unpolar liquids and able to dissolve fats. Why should not we utilise the extraordinary properties of such solvents in electrochemistry? The methods presented in this book further down will show that we can do experiments of this kind even with everyday instruments, without application of external pressure or spending a lot of heat energy. Examples for the novel experimental facilities offered by the scientific field named here "modern thermoelectrochemistry" or alternatively "in situ thermoelectrochemistry" will be presented in this book.

The term "thermoelectrochemistry" is not new [1, 2]. It has never been used very frequently, but from time to time it appeared in the literature [3–9]. As in all branches of science, also in electrochemistry it is common practice to study phenomena as a function of temperature. Most interesting have been temperature dependencies of potential (as an expression for the thermodynamic driving force) and of limiting current (as a measure of reaction rate). Also, heat generation as a by-product of electrochemical energy generation has been a well-studied object. A prominent example of in situ calorimetry in an electrochemical cell was the famous paper of Fleischmann and Pons [10], where they believed to have found a path to "cold nuclear fusion"—an unfortunate error. In this book, we define all such investigations as "classical thermoelectrochemistry", since we believe that a new method of approach now has led to a "modern thermoelectrochemistry" which will be discussed further down in more detail. Briefly: Modern thermoelectrochemistry is considering temperature as an independent variable, which should be varied arbitrarily and fast, i.e. the investigator should be able to impose a certain temperature value to an electrode in the same way as this is common practice with the classical variables' potential and current in electrochemistry.

Traditional electrochemistry knows the three variables: voltage (potential), current, and time. When working experimentally throughout with only these

P. Gründler, *In-situ Thermoelectrochemistry*, Monographs in Electrochemistry,
DOI 10.1007/978-3-662-45818-1_1

quantities, restrictions became obvious more and more within the second half of the last century. This resulted in the development of combination methods, among them, e.g. photoelectrochemistry, triboelectrochemistry or sonoelectrochemistry, where "non-electrochemical" quantities like light, mechanical attack or ultrasound have been applied in order to stimulate reactions or alternatively to find better diagnostic means. In every case, the new combination techniques opened up new ways for a better understanding of electrochemical processes. It is amazing to see that a similar development could not be seen in the case of temperature for a long time. Unless the quantities mentioned above, temperature hardly has been used intentionally to affect electrochemical reactions. This situation changed when methods appeared which allowed to vary electrode temperature arbitrarily, mainly by "imposing" heat or heat pulses similar to imposing potential pulses in traditional electrochemistry. Hence, the techniques of electrode heating form a substantial part of this book. The focus will be on electrically heated microelectrodes ("hot-wire electrochemistry" or "hot-layer electrochemistry"), since these techniques have reached a high level of perfection and since they may be applied with low effort in every electrochemical laboratory.

Till now, there are not many reviews on thermoelectrochemistry [11–14]. The subject named here *modern thermoelectrochemistry* has been considered in one of them [14].

References

1. Van Rysselberghe P (1955) Electrochemical affinity—studies in electrochemical thermodynamics and kinetics. Edition Herman, Paris
2. Van Rysselberghe P (1963) Thermodynamics of irreversible processes. Edition Herman, Paris, pp 133
3. Spritzer MS (1975) Abstr Papers Am Chem Soc 169:105
4. Bilal BA, Tributsch H (1998) J Appl Electrochem 28:1073
5. Fang Z, Guo L, Zhang H, Zhang P (1998) J Central South Univ Technol (English Ed) 5:38
6. Yi JL, Tang XJ, Zeng Y (2005) J Nat Sci Hunan Normal Univ 28:49
7. Wang SF, Fang Z, Tai YF (2006) J Therm Anal Calorim 85:741
8. Jung YS, Lee KT, Kim JH, Kwon JY, Oh SM (2008) Adv Funct Mat 18:3010
9. Ke JH, Tseng HJ, Hsu CT, Chen JC, Muthuraman G, Zen JM (2008) Sens Actuat B 130:614
10. Fleischmann M, Pons S (1989) J Electroanal Chem 261:301
11. Wildgoose GG, Giovanelli D, Lawrence NS, Compton RG (2004) Electroanalysis 16:421
12. Zhang W, Charles EA, Congleton J (2004) Chem Res Chin Univ 20:494
13. Gründler P, Flechsig GU (2006) Microchim Acta 154:175
14. Gründler P, Kirbs A, Dunsch L (2009) ChemPhysChem 10:1722

Chapter 2
Fundamentals

2.1 Reasons to Reconsider Thermoelectrochemistry

There are good reasons to reconsider thermoelectrochemistry and to develop in situ techniques which should broaden its suitability.

Electrochemistry is faced with new challenges. As an example, we may consider the utilisation of "heat waste" as a source of electric energy. Nuclear power stations generate a huge amount of such heat which cannot be utilised and has to be dissipated. Electrochemistry might contribute ways to convert a part of it into useful energy. Further examples are battery research and development of fuel cells. Modern thermoelectrochemistry can provide ways to obtain important characteristics like entropy in a very fast and efficient way. Better utilisation of natural processes like, e.g., enzymatic redox reactions may become an extremely important task in future. Biofuel cells are not the only potentiality. In enzymatic reactions, the most important quantity is entropy. Its knowledge is substantial to understand how nature brings about "cold combustion" and further extremely efficient reactions under mild conditions. Modern thermoelectrochemical methods make it easy to determine entropy values under practical aspects.

As an interesting side effect of reconsidered thermoelectrochemistry, some older uncertainties and errors of electrochemical theory can be corrected in a plausible way since modern thermoelectrochemistry is directing attention to *single-electrode quantities*.

2.2 Isothermal and Non-isothermal Cells

Electrochemical cells where electrodes are heated, obviously are non-isothermal cells, i.e. there exists a thermal gradient somewhere between working and reference electrodes, respectively. In isothermal cells, such a gradient does not exist since

P. Gründler, *In-situ Thermoelectrochemistry*, Monographs in Electrochemistry,
DOI 10.1007/978-3-662-45818-1_2

working electrode and its surrounding solution are of equal temperature. Isothermal cells are characteristic for classical thermoelectrochemistry. They can be subject to temperature programming and even to temperature jumps, but in all cases not alone the working electrode has to be exposed to temperature changes but also large part of the electrolyte solution. The reference electrode may give rise to problems if it is subject to temperature variations, since common types need considerable time to equilibrate after temperature changes. Consequently, in classical thermoelectrochemical experiments also frequently non-isothermal cells were preferred, where a thermostated container with the working electrode is connected via a salt bridge to an external reference electrode container at ambient temperature.

With non-isothermal cells, which are an inherent feature of modern thermoelectrochemical methods, several phenomena have to be considered which otherwise would not be meaningful. Some of them, like the thermodiffusion (Soret effect) can be interpreted on a thermodynamic basis, others, like diffusion or convection effects, are considered to be dynamic processes and need a specific dynamic interpretation.

Non-isothermal electrochemical cells have been mentioned first in 1858 by Wild [1]. A special variant of them, the *thermocells*, consist of two half-cell compartments with equal electrodes and equal electrolyte. They play a role in efforts for direct conversion of heat to electric energy (see Chap. 3). An example of sources of dispensable heat is nuclear power plants. If one half-cell of a thermocell is heated by waste heat, whereas the second half-cell keeps at ambient temperature, and if the electrode reaction has a high numeric value of reaction entropy, the resulting voltage between the half-cells may be utilised as source of electric energy. Unfortunately, the efficiency of such thermocells is extremely low.

The temperature gradient which is found always in non-isothermal cells may be located somewhere between working and reference electrodes. In cells with heated electrodes, it is located always in close vicinity to the electrode/electrolyte interface, i.e. thermal and concentration gradients are overlapping each other. This fact has a lot of consequences and became the origin of some interesting discoveries (see Chap. 5). Half-cells with heated electrodes can be named *non-isothermal half-cells* (“half”, since the reference electrode keeps off varied temperature), in contrast to *isothermal half-cells* where the electrode surface is in thermal equilibrium with its surrounding electrolyte solution. In *isothermal half-cells*, working electrode plus surrounding solution are subject to temperature variation, whereas the reference electrode keeps at constant (mostly ambient) temperature. *Non-isothermal half-cells* are characterised by a temperature gradient between working electrode surface and solution.

2.3 Thermodynamics

2.3.1 Voltage and Potential in Non-isothermal Cells

Thermodynamic interpretation of non-isothermal cells directs attention to some old electrochemical principles, which are underrepresented in textbooks and should be reconsidered while we are at it.

The problems start with two of the most fundamental electrochemical terms: voltage and potential. *Voltage* is a quantity measured between two points, *potential,* however, originally, is a property of one single point. Many terms and relations important for the thermodynamic basis of electrochemistry have been expressed by the father of electrochemical thermodynamics, Walter Nernst. Unfortunately, even Nernst himself has introduced a serious uncertainty by defining the important *electrode potential E* as the voltage between an electrode versus another electrode (the reference electrode). The *standard electrode potential* $E^{\ominus}$, consequently, is the voltage between the considered electrode and a universal standard electrode, the *standard hydrogen electrode (SHE)*.In other words, Nernst discusses a *two-point quantity*, but he names it for a term which should be a *single-point quantity*. The problems arising from this sloppiness are manifesting in a detailed consideration of non-isothermal electrochemical cells.

If we compare the thermal behaviour of any studied electrode versus hydrogen electrode, either in an isothermal cell (studied electrode as well as reference electrode both at equal but not standard temperature) or in a non-isothermal cell (studied electrode with varied temperature, reference electrode remaining at standard temperature), then we will get two different values of $dE^{\ominus}/dT$, since in one of both cases the temperature coefficient of the hydrogen electrode potential is included. Confusion could occur especially by an unreflected consideration of the old definition "the *electrode potential* of the *standard hydrogen electrode* is *zero at all temperatures*". Possible misunderstandings can be avoided if we keep in mind that the electrode potential indeed is *not a potential but a voltage* (named also by the outdated noun *electromotive force, EMF*) between the actual electrode and the standard reference electrode. Clearly, the voltage *between the standard hydrogen electrode* and the *standard hydrogen electrode* is zero at all temperatures. A further consequence which we should never forget is the origin of the Nernst equation. A correct derivation (not that of Nernst!) of this equation starts with the complete cell reaction consisting of simultaneous reduction and oxidation processes. Accordingly, *Gibbs Free Energy* ΔG is divided by the corresponding *molar charge zF* (often written *nF*), and the result is a cell voltage (EMF) with a concentration dependence following Nernst's well-known equation. Consequently, the "Nernst equation for an *electrode potential*" $E = f(a)$ means the equation for an EMF of cells consisting of the considered electrode and a standard reference electrode (normally the SHE). Such considerations are highly important for non-isothermal electrochemical cells. The thermal behaviour of an electrode in a non-isothermal cell, where the reference electrode is kept at standard temperature, can be considered to

be free from distortions caused by the reference electrode. On the other hand, we get distortions which are not found with isothermal cells, e.g. the thermodiffusion (Soret effect).

The most important conclusion of the above considerations is that measurements with non-isothermal cells may provide true single-electrode potentials (in this case, indeed *potentials*, not voltages!). The very important *entropy of a single electrode* S_e can be determined this way. The corresponding relation is $dE/dT = S_e/zF$.

Single-electrode potentials are important for some fundamental but unmeasurable quantities. The problem has been discussed in literature [2, 3]. *Relative* potential values (not *absolute* values which refer to an imaginary point in the universe!) can be calculated. Also *single-electrode entropy* values can be calculated by means of non-isothermal cells, but it is necessary to make use of some non-thermodynamic assumptions.

2.3.2 Heat and Entropy Flow in Open Non-isothermal Cells

Open electrochemical cells do not have any external connection between electrodes. Consequently, no electrolytic current will flow. In open, non-isothermal cells, nevertheless, some exchange processes will take place. The necessity to maintain a stationary temperature difference, e.g., means that heat is flowing continuously from hot to cool place. Consequently, there must be some transfer of entropy even without any kind of electrolysis. We have to discuss such effects first in terms of thermodynamics.

Consideration of entropy flow through a non-isothermal cell is a good starting point. There are at least two contributions. The "thermodynamic contribution" corresponds to the *change in Free Energy* of both redox half-reactions just by temperature variation of the corresponding species. In other words: Since the Gibbs Free Energy G is temperature dependent, species coming from a cooler region and going to a hot place will attain a higher value of G, even if their concentration would keep constant. The second entropy contribution is caused by the *heat flow* from a hot to a cold place inside the cell.

The considerations mentioned lead to the following consequence: In an electrolyte solution, the existence of a temperature difference must give rise to a voltage across the zone of temperature profile, the so-called thermal liquid junction potential, E_{TLJP}. If the contributions have to be determined, the "thermodynamic contribution" mentioned above can be made reversible just by measuring cell voltage under "open circuit condition", i.e. without current flow. The second contribution, in contrast, is irreversible and not constant with time.

For calculation of entropy contributions, it is useful to start with a simple thermocell, e.g. a cell consisting of two equal silver/silver chloride electrodes connected via a KCl salt bridge:

$$\begin{array}{l} \mathrm{Cu}\,|\,\mathrm{Ag}\,|\,\mathrm{AgCl}\,|\,\mathrm{KCl}\,\vdots\,\mathrm{KCl}\,|\,\mathrm{AgCl}\,|\,\mathrm{Ag}\ldots\mathrm{Ag}\,|\,\mathrm{Cu} \\ |\quad\ T_1\quad\ |\quad\ T_2\quad\ |\quad\ T_1\ | \end{array}$$

The external copper leads of the above example thermocell should be of equal temperature to compensate for voltage contributions from metal/metal interfaces (Seebeck effect). The thermodynamic part of the overall cell voltage can be calculated easily by evaluating the simple relation $E_{\mathrm{cell}}(1) = \Delta G/F$ using the available values of chemical potentials μ_i. The second part of overall cell voltage, the thermal liquid potential E_{TLJP}, is unmeasurable. It can be estimated using the following equation).

$$E_{\mathrm{TLJP}} = -\frac{1}{F}[\mu_{\mathrm{Cl}^-}(T_2) - \mu_{\mathrm{Cl}^-}(T_1)] - \frac{1}{F}\int_{T_1}^{T_2}\left(\frac{t_{\mathrm{K}^+}\cdot S^*_{\mathrm{K}^+}}{z_{\mathrm{K}^+}} + \frac{t_{\mathrm{Cl}^-}\cdot S^*_{\mathrm{Cl}^-}}{z_{\mathrm{Cl}^-}}\right)\mathrm{d}T \qquad (2.1)$$

In Eq. (2.1) mean μ_i are the chemical potentials, t_i the Hittorf numbers, z_i the charges of the corresponding ions. and S_i^* are their entropies of transport. The latter have been extrapolated from standard values at lower temperature following the hydrodynamic theory given by Agar [4]. All the remaining quantities are available. Many authors have dealt with estimation of the magnitude of E_{TLJP} [4–11]. The reason is that this quantity is meaningful for discussing the important phenomenon of *thermodiffusion* (*Soret effect*).

Thermodiffusion is occurring at the boundary between two zones of different temperatures in a homogeneous solution. In electrolyte solutions, ions tend to move from hot to cold region. Due to differences in mobility between ion sorts, a partial charge separation is occurring with the result of voltage formation at the hot/cold interface. Furthermore, ion movement at this place is generating a concentration profile. The latter causes increasing back diffusion, until a stationary state will be attained. This state is named as the *Soret equilibrium*. Thermodiffusion is a slow process, thereby the initial state (without equilibration) often persists for long time. It is sufficient to calculate the value of E_{TLJP} for this initial state. Some examples are given in Table 2.1 [12]. Obviously, in concentrated KCl salt bridges, the thermal liquid junction potential can be neglected in most cases. A different behaviour was found in acidic and in strongly alkaline solutions. In dilute HCl, the TLJP can attain values of up to 40 mV for $\Delta T = 150$ K. Reason is the much higher transport entropy of hydrogen and hydroxide ions. The resulting error can be avoided by inserting a concentrated KCl bridge where the temperature profile must be located. If this is not possible, e.g., in non-isothermal, autoclaved high-temperature cells working with subcritical or supercritical water, thermodiffusion has a higher effect, and even the Soret equilibrium may be established. High values of E_{TLJP} also may be encountered with strongly heated electrodes in acidic solution. Baranski and Boika emphasise in their work, with very hot solution spots generated by high-frequency ohmic heating that the influence of the Soret effect has to be encountered for [13, 14].

Table 2.1 Thermal liquid junction potentials in aqueous KCl solution and their temperature coefficients for $T_{cold} = 298$ K [12]

T_{hot}/K	E_{TLJ}/mV	$\Delta E_{TLJP}/\Delta T$/mV K^{-1}
473	−4.74	−0.024
448	−4.44	−0.025
423	−4.18	−0.028
398	−4.15	−0.033
373	−3.9	−0.039
353	−3.94	−0.049

Table 2.2 Temperature coefficients of single-electrode potentials of common reference electrodes [5]

Electrode	$\frac{dE^\circ}{dT}$ /mV K^{-1}	Reference
SHE (298.5 K)	+0.871	[5]
Calomel el., 3.5 M KCl	+0.48	[5]
Calomel el., 1 M KCl	+0.5814	[2]
Ag/AgCl, 1 M KCl	+0.235	[5]

By means of entropy calculations as mentioned above, E_{TLJP} values of common reference electrodes have been calculated. On this basis, the non-isothermal temperature coefficient of some single-electrode potentials became available. Some results of such single-electrode potentials are given in Table 2.2. A comprehensive list for a large variety of electrodes has been published [5].

2.3.3 *Entropy Flow with Charge Transfer: The Electrochemical Peltier Effect*

Before we discuss energetic phenomena as a whole in non-isothermal cells, we have to consider the question, which reversible heat transfer will occur when charges are transferred over an electrode interface. To this end, we have to return to an isothermal electrochemical cell where reversible charge transfer takes place. In the special case, if we focus on *heat transport* connected to charge transfer, the so-called *electrochemical Peltier effect* must be considered. The latter has been defined as an analogue to the well-known "general" Peltier effect observed at a contact interface between two different metallic (later semiconducting) materials. It means that heat is transferred if electric current flows through the contact, i.e. either the contact is cooling or it is heating up. The opposite phenomenon, the *Seebeck effect*, means formation of a voltage at the contact if its temperature is changed. It can be expected that such effects will occur also at electrodes of electrochemical cells. Indeed, the "electrochemical Peltier effect" has been described [15, 16]. Theoretical considerations often have been done by means of irreversible thermodynamics [16]. Following such considerations, the heat balance of an electrochemical cell can be considered to be determined mainly by three contributions, namely (I) the electrochemical Peltier heat, which is the heat absorbed or evolved at the electrode interface when an electric charge unit passes through this interface at

constant temperature and pressure [17]. Contribution (II) is the irreversible heat produced when current is flowing in a situation far from equilibrium. In this case, an overvoltage is necessary to drive the reaction. A further contribution (III) is the Joule heat generated when current is flowing through an electrolyte reservoir, corresponding to its *iR* drop [16]. We have to consider here preferably the Peltier heat. The molar electrochemical Peltier heat Π is connected to a change in entropy ΔS in the course of an electrode reaction and the entropy of ions transported by migration ΔS^* (transport entropy or Eastman entropy). Π is defined to be positive for an exothermic anodic reaction. For a molar conversion of the redox reaction $\mathrm{Ox} + z\mathrm{e}^- \leftrightarrows \mathrm{Red}$, we can write

$$\Pi = \Pi_{\mathrm{Ox}} = -T(\Delta S_{\mathrm{Ox}} + \Delta S^*) = -\Pi_{\mathrm{Red}} = T(\Delta S_{\mathrm{Red}} - \Delta S^*) \tag{2.2}$$

with

$$\Delta S_{\mathrm{Ox}} = S_{\mathrm{Ox}} - S_{\mathrm{Red}} + zS_{\mathrm{e}}$$
$$S_i = S_i^{\theta} - R\ln a_i - RT\frac{\mathrm{d}\ln a_i}{\mathrm{d}T}$$

The transport entropy is written as

$$\Delta S^* = z\left(\sum \frac{t_j S_j^*}{z_j} + S_{\mathrm{e}}^*\right) \tag{2.3}$$

The subscript i refers to species participating in the reaction, while j denotes the species migrating in an electric field. Further symbols are t_j, the ion transport number and z_j, the ionic charge. S_j^* means the transport entropy for the considered ion.

In modern thermoelectrochemistry, the electrochemical Peltier effect has to be considered preferably with in-situ calorimetric measurements. Examples will be given in Sect. 3.4.

2.4 Properties of the Interface Electrode/Solution

The place where charge carriers cross the interface between electrode and solution is characterised by the electrolytic double layer. This is a very thin layer of molecular dimensions in the range of some nanometers. It can be considered as composed of two layers of particles carrying charges of opposite signs. Consequently, across the double layer, a voltage exists. Defining this voltage as the difference between the *inner electric potentials* (*Galvani potentials*) between both phases, we speak about a *Galvani voltage*. If a voltage is imposed externally between both phases, an electric field is generated which is localised nearly completely between both sides of the double layer. The reason is that inside a homogeneous electrolyte solution, no remarkable electric fields can exist. An

overall voltage amounting to some volts between a distance of some nanometers will then cause a field strength of megavolts per metre. This high field strength is the reason for the high power of electrochemistry which is potent to affect strongly the chemical reactions proceeding at the interface between electrode and solution. It seems useful to consider temperature effects at this highly important place.

There are different models depicting the double layer structure. The oldest model, created by Helmholtz, assumed that the excess charge on the electrode metal would be neutralised by a monomolecular layer of ions of opposite charge at the solution side. Later, this model was modified since it became clear that there must exist an additional layer consisting of a space charge of carriers driven away from the interface by thermal motion. The result is a "diffuse double layer" of charge, where the concentration of charge is maximum at the electrode surface and decreases progressively up to a homogeneous distribution of ions pertaining in the bulk electrolyte. Other authors refined this model. The generally accepted model now is based on the considerations of Grahame [18]. This model defines two planes of closest approach, one for specifically adsorbed ions (mainly anions) and another for non-specifically adsorbed ions. These planes are named inner Helmholtz plane (IHP) and outer Helmholtz plane (OHP), respectively. Adsorbed solvent dipoles also are located in the IHP. Further, a diffuse charge layer region exists which extends to the bulk electrolyte phase. Figure 2.1 gives an impression of the structure.

An alternative interpretation of the electrochemical double layer comes from a more thermodynamic approach. As an initial point, considering the *Gibbs adsorption equation* proved useful. This equation originally describes the dependence of the surface tension on the two-dimensional surface concentration (the surface excess Γ) of adsorbed particles as well as on their chemical potential μ. The equation can be extended by introducing an electric term which considers the potential dependence of the surface tension. The Gibbs adsorption equation in its complete form is as follows:

$$\mathrm{d}\sigma = -\Sigma \Gamma \,\mathrm{d}\mu_i - Q\,\mathrm{d}(\varphi_\mathrm{m} - \varphi_\mathrm{s}) \tag{2.4}$$

or

$$\mathrm{d}\sigma = -\Sigma \Gamma \,\mathrm{d}\mu_i - Q\,\mathrm{d}E \tag{2.5}$$

with

σ	surface tension
Γ	surface concentration (excess concentration per unit area compared to bulk concentration) of adsorbed species
μ_i	chemical potential of adsorbed species
Q	charge per unit area at the electrolyte side (charge density)
$\varphi_\mathrm{m}-\varphi_\mathrm{s}$	Galvani potential difference between metallic and solution phases

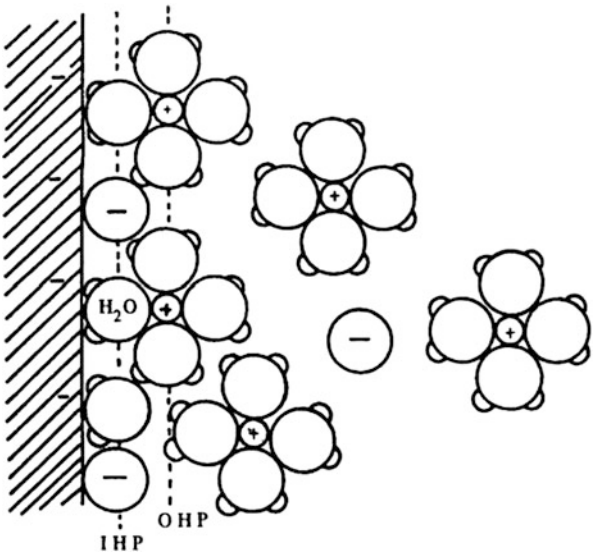

Fig. 2.1 Grahame's model of the electrochemical double layer. Anions and cations characterised by − or + signs, respectively. *IHP* inner Helmholtz plane and *OHP* outer Helmholtz plane. Reproduced from [19], with permission

The two terms at the right hand side of Eq. (2.4) can be discussed separately. The partial equation

$$\frac{\mathrm{d}\sigma}{\mathrm{d}\mu} = -\Gamma \tag{2.6}$$

often alone is referred to as Gibbs adsorption equation. It gives a mathematical expression for the fact that substances, which decrease the surface tension, are accumulated at the surface. The second term in Eq. (2.4) describes the potential dependence of the surface tension for constant concentration. The amount of work necessary to increase the surface, $\mathrm{d}\sigma$, corresponds to the amount of electric work, $Q\mathrm{d}\varphi$. We may write then

$$\mathrm{d}\sigma = -Q\,\mathrm{d}E \tag{2.7}$$

The above equation, written as follows

$$Q = -\left(\frac{\partial\sigma}{\partial E}\right)_{\mu} \tag{2.8}$$

is the well-known Lippmann equation (sometimes referred to as Lippmann–Helmholtz equation). Integration of this differential equation yields the function of a parabola

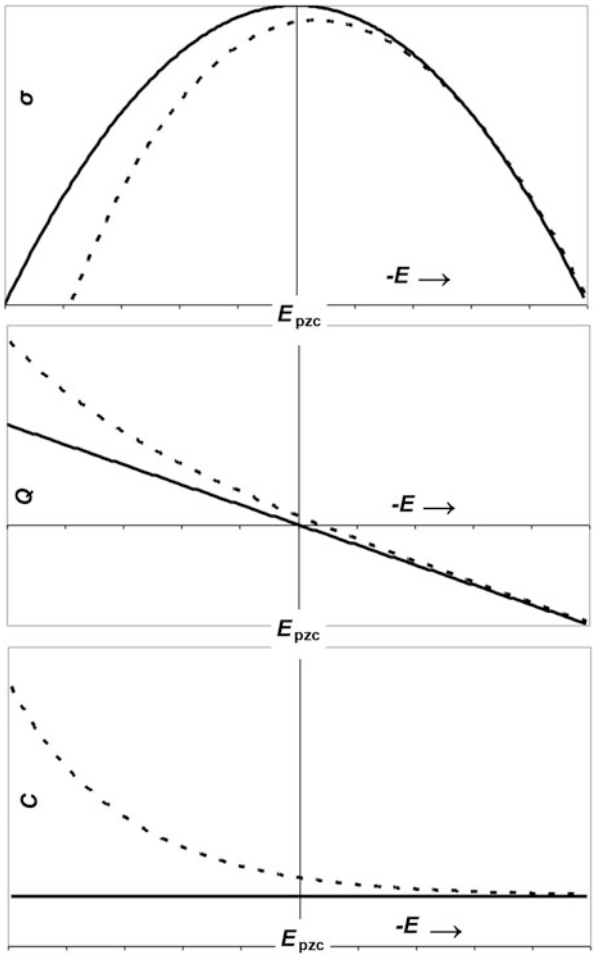

Fig. 2.2 Surface tension and its first and second derivatives versus potential E. From *top* to *bottom*: Surface tension per unit area σ; surface charge $Q = (\partial\sigma/E)_\mu$; differential capacity $C = (\partial Q/\partial E)_\mu = -(\partial^2\sigma/\mathrm{d}E^2)_\mu$. *Solid lines*: no adsorption; *dotted lines*: adsorbed anions

(Fig. 2.2, top). At the maximum of this parabola, the surface should be free from any excess charges, since every electric charging should generate repulsion forces between molecules, which would decrease the surface tension. Consequently, the first derivative of σ, i.e. the charge $Q = \mathrm{d}\sigma/\mathrm{d}E$, should be zero for the potential value at electrocapillary maximum, E_{pzc} (Fig. 2.2, centre). A further relation depicted in Fig. 2.2 is

$$C = \left(\frac{\partial Q}{\partial E}\right)_\mu = \left(\frac{\partial^2 \sigma}{\partial E^2}\right)_\mu \tag{2.9}$$

The *potential of zero charge* E_{pzc} has been considered as a characteristic of electrodes which should express their individuality more than the standard electrode potential E^Θ. Electrochemical series with E_{pzc} instead of E^Θ have been published. Electrocapillarity curves are not easily available for solid electrodes. It

proved very useful to study instead the differential capacity C, the second derivative of σ, in relation to the potential.

Adsorbed ions at the electrode surface cause deformation of the curves given in Fig. 2.2. The slope of the electrocapillary parabola becomes more steep for positive potentials, if anions are adsorbed. At negative potentials, the slope is becoming more steep with adsorbed cations. In Fig. 2.2 the effect is shown for adsorbed anions. The curves show that with adsorbed ions, the electrocapillary maximum is not achieved, and the surface is not free from charges at the point with the highest measured surface tension. Adsorbed solvent dipoles, e.g., contain charges inside the inner Helmholtz layer. Further it can be seen that the differential capacity is much more sensitive to adsorptive effects than σ. If both sorts of ions are adsorbed, the diagram $C = f(E)$ shows a minimum in vicinity of E_{pzc}, the so-called *capacitive minimum*. The latter is of high value for double layer studies. Consequently, as the standard method to investigate the interface electrode solution, nowadays the measurement of electrode impedance has established. Originally, the impedance (the complex resistivity containing ohmic and capacitive parts) had to be determined point by point by means of a modified Wheatstone bridge Fig. 2.3. Actually, automated instruments allow much more convenient measurement. Capacity can be studied in dependence of frequency over a large range. The resulting method is named electrochemical impedance spectroscopy.

Important thermoelectrochemical insight has been obtained by investigating the temperature dependencies of σ, C and E_{pzc}. The temperature coefficients of σ at the electrocapillary maximum, of C at the capacitive minimum and of E_{pzc} are important sources for information about the double layer structure. The latter depends on temperature dependent changes of physical solution properties (see Sect. 2.5). Classical investigations have been done at "ideal polarizable electrodes", i.e. at electrodes where no charge transfer across the interface electrode/solution is occurring during polarisation. Very often, the mercury drop electrode has been used as an example of an ideal polarisable electrode.

Grahame [21] has deduced the significant relationships between surface tension of an ideal polarised electrode at its electrocapillary maximum σ_{max} and the corresponding free energy as well as entropy of double layer formation. Based on these fundamental considerations, Randles [22] utilised the temperature coefficient of σ_{max} at mercury electrodes in KCl solution to establish a relation to localise single-electrode entropies and single-ion entropies. The temperature dependency of E_{pzc} was identified as a most important quantity in this context. An overview on theoretical concepts about the structure of the double layer and a connection to the "absolute electrode potential" has been given by Trasatti [23].

Soon it became obvious that measurement of capacity is the better way to determine the three variables mentioned above in dependence of temperature. First time such studies have been done with mercury electrodes [24], later also with an alternative liquid electrode, i.e. with gallium [25]. Studies with polycrystalline solid electrodes are difficult, since their charge density distribution is not uniform. This was the reason that many investigations of temperature dependent double layer parameters have been done with single crystal electrodes, among them

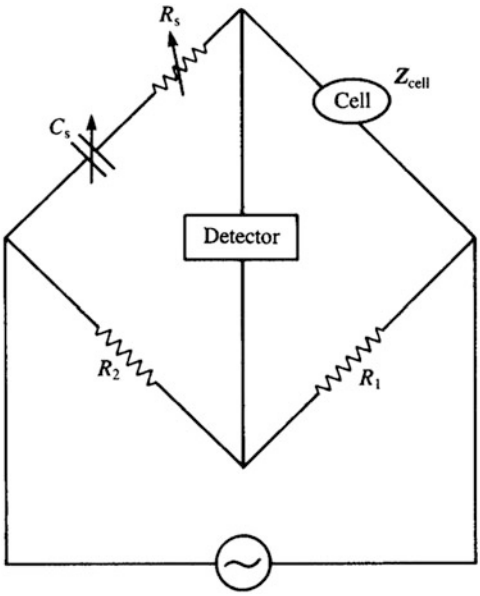

Fig. 2.3 A.c. bridge for the measurement of the impedance of electrochemical cells. The bridge is balanced when the current is zero. In this case $Z_{cell}/R_1 = Zs/R_2 = R_s - i/\omega C_s$. From [20], with permission

silver [26–29], gold [30–33] and cadmium [34]. This way, it was even possible to determine adsorption entropies of specifically adsorbable anions [29].

Without a deeper knowledge of theory, some deductions are obvious. Assuming that adsorbed water dipoles are oriented inside the IHP with their negative charge towards the electrode surface, a temperature rise would tend to disorder the dipole layer resulting in a decrease of the negative potential shift in the inner plane. Consequently, E_{pzc} should shift towards more positive values. This has been confirmed experimentally [34]. This means that typically the differential capacity is decreasing with temperature. With extremely negative potentials, this tendency may invert [34]. As an example, results with a single crystal Cd electrode are presented in Fig. 2.4. The anomaly in temperature coefficient depends on different factors. The latter have been stated by mathematical simulation, e.g., in [35].

Also it is easily understood that the diffuse part of the double layer will extend with temperature due to increasing thermal motion of the particles. The extension factor is assumed generally to be 0.22 % per Kelvin, as stated in many textbooks of electrochemistry. The interface capacity at capacitive minimum C_{min} reflects this extension.

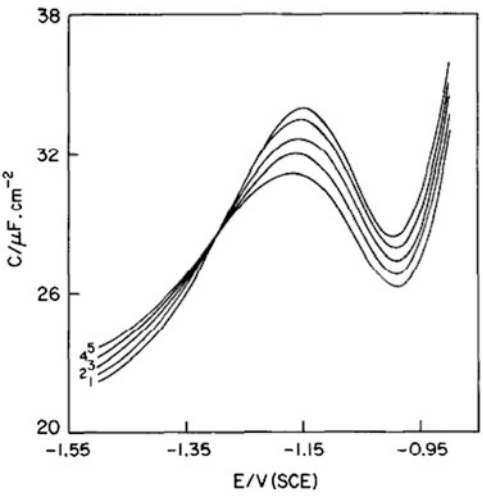

Fig. 2.4 Capacity versus potential on Cadmium(001) in 50 mM KF solution at varied temperature (1) 283 K, (2) 293 K, (3) 303 K, (4) 313 K, (5) 323 K. Cited from [34], with permission

2.5 Properties of Solvent and of Ions in Solution

As mentioned above, many solvent properties depend on temperature. This temperature dependence affects all the properties discussed above and in following.

The tendency of solvent molecules to associate and to form an inner structure is decreased. The internal friction between molecules is reduced. This means that the temperature coefficient of viscosity is always negative, i.e. the viscosity is decreasing with increasing temperature. As a general rule, the viscosity decreases by ca. 2 % [36]. The temperature dependence for many liquids is expressed by a relationship of the Arrhenius type (Fig. 2.5):

$$\eta = A \cdot \exp(-E_{\mathrm{A,vis}}/RT) \tag{2.10}$$

The activation energy of the liquid flow in Eq. (2.10), $E_{\mathrm{A,vis}}$, corresponds to the energy barrier which has to be overcome by a molecule until it will be able to pass the adjacent molecules.

As a consequence of viscosity decrease, the rate of transport of electroactive species towards the electrode surface can increase markedly. The diffusion coefficients of dissolved particles are related to the viscosity and the density of the solvent via two simple relations:

$$D \cdot \eta = \mathrm{const} \tag{2.11}$$

$$\eta = \rho \cdot D \tag{2.12}$$

The relations given above can be used to estimate values of D for varied temperatures.

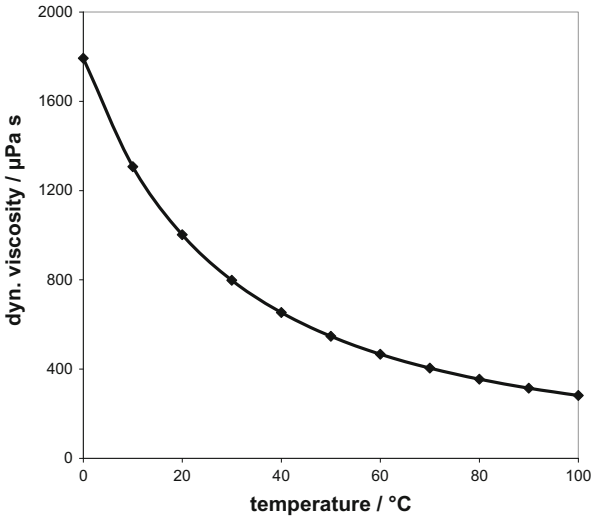

Fig. 2.5 Temperature dependence of the dynamic viscosity of water. Values from [36]

Electric conductivity of electrolyte solutions strongly depends on temperature. To a certain point, typically the conductance is increasing due to decreasing viscosity of solvent. There are, however, counteracting factors. In aqueous solution, e.g. above 90 °C, the conductance is decreasing due to decreasing dielectric constant of the solvent [37]. The solvent shell is reduced, and ionic interactions tend to affect the mobility of ions more and more.

A very important thermodynamic parameter in electrolyte solution is the activity coefficient. Its temperature dependence can be studied by potentiometry, since activity manifests directly in the value of the electrode potential. Studies of such kind have been done, e.g., for solutions of HBr and KBr in aqueous solution [38]. Summarising all the mentioned temperature effects, it can be said as a general rule, that activity a of electrolytes with increasing temperature tends to approach the value of the analytical concentration c. In other words, the higher the temperature of a nonideal solution, the smaller the deviation of its components from ideal behaviour. The activity coefficient f_i will approach the value one with increasing temperature.

The discussed temperature effects can be summarised to obtain the following important consequences:

- The structures in the bulk solution are loosened by temperature increase. As a result, transport processes towards the electrode and away from it, respectively, are enhanced.
- Solvent adsorption at the electrode surface is changed. Primarily, the compact structure of the double layer is disturbed. As a result, double layer capacity is altered.
- Electric conductivity of electrolyte solution, as a rule, is increasing.

– The dielectric constant of polar solvents decreases with temperature. As a result, the solvent shell will be reduced.
– Activity of ions is changing with temperature such a way that their properties tend to approach the ideal state, i.e. the activity coefficient f_i tends to attain the value 1.

2.6 Kinetics and Transport Processes

The overall reaction process taking place in an electrochemical cell consists of a manifold of partial processes. Relevant processes are the following:

– Transport of reactants toward the electrode (by diffusion, convection or ion migration)
– Preceding homogeneous chemical reactions (dissociation equilibria, etc.)
– Adsorption of reactants at the electrode surface
– Charge transfer through the interface electrode/solution
– Desorption of reaction products
– Transport of products away from the electrode

Every partial process is temperature dependent. Kinetic behaviour of any type of electrode reaction and even of the transport of particles by diffusion is reflected by the Arrhenius equation which relates the activation energy E_A to the rate constant, k:

$$k = A \cdot \exp\left(-\frac{E_A}{RT}\right) \tag{2.13}$$

If ln k is plotted versus T^{-1}, the activation energy E_A corresponds to the slope of the resulting straight line, whereas the pre-exponential factor A can be determined from the intersection with the T^{-1} axis. By Eyring's theory of the *activated complex*, rearrangement processes of the ionic atmosphere are important in electrochemical reactions. Hence it is useful to introduce the activation entropy ΔS^*. Since the pre-exponential factor A of Arrhenius equation can be expressed as a function of entropy, we get (with activation enthalpy, ΔH^* and Boltzmann constant k_B):

$$k = \frac{k_B T}{h} \cdot \exp\left(\frac{\Delta S^*}{R}\right) \cdot \exp\left(-\frac{\Delta H^*}{RT}\right) \tag{2.14}$$

Equation (2.14) points to the opportunity to determine the thermodynamic quantities ΔH^* and ΔS^* by means of kinetic measurements at varied temperature.

Charge transfer across the interface electrode-solution is the central step inside the overall reaction. The amplitude of the electrolysis current, expressed by the current density j (current per electrode surface area), is directly proportional to the heterogeneous rate constant of charge transfers through the interface electrode

solution. The well-known Butler–Volmer equation relates the current density to all relevant quantities contributing to kinetics of charge transfer. The following simplified equation can be derived:

$$j = j_0 \cdot \exp\left(\frac{\alpha \eta F}{RT}\right) \tag{2.15}$$

In this equation, j is correlated with the overvoltage η using the kinetic parameters transfer coefficient α and the exchange current density j_0. The term overvoltage reflects the fact that kinetic hindrance in electrochemistry can be compensated by imposing an additional voltage difference. The difference between imposed and equilibrium potential means overvoltage (sometimes named overpotential) η. The kinetic parameter α (*transfer coefficient* or *symmetry factor*) is an expression for the influence of a potential difference across the electrochemical double layer if an external voltage is imposed between the electrodes of a cell. The parameter *exchange current density* j_0 gives an impression of the charge transfer amplitude across the interface in *electrode equilibrium*. The higher j_0, the smaller is the effect of an external, imposed current on the deviation of the electrode from equilibrium, i.e. the smaller is the resulting charge transfer overvoltage.

Equation (2.15) is valid only for potential values far from the equilibrium potential. Limitations by mass transport should be negligible. If these assumptions are met, the conditions correspond to the so-called *Tafel region*, where j depends exponentially on the electrode potential. The *Tafel region* is defined by the *Tafel equation*, which can be written in a general form (for anodic current density j_a) as,

$$\ln j_a = b + \frac{\alpha_a z F E}{RT} \tag{2.16}$$

Plots of $\ln \left| j \right|$ versus E give the transfer coefficient α (from the slope) as well as the exchange current density j_0 (from the intercept with the $\ln j$ axis). It is assumed that the transfer coefficient α should be independent from temperature and electrode potential. There are many controversies in literature about the question whether α is temperature dependent or not [39–50]. An anomalous behaviour of α has been observed frequently. A comprehensive discussion has been given by Bockris [41]. Gileadi has proposed an equation for the temperature dependence of α [42].

The temperature dependence of the exchange current density j_0 follows the Arrhenius equation analogous to the relationship given above for k.

The kinetics of the overall electrochemical reaction is not only determined by the electron transfer process but also by transport processes, mainly diffusion, furthermore adsorption/desorption of reactants and reactions in homogeneous solution preceding or following the charge transfer. If new phases are formed in the course of an electrolysis (e.g. with metal deposition at a solid surface or with gas evolution), the kinetics of phase formation (mainly the nucleation step for depositions) also controls the overall reaction rate. All partial processes have their own special temperature dependence.

The different overall reaction pathways occurring in an electrochemical cell often are classified by defining reactions in homogeneous solution (*preceding* or *following* reactions) as "chemical" reactions abbreviated by "C" and the charge transfer through the interface as "electrochemical" reaction symbolised by "E". This way, as an example, an overall reaction starting with a preceding reaction C, followed by charge transfer E, and by a following reaction (again C) is symbolised as "ECE mechanism". Among *preceding reactions* (in CE processes), the dissociation of water is permanently existing in aqueous solution. As an extremely fast reaction without any direct influence on electrode kinetics, the dissociation equilibrium is temperature dependent as well. This can be expressed by the ion product of water, represented by the pK_W value. Its value is 14.89 for 0 °C, 13.90 for 22 °C and 11.30 for 200 °C. The thermoelectrochemical consequence of this equilibrium is that the pH in aqueous solution is temperature dependent, and consequently, all pH sensitive equilibria also depend on temperature.

Adsorption or desorption processes often precede or follow an electrochemical reaction. They can be rate determining for the overall electrode–electrode reaction and they are strongly temperature dependent. With increasing temperature, the effect of adsorption–desorption equilibria on electrode reactions is decreasing, since the degree of interaction at a surface is reduced with temperature. Electrode processes under participation of solvent species are most important in electrode reaction. Adsorption layers of solvent molecules strongly affect the double layer capacity, and therefore the temperature dependence of the latter can provide information on the adsorptivity of ions involved in electrode processes. Thus, the temperature dependence of oxygen species generally is higher than those of hydrogen species.

Among the transport processes in electrochemistry, diffusion is the most significant one. Diffusion is strongly temperature dependent. The diffusion limited current I_L increases by ca. +1.6 % per Kelvin. This can be ascribed to two different reasons:

(a) The kinetic energy of species increases with temperature, hence more particles achieve the necessary energy to cross the energy barrier formed by the "cage" of surrounding solvent molecules. Temperature dependence of the diffusion coefficient D follows a relationship analogous to Arrhenius equation:

$$D = D^* \cdot \exp\left(-\frac{E_D}{RT}\right) \tag{2.17}$$

The pre-exponential factor D^* can be approximately considered to be temperature independent. The molar activation energy of diffusion E_D is about 8–20 kJ mol^{-1} in liquids. It can be determined from the correlation $D = f(T^{-1})$.

(b) The viscosity of solvents is decreasing with temperature according to an Arrhenius type relationship. The resulting increase of D is expressed by the

Stokes–Einstein relation (with k_B the Boltzmann constant, η the dynamic viscosity and r the hydrodynamic radius of the diffusing species):

$$D = \frac{k_B \cdot T}{6\pi\eta r} \tag{2.18}$$

As mentioned in Sect. 2.5, solvent density and solvent viscosity are determining for the value of the diffusion coefficient [see Eqs. (2.11) and (2.12)]. Consequently, the temperature dependence of these quantities is found in the value of D.

The temperature dependence of conductivity (see Sect. 2.5) depends on temperature in the same way as the diffusion coefficient of ions. Often it is convenient to estimate actual values of D by means of its relation to conductivity. Two fundamental equations describe this relation. It is Eq. (2.19), the Einstein relation (with u the molar ion mobility and F the Faraday constant), and Eq. (2.20), the Nernst–Einstein relation (with λ the molar ion conductivity).

$$D = \frac{u \cdot RT}{zF} \tag{2.19}$$

$$\lambda = \frac{z^2F^2}{RT}D \tag{2.20}$$

References

1. Wild H (1858) Pogg Ann 103:353
2. Parsons R (1985) The single electrode potential: its significance and calculation. In: Bard AJ, Parsons R, Jordan J (eds) Standard potentials in aqueous solution. Marcel Dekker, New York, NY, Chapter 2
3. Trasatti S (1985) Pure Appl Chem 58:955
4. Agar JN, Breck WG (1957) Trans Faraday Soc 53:167–178
5. Debethune AJ, Licht TS, Swendeman N (1959) J Electrochem Soc 106:616–625
6. Eastman ED (1926) J Am Chem Soc 48:1482–1493
7. Tyrrell HJV, Hollis GL (1949) Trans Faraday Soc 45:411–423
8. Macdonald DD, Scott AC, Wentrcek P (1979) J Electrochem Soc 126:908–911
9. Macdonald DD, Scott AC, Wentrcek P (1979) J Electrochem Soc 126:1618–1624
10. Lvov SN, Macdonald DD (1996) J Electroanal Chem 403:25–30
11. Engelhardt GR, Lvov SN, Macdonald DD (1997) J Electroanal Chem 429:193–201
12. Nickchi T, Alfantazi A (2012) Corrosion Sci 63:174–181
13. Baranski AS (2002) Anal Chem 74:1294–1301
14. Boika A, Baranski AS (2011) Electrochim Acta 56:7288–7297
15. Vetter KJ (1961) Elektrochemische Kinetik. Springer, Berlin
16. Agar JN (1963) Thermogalvanic cells. In: Delahay P (ed) Advances in electrochemistry and electrochemical engineering. Interscience Publishers, London, pp 31–121
17. Boudeville P, Tallec A (1988) Thermochim Acta 126:221–234
18. Grahame DC (1947) Chem Rev 41:441–501
19. Southampton Electrochemistry Group (1985) Instrumental methods in electrochemistry. Ellis Horwood, Chichester
20. Brett CMA, Oliveira Brett AM (1993) Electrochemistry. Oxford University Press, Oxford
21. Grahame DC (1948) J Chem Phys 16:1117–1123

22. Randles JEB, Whiteley KS (1956) Trans Faraday Soc 52:1509–1512
23. Trasatti S (1991) Electrochim Acta 36:1657–1658
24. Hills GJ, Payne R (1965) Trans Faraday Soc 61:326–349
25. Szabo K, Mika J (1991) Acta Chim Hung 128:195–205
26. Bacchetta M, Francesconi A, Trasatti S, Doubova L, Hamelin A (1987) J Electroanal Chem 218:355–360
27. Hamelin A, Doubova L, Stoicoviciu L, Trasatti S (1988) J Electroanal Chem 244:133–145
28. Popov A, Velev O, Vitanov T, Tonchev D (1988) J Electroanal Chem 257:95–100
29. Popov A (1995) J Electroanal Chem 384:179–181
30. Hamelin A, Stoicoviciu L, Silva F (1987) J Electroanal Chem 236:283–294
31. Silva F, Sottomayor MJ, Hamelin A, Stoicoviciu L (1990) J Electroanal Chem 295:301–316
32. Silva F, Sottomayor MJ, Hamelin A (1990) J Electroanal Chem 294:239–251
33. Silva F, Sottomayor MJ, Martins A (1993) J Electroanal Chem 360:199–210
34. Popov A, Dimitrov N, Naneva R, Vitanov T (1994) J Electroanal Chem 376:97–100
35. Alawneh M, Henderson D, Outhwaite CW, Bhuiyan LB (2008) Mol Simulat 34:501–507
36. Lide DR (1995) CRC handbook of chemistry and physics, 76th edn. CRC Press, Boca Raton, FL, pp 6–10
37. Uematsu M, Franck EU (1980) J Phys Chem Ref Data 9:1291
38. Lietzke MH, Stoughton RW (1963) J Phys Chem 67:2573–2576
39. Ulstrup J (1984) Electrochim Acta 29:1377–1380
40. Conway BE, Tessier DF, Wilkinson DP (1986) J Electroanal Chem 199:249–269
41. Bockris JO, Gochev A (1986) J Electroanal Chem 214:655–674
42. Gileadi E (1987) J Electrochem Soc 134:117–120
43. Tsionskii VM, Krishtalik LI, Kriksunov LB (1988) Electrochim Acta 33:623–630
44. Conway BE, Tessier DF, Wilkinson DP (1989) J Electrochem Soc 136:2486–2493
45. Schmickler W (1990) J Electroanal Chem 284:269–277
46. Damjanovic A, Walsh AT, Sepa DB (1990) J Phys Chem 94:1967–1973
47. Damjanovic A (1993) J Electroanal Chem 355:57–77
48. Damjanovic A, Utz AL, Walsh AT (1993) J Phys Chem 97:9177–9180
49. Kriksunov LB, Bunakova LV, Zabusova SE, Krishtalik LI (1994) Electrochim Acta 39:137–142
50. Kirowa-Eisner E, Rosenblum M, Schwarz M, Gileadi E (1996) J Electroanal Chem 410:189–197

Chapter 3
History of Modern Thermoelectrochemistry

3.1 Classical Thermoelectrochemistry in Isothermal Open Cells and Half-Cells

Classical industrial processes like electrodeposition, galvanising, or electrochemical oxidation of materials are temperature dependent. Traditional processing takes place in open cells. Consequently, many "trivial" thermoelectrochemical investigations in open cells, at moderate temperature variation, have been described. The majority of such studies are dedicated to the improvement of efficiency [1–26]. Deposition of metals, among them copper [1, 2], zinc [3–5], nickel and its alloys [6, 7], chromium [8] and cobalt [9, 10] has been studied. Also electrochemical generation of oxide layers on zinc and on aluminium [4, 12] was subject of papers. Temperature dependence of less common phenomena, e.g., calcareous scaling [13], electrostimulated leaching of minerals [14, 15] or growth of nanocables [16] has been studied. Classical thermoelectrochemical experiments provided information about important partial processes as hydrogen electrosorption [17] or lithium ion intercalation into graphite [18]. Deposition processes have been investigated by means of the electrochemical quartz microbalance under temperature variation [19]. Uncommon electrode materials were single crystal platinum [20] and diamond electrodes [21], as well as paste electrodes made of graphite and ionic liquids [22]. Ionic liquids as solvents have been applied in open cells at moderate temperature variation [23, 24]. An interesting application of classical thermoelectrochemistry dealt with a process named electrodialysis [25].

Processes of industrial interest as corrosion [27–30] and electrochemical machining [31–34] also were subject of classical thermoelectrochemistry.

In all the examples mentioned above, the intention has been just to improve existing methods by means of temperature variation. There is doubt whether it is allowed to speak about thermoelectrochemistry in such cases. On the other hand, there are many examples where real thermoelectrochemical questions are studied in open, isothermal cells and half-cells. First of all, potentiometric methods must be

P. Gründler, *In-situ Thermoelectrochemistry*, Monographs in Electrochemistry,
DOI 10.1007/978-3-662-45818-1_3

mentioned. Early in nineteenth century, potential differences between electrodes in a thermocell have been observed. The opposite case, i.e. temperature changes between electrodes as a result of current flow, has been found first in 1877 by Mills [35], but the observation was misinterpreted. The first correct interpretation of such heat effects has been given by Bouty in 1879 [36]. The phenomena were considered to be some kind of an "electrochemical Peltier effect". An early review can be found in [37].

As outlined in Chap. 2, the temperature coefficient of standard electrode potential is closely connected with the entropy of the cell reaction. Consequently, potential measurements in thermocells as well as in isothermal and in non-isothermal cells or half-cells are highly important sources of the important thermodynamic quantity entropy. In a very important work of Debethune et al. [38, 39] the cell voltage (EMF) of a large variety of thermocells and of isothermal half-cells has been studied. A clear distinction was given between the "isothermal" and the "thermal" temperature coefficients of standard potentials. The former can be obtained by measuring temperature-dependent potential changes at a cell where the electrode of interest is combined with the standard hydrogen electrode (SHE), both of equal temperature, whereas the latter results from a cell where the reference electrode SHE is held at constant temperature, and the temperature of the half-cell containing the electrode of interest is varied. Additional information is obtained with potential measurement at *thermocells*. This way, standard entropy values of 300 electrodes have been determined, also the entropy of the hydrogen electrode half-cell itself, which is considered to be the "entropy of the electrochemical transport of the hydrogen ion". The results represent an important source of thermodynamic *single-electrode quantities*. Instead of potentiometry, voltammetry has been utilised to determine important thermodynamic properties [40].

Among the papers dealing with potential measurements at isothermal half-cells at normal pressure, such of industrial interest are remarkable, e.g. of the chlorine electrode [41]. Very precise studies at thermocells with the hydrogen electrode, the silver–silver chloride electrode and the silver electrode [42] provided single ion entropies and activation entropies.

Among electrochemical processes which might be of future interest, the conversion of "heat waste" into electric energy is important. Heat generated in nuclear power plants, as mentioned further above, cannot be evaluated for heating of buildings, etc., hence alternative processes are of interest. One way is the use of thermocells, where the resulting voltage difference is utilised. Another way was to make use of special electrolysis cells which generate hydrogen at higher temperature. Most of the corresponding processes are running under pressure, diagnostic studies also are done preferably in autoclave cells. Examples are given later below. As an exception, fundamental experiments in a normal ambient pressure cell consisting of a cupric/cuprous electrode and a hydrogen electrode have been described [43]. The intention of this paper was to determine important thermodynamic quantities, mainly entropy (Fig. 3.1).

In cells with moderate temperature variation under ambient pressure, double-layer studies have been done, mainly by investigating the capacitive minimum,

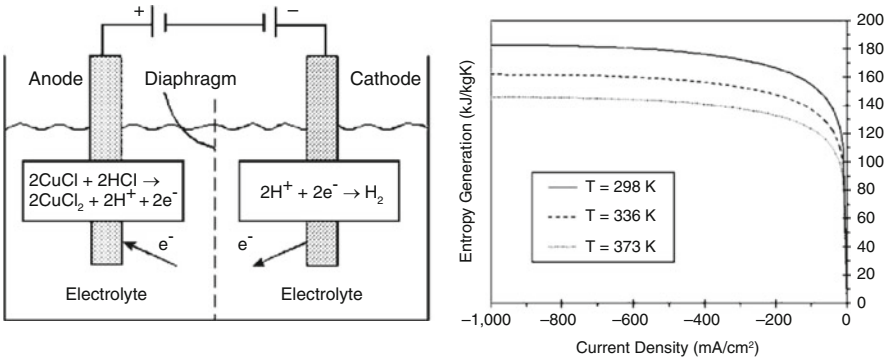

Fig. 3.1 *Left*: Scheme of a hydrogen producing thermoelectrochemical cell; *Right*: Temperature dependence of entropy generation in the CuCl cell. From [43], with permission

mentioned in Chap. 2. The mercury electrode was the preferred object [44–46]. A typical temperature effect is demonstrated in Fig. 3.2. The advantages of a liquid electrode, especially its ideal flat surface, are also found with the gallium electrode; however, thermoelectrochemical double-layer studies with Ga kept a rare exception [47]. The charge distribution at polycrystalline solid electrodes is non-uniform. Double-layer studies at polycrystalline metals are problematic thereby. The temperature dependence of C_{DL} has been studied at the polycrystalline gold electrode [48], but the big majority of studies were with single crystal electrodes, among them silver [49, 50], gold [51], and cadmium [52]. Fundamental thermoelectrochemical investigations with large surface area materials [53–55] have not been done frequently. More representative were simple tests with slight temperature variations just to improve the efficiency of super capacitors and related devices. Examples are cited later below.

Impedance analysis is a powerful thermoelectrochemical instrument. It proved useful to study the capacity of cobalt hydroxide film formation in double-layer electrolyte capacitors [56]. Also, experiments with the capacity of electrodes in solid state electrolytes have been published, e.g. with silver halide/graphite mixtures [57].

Experiments under the restrictions of classical thermoelectrochemistry in open cells with moderate temperature variation addressed, to some extent, also the conditions in the bulk electrolyte solution and the properties of ions. Potentiometric measurements in aqueous solutions of hydrogen and potassium bromides yielded the temperature dependence of activity coefficients of important ions [58]. As mentioned in Chap. 2, all electrolyte solutions tend to approach the ideal state with increasing temperature. The conductance of various electrolytes has been studied in dependence on temperature [59–66]. Solvents studied were propanol [59], propylene carbonate [60, 64], dimethoxyethane [65], primary alcohols and acetonitrile [62]. Conductance values were used to determine transference numbers of ions in non-aqueous solution [62]. Salt melts of sodium and caesium halides also have been studied [66]. Theoretical considerations were subject of [63].

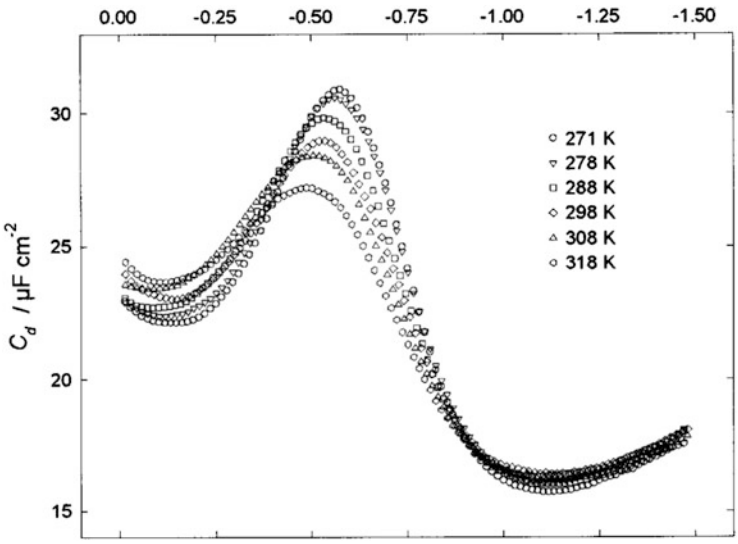

Fig. 3.2 Variation of the differential capacity of the mercury/aqueous solution interphase with temperature for a 1 M $NaClO_4$ solution. From [45], with permission

There are not many experiments at open cells with small T variations which are directed to determination of fundamental kinetic quantities like transfer coefficients of homogeneous redox couples [67], heterogeneous rate constant of the charge transfer [68], or nucleation at solid electrodes [21] system described in [21, 69], deposition of lead at the boron-doped diamond electrode, is a good example for a possible new role of thermoelectrochemistry which could provide important information about the nucleation process at non-metallic electrodes without underpotential deposition. The temperature dependence of this type of nucleation has been studied, yet only scarcely.

Gas evolution, especially of hydrogen and oxygen, was subject of thermoelectrochemical studies in open cells [69–71]. Hydrogen evolution kinetics at single crystal platinum electrodes [71] is of great practical interest; this holds true also for oxygen evolution at lead dioxide electrodes [72]. At a PbO_2 electrode in aqueous solution, oxygen formation is characterised by a high overvoltage. This is the reason that other anodic processes of industrial interest can proceed without distortion by solvent oxidation. Interesting processes are, e.g., chlorine evolution or anodic oxidation of organic compounds, among them water pollutants.

Kinetics of oxygen reduction was subject of thermoelectrochemical studies [73–77], among them at platinum single crystal electrodes [74], and at graphite with and without catalysts [75–77].

Anodic oxidation at different solid electrodes has been investigated in connection with temperature variation [78–82]. Anodic oxidation of carbon, catalysed by Fe^{2+}/Fe^{3+} [78], anodic dissolution of titanium [79]and of copper [82] and furthermore oxidation of dissolved formic acid [80] and of methanol [81] have been

reported. Electrochemical oscillations are interesting phenomena with a strong temperature influence [80, 82, 83]. Oscillations have been observed also in melts of lithium/sodium carbonates [84], with microcrystals of platinum phthalocyanine adhering at the surface of a platinum electrode [85]. Thermal fluctuation in electrochemical cells has been discussed from a general point of view [86].

In a thermoelectrochemical context, last but not least, there should be mentioned experiments with important phenomena present in modern devices. Examples are the behaviour of the lithium electrode in propylene carbonate, where the passive layer was subject of interest [88]. This layer is significant for the function of lithium accumulators. Another process which is meaningful for modern battery research was reduction of sulphate to give sulphide at graphite electrodes [87].

In many classical thermoelectrochemical experiments in open cells, which are directed at modern substances or actual processes, transport properties were of interest [89–93]. In a comprehensive impedance study of a conducting polymer, poly(tetracyanoquinodimethane) (polyTCMQ), Inzelt determined fundamental constants like diffusion coefficient, double-layer capacity and other quantities of the semiconductor layer as a function of temperature [89]. Reduction kinetics of buckminsterfullerene C_{60} has been studied [90]; diffusion coefficients of different systems have been determined [91–93], among them D of ferrocene/ferricinium in acetonitrile [92] and of vanadium ions [93]. In the latter example, activation energy of diffusion was also of interest.

There is a rich literature where just temperature dependence of electrochemical parameters is of interest. It is no wonder that large part of those papers cannot really be classified to belong to thermoelectrochemistry. In fact, many experiments have been done just to improve the efficiency of common processes by means of certain temperature variation. The majority of these types of publications are found in battery research [94–118]. Theoretical considerations from a fundamental point of view are a rare exception [94]. Nearly all papers are dealing with special battery types. Nickel batteries of the Ni-Cd or the NiMH type actually are not preferably in the focus of interest. All actual papers are directed to the nickel hydroxide layer at the positive electrode [95, 96]. Also, the lead–acid battery is considered scarcely at present [27].

In battery research, the large majority of thermal effects studied belong to lithium batteries [98–120]. Some general considerations are subject of [98–100]. Electrode materials like $LiFePO_4$ have been discussed [101–111]. Remarkable is the use of ionic liquids [110], the special behaviour of lithium intercalation in graphite electrodes [112–115] and thermal effects on polymer electrolytes [116–119] and on ceramic solid electrolyte [120].

Technically, fuel cell research belongs to battery research. Most fuel cell types are run at increased temperature, hence T is an important parameter [121–143]. On the other hand, nearly all the references cited deal with simple optimisation experiments; whereas papers dealing with a fundamental background do not occur frequently [126]. Investigations with cells containing classic, liquid electrolytes are similar to many other classical thermoelectrochemical studies [121–126]. Not very far from classic experiments are fuel cells with polymer electrolyte

[127–132], preferably proton exchange membrane fuel cells (PEMFC) [128–132]. Different characteristics are found with solid oxide fuel cells (SOFC) [138–143]. The latter work with gaseous reactants, thereby belongs to autoclaved cells, but in some cases experiments in open solid electrolyte cells have been described.

New materials with an extremely high surface-to-volume ratio allow construction of "super capacitors". Super capacitors are capable to store a high amount of electric charge similar to the charge storage in rechargeable batteries. The classical distinction is that on capacitors the charge is stored in a pure physical way; whereas batteries store charges by means of reduction and oxidation processes forming new chemical substances. This distinction, in modern electrochemistry, cannot be hold strictly, since, e.g., in cells with lithium ions and graphite electrodes, the charge separation is somehow between electrostatic separation and redox reaction. In any case, temperature is a very important parameter for super capacitors [144, 145]. Figure 3.3 gives an impression on the enormous capacity. The temperature influence is not very strong.

Among research interest of classical thermoelectrochemistry in open cells with small T variation was the process of electropolymerisation [146, 147], the large field of electrode surface layers [148–159]. Formation of oxide films or layers of adsorbed oxygen species at noble metal electrodes (Ir, Pd, Pt, Ru) or at alloy 600 (a nickel–chromium–iron alloy) has been studied in dependence on temperature [148–151]. The temperature dependence of self-assembled monolayers (SAMs) also was subject of interest [152, 153]. SAMs are examples of well-organised, highly ordered surface layers. Linear molecules are immobilised by an anchoring group (frequently a group containing a disulphide bond), which coordinates with the electrode surface, in most cases a gold surface. This way, linear molecules are arranged perpendicular to the surface, forming some kind of a dense "brush". Transport properties, heat conduction and other characteristics are of high

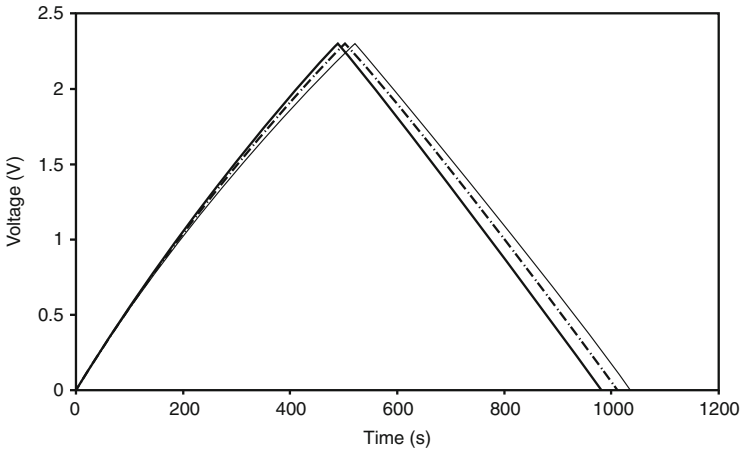

Fig. 3.3 Charge/discharge curves for a commercial 10 F capacitor; 0.032 A; 15 °C (*solid line*); 25 °C (*dashed line*); 40 °C (*dotted line*). From [144], with permission

interest for practical application of SAMs. In a perfect SAM, the underlying metal surface is nearly completely "masked". Thermoelectrochemistry is useful for determining SAM parameters. Formation of foreign layers on substrates has been studied by classical thermoelectrochemistry in open cells [154–157]. Examples are TiO_2 in photoelectrochemical cells (PECs) [154], electrodeposition of CoWP films [155] and deposition of metals on silicon substrates [156] and of zinc oxide layers on SnO_2 semiconductor films [157]. Protein membranes and immobilised enzyme layers have been studied [158, 159]. Finally, there is an example where the temperature dependence of the ionic transport across the boundary between immiscible liquids has been subject of thermoelectrochemical studies [160].

Analytical applications often play a role in electrochemical experiments with temperature variation [161–168]. Beginning already in 1930, pH sensors with higher temperature stability were looked for [161–163]. In a structural analysis of complex compounds, thermoelectrochemistry provided valuable results concerning thermodynamic constants as well as the presence of different isomers [164]. Phase transitions in adenine layers adsorbed at mercury have been found also by electrochemical experiments with T variation [165]. T variation also has been applied to improve peak separation of overlapping electroanalytical signals, e.g., in the determination of dopamine in presence of uric acid and of ascorbic acid [166]. This principle later proved highly successful with heated electrodes. In many papers, however, just improvement of existing analytical procedures was of interest, e.g. sulphide determination at preoxidised nickel electrodes [167] or the sensitivity of modified electrodes [168].

Electrochemical investigation of biomolecules preferably is done in aqueous solution and with a moderate temperature variation. Also, biosensors are run under those conditions. Nevertheless, there are not many classical thermoelectrochemical publications on these subjects. Electrochemical sensors, which allow identification of individual DNA became substantial part of research with heated electrodes and microthermostats. In [169], some research was done in open cells. The hybridisation process (the process when the complete DNA double strand is formed by combination of two perfectly fitting single strands) is one way to identify an individual DNA molecule, consequently, to detect traces of a single individual. A hybridisation sensor is made by immobilising an oligonucleotide, i.e. a characteristic section of a natural DNA single strand at the sensor surface. If this sensor will meet the fitting opposite strand, a hybrid is formed, i.e. a section of the double strand. Successful hybridisation means successful detection of an individual molecule. It is essential to find a method which will indicate that the studied actual hybridisation action was successful. Different electrochemical methods are useful for this purpose. Temperature plays a crucial role in hybridisation detection, since characteristic temperature values are necessary for the process of denaturation (splitting double strand into single strands), as well as for the opposite process of hybridisation. The necessary extensive thermostatting can be done rather elegant by means of heated electrodes or micro thermostats, but there are also some classic experiments. In [169], capacitance change of an immobilised oligonucleotide layer

is used to detect hybridisation. Electrochemical impedance spectroscopy was utilised to obtain further information.

Redox active biomolecules have been studied by open cell thermoelectrochemistry. By potentiometry of cytochrome C at a gold electrode, thermodynamic quantities like ΔG have been identified [170]. Important thermodynamic constants, among them the entropic term of the redox processes in an immobilised myoglobin layer, have been determined in a similar way [171].

Energy conversion has been always a preferred application of thermoelectrochemical methods. PECs work with semiconductor films in contact with reversible redox couples. Intense sunlight illumination generates free charge carriers and induces a cell voltage. In [172], temperature increase enhances the usable current at a tungsten selenide electrode in contact with iodine/iodide solution.

Thermocells (see Chap. 2 and Fig. 3.4) are the primary means to convert chemical into electric energy. The principle was demonstrated in [173], where electrodes of doped nanotubes in contact with aqueous ferri/ferrocyanide solution are used to obtain a utilisable cell voltage by imposing a temperature difference between both equal electrodes. Instead of classic solvents, in [174] a eutectic melt

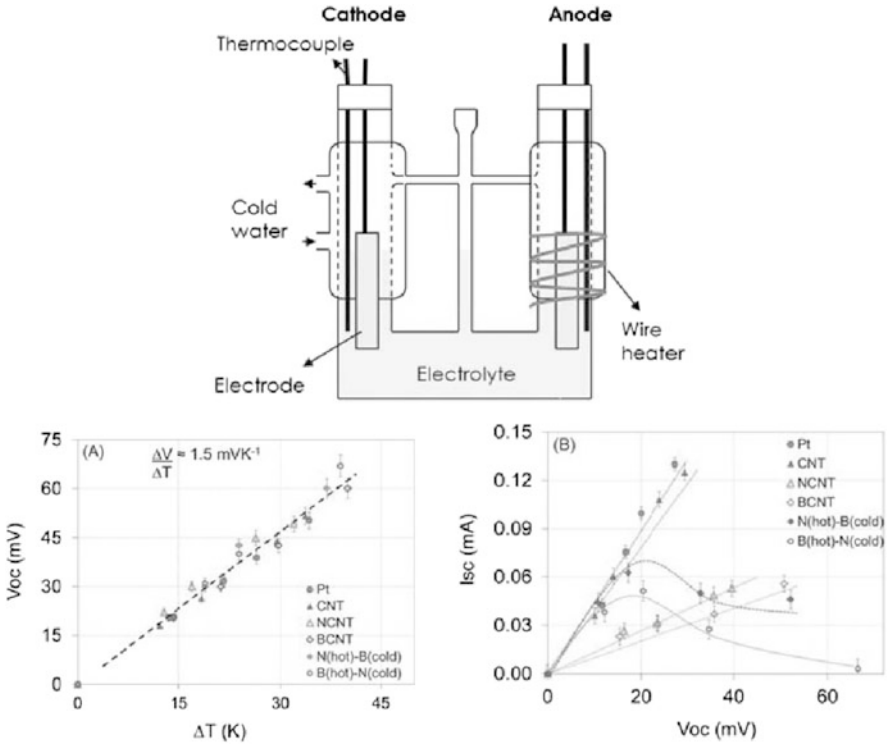

Fig. 3.4 *Top*: Scheme of a typical thermocell. *Bottom left*: Open circuit potential of $Fe(CN)_6^{3+}/Fe(CN)_6^{4+}$. *Bottom right*: Short circuit current. From [173], with permission

of LiCl, KCl and RuCl was used as electrolyte. The system Li(Fe)-FeS_2 was used as working electrode.

Alternatively to the energy conversion methods mentioned above, thermo-electrochemical methods are used where chemical substances like hydrogen or carbonaceous fuels are generated by temperature enhanced electrolysis. Among them, the so-called S.T.E.P. process combines photovoltaics, utilisation of waste energy and electrochemistry [175, 176]. The idea behind this process is that light alone would not be sufficient to raise energy for water electrolysis but additional heating by solar IR will bring about it (Fig. 3.5).

An uncommon, rather new technique where temperature affects electrochemical processes is DEMS (differential electrochemical mass spectrometry) [100, 177–180]. In this method, tiny amounts of organic substances, e.g., in adsorption films, are desorbed and/or oxidised and the volatile reaction products are determined by mass spectrometry. This technique is useful to detect organic substances adsorbed at the metal–electrolyte interface. In a thin-layer cell, adsorbed molecules are desorbed by potential variation. The desorbed material diffuses through a porous PTFE membrane and is detected by mass spectrometry. Besides potential, also temperature variation influences the desorption process. This way, temperature dependence of adsorption at single crystal platinum surfaces has been studied [178]. Other DEMS experiments have been done under pressure in autoclave cells [179, 180].

Methods, where the temperature is intentionally varied during an electrochemical experiment, can be seen as an analogue of spectroelectrochemistry, where the illumination of an electrode by light or other radiation is varied. In situ

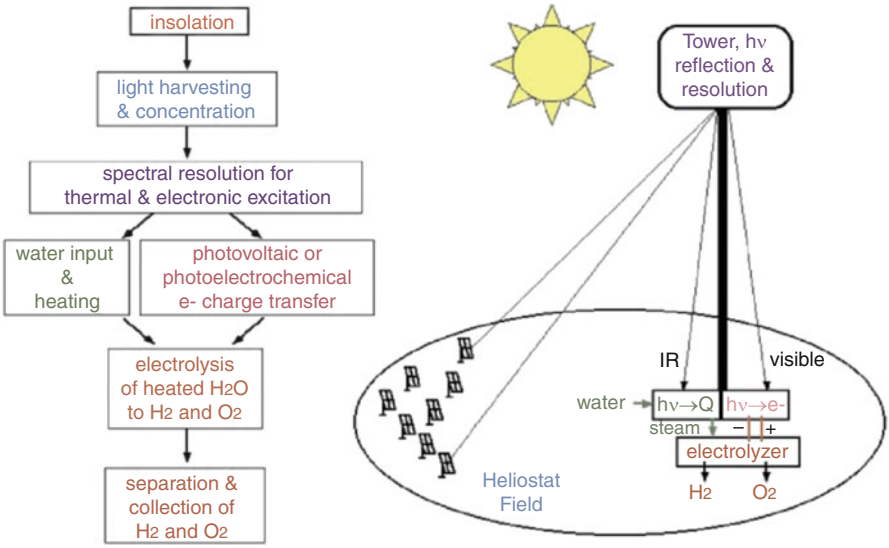

Fig. 3.5 Solar water electrolysis improvement through excess solar heat utilisation via thermal electrochemical hybrid H_2 generation (STEP). From [175], with permission

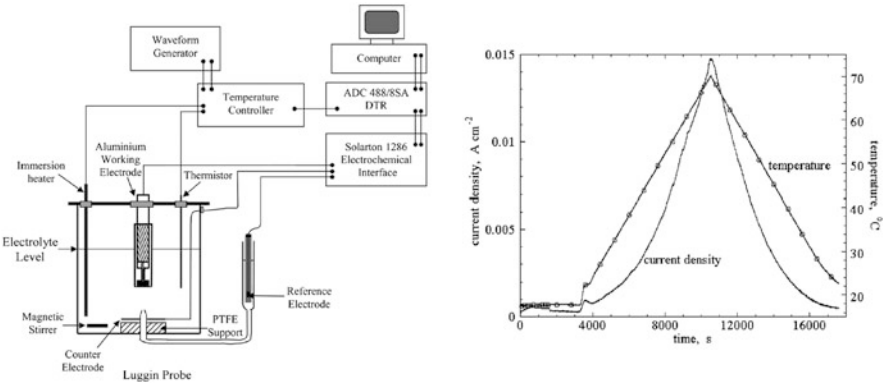

Fig. 3.6 *Left*: Experimental set-up for cyclic thermammetry. *Right*: Cyclic thermammetry of aluminium in 0.3 M HNO_3, temperature scan rate 7 mK s^{-1}, potential 0.00 V (SCE). From [182], with permission

temperature variation can be made easily by means of electrode heating. Executing such variation in isothermal cells or half-cells, however, requires elaborate equipment [181]. Nevertheless, in a method named "thermammetry", the idea has been realised. A current is passing through an electrode interface and measured as a function of an imposed temperature programme whilst the electrode is held at a constant potential. Using a thermal programme in which the temperature is ramped linearly to a maximum value and then reversed to give a linear cooling ramp again is called "cyclic thermammetry". Equipment and some results are given in Fig. 3.6. The pitting corrosion of aluminium in nitric acid solution has been investigated [182].

3.2 High-Temperature Electrochemistry: Electrochemistry in Subcritical and Supercritical Fluids

High-temperature electrochemistry is a well-defined, independent branch of thermoelectrochemistry, although, on the other hand, the term "high temperature" in this context is not really well defined. It is, however, generally accepted that, as a rule, values above 100 °C mean *high temperature* in electrochemistry. There is practical interest in electrochemical processes at increased temperature, as outlined in two reviews on the subject [183, 184].

3.2.1 *Open High-Temperature Cells*

Defining temperature values above 100 °C as "high temperature" means that many non-classical arrangements like cells with solid electrolyte and gaseous reactants belong to the group of high-temperature cells. Among them are the SOFC mentioned already [133–143]. The latter do not fit perfectly into the classification scheme used below. It is tried, in following, to distinguish *open cells*, working at ambient pressure, from *pressurised* (*autoclaved*) cells. In the case of fuel cells, not always both compartments of the cell must be under increased pressure. Cells using atmospheric oxygen, e.g., have a compartment working with ambient pressure. Similar considerations are valid for electrochemical gas sensors on the basis of solid electrolytes, which preferably consist of solid conducting oxides like the dioxides of tin, zirconium or titanium, respectively [185–190]. Such sensors cannot be classified clearly to be either pressurised or non pressurised cells. This is becoming obvious when the well-known Lambda sensor is considered (Fig. 3.7). This sensor was designed to analyse hot gas mixtures containing oxygen, e.g. the exhaust gas of combustion engines like Otto or Diesel motors. The result of this analysis can be used to modify the working parameters of the motor in such a way that the combustion process of the fuel is made as efficient as possible. In modern cars, the Lambda Sensor can be found at two places, namely, at the motor exhaust pipe, also behind the catalytic converter used to oxidise fuel residues as well as carbon monoxide from incomplete combustion. Such sensors normally are concentration cells with two compartments, each in contact with a gas atmosphere, one of them with known analyte content, the second one with unknown content. The analytical signal in most cases is potentiometric, i.e. the voltage between both compartments is measured and evaluated following the Nernst equation. Alternatively, typically in miniaturised cells, an external voltage is applied and the electrolytic current is determined as an expression of concentration difference (voltammetric or coulometric processing, respectively).

Further important application examples of electrochemical sensors with solid oxide electrolyte are analysis of CO_2 and SO_2 [186], of reducing vapours [187] and of nitrogen oxides [188–190].

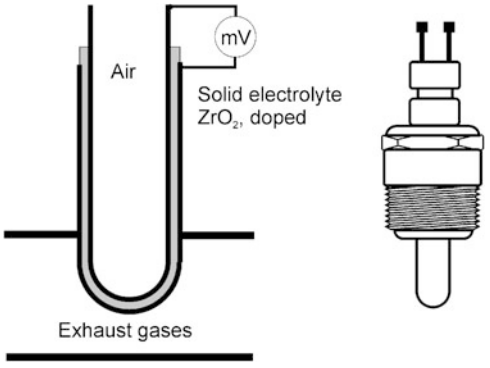

Fig. 3.7 Lambda sensor designed to control the catalytic converter of combustion engines. From [185], p. 157, with permission

High temperature can be achieved in open cells, if the solvent used has a higher boiling point than water [191–196]. Most popular for that purpose was polyethylene oxide as a solvent, a polymer with properties of a liquid or a low-melting solid, depending on its molecular weight [191]. Electrochemical studies have been made at enhanced temperatures in pure phosphoric acid [192] as well as in 85 % acid solution [193, 194]. Highly concentrated aqueous salt solutions, preferably with alkaline earth halides, were also used for high-temperature electrochemical investigations [195, 196]. A medium for high-temperature experiments used in the early days of electrochemistry are classical molten salt mixtures. Beginning with Humphry Davy's successful deposition of alkali metal elements, salt melts have found numerous applications, preferably in technical electrochemistry. Recent studies concern with electrochemical deposition of thin semiconducting [197, 198] or protecting [199, 200] layers. By deposition in such media, much better morphology of the layers can often be achieved than in common solvents. In many papers, the determination of redox potentials in molten salt media has been described (see, e.g. [201, 202]). In fuel cell research, molten salts also play a role [203].

During the last years, electrochemistry in ionic liquids became more and more interesting. Such liquids have properties similar to those of high-temperature molten salts, but they can be handled much more convenient. Ionic liquids are characterised by extremely low vapour pressure and can be used thereby in open cells without problems. In many cases, they are stable at increased temperatures but nearly no thermoelectrochemical studies in IL are reported up till now. An interesting example is a high-temperature electrochemical scanning tunnelling microscope [204] suited for room-temperature ionic liquids as well as for high-temperature salt melts (Fig. 3.8).

3.2.2 Autoclave Cells

As mentioned in aforegoing Chapter, classical high-temperature electrochemical experiments in open cells can be done only up to the boiling point of electrolyte solution. Later, this restriction has been overcome by modern thermoelectrochemical methods, where short electrolysis time periods are used to make point-by-point measurements to build voltammograms and other curves. The time intervals used for electrolysis must be short enough to avoid solution boiling. Such measurements can be performed only by heating of microelectrodes, as will be described further down. Alternatively, in classical thermoelectrochemistry, the temperature restriction was overcome by application of increased pressure, i.e. measurement in closed, autoclaved electrolysis cells. Such measurements are nothing else than a simple extension of work in open cells, towards higher temperature. Isothermal cells as well as isothermal half-cells have been utilised.

Increased pressure allows working at higher temperature, but this is not the only potential of autoclave cells. A second motivation for higher pressure applications is

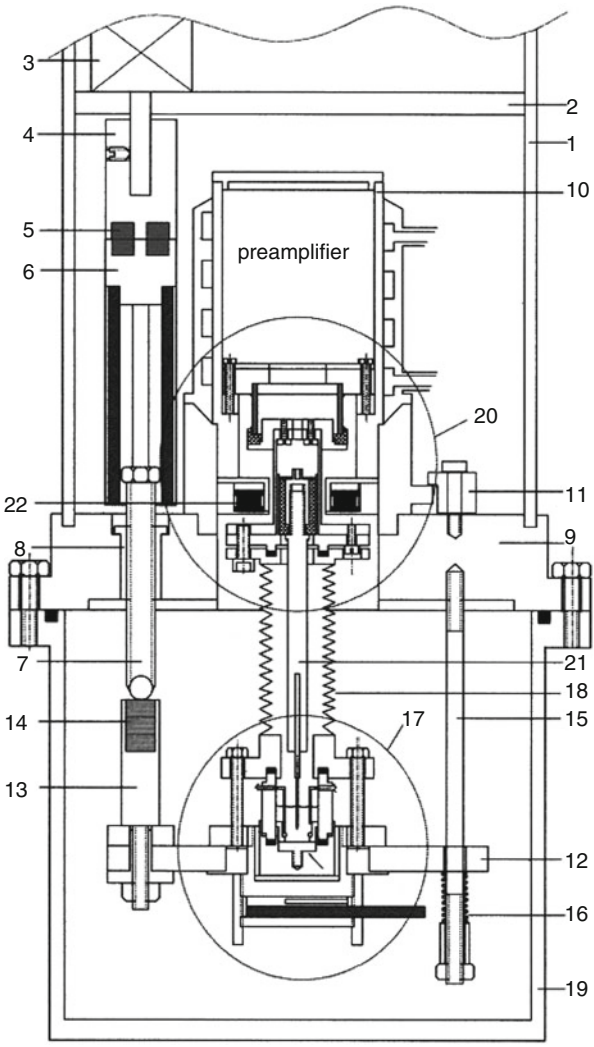

Fig. 3.8 High temperature electrochemical scanning tunnelling microscope. (1) aluminium cylinder, (2) upper aluminium plate, (3) step motor, (4) coupling, (5) NdFeB magnets, (6) connecting leg, (7) micrometere screw, (8) counterthread fixed into main plate (9), (10) scanner housing, (11) screw with fixing leg, (12) quartz sample plate, (13) leg from stainless steel, (14) SmCo magnets, (15) guiding rod, (16) spring, (17) electrochemical cell, (18) bellow, (19) chamber, (20) scanner, (21) tip holder, (22) Peltier cooling. From [204], with permission

the use of solvents which do not exist at atmospheric pressure, e.g. gases that have to be liquefied by pressure or even supercritical gases. An alternative terminology for this case is *subcritical* electrochemistry (electrochemistry below critical temperature, in a liquid/vapour two-phase system under increased pressure) or *supercritical* electrochemistry (working above critical temperature in a one-phase gaseous system with high density, enforced by high pressure).

Summarising these points, only a part of *high-pressure* electrochemistry belongs to *high-temperature* electrochemistry. Supercritical electrochemistry in gases with low critical temperature like carbon dioxide or sulphur dioxide, however, is not

done at higher temperatures, since pressure is merely applied to convert gases into solvents useful for electrochemistry.

Systematic and detailed investigations of electrochemistry in autoclaves started in the 1970s. Pioneering work has been done by the groups of D. D. Macdonald [205–222] and of A. J. Bard [223–231]. Subcritical experiments in water [213–215, 217, 222, 225, 235] as well as in non-aqueous solvents are not different from ordinary electrochemical studies in open cells.

An important motivation to do electrochemical studies in pressurised aqueous solutions was caused by the need to analyse solutions in nuclear reactors, where high pressure is common [208, 211, 215, 232–234]. Also, geothermal brines were interesting subjects. Many papers deal with corrosion of construction materials and electrode compositions exposed to high pressure and high temperature [215, 221, 234–245]. Related processes were the anodic oxidation of gold [240] and the passivation of metals like zirconium [222]. Non-aqueous-pressurised solutions are investigated, since lithium batteries became important due to their applications [246, 247]. Other innovative batteries, like the Na–Ni battery [248], also fuel cell types [249] have been studied, since they are running under increased pressure.

Prominent example of chemical analysis under high pressure and high temperature is pH measurement. The well-known glass electrode has been adapted for such conditions [213], but full solid state arrangements with ceramic and oxidic materials attracted more interest [207, 208, 210, 214, 237]. High-pressure, high-temperature determination of sulphides and hydrogen sulphide [250, 251] seems to be interesting, since such conditions exist in deep sea near the so-called hot spots (underwater volcanoes).

Reference electrodes constructed similar to high-pressure pH sensors have been proposed, among them internal [209, 252–254] as well as external types [205, 255]. Cell design [257–260] suited for extreme conditions has been given, especially a wall-tube cell [259] (Fig. 3.9).

With aqueous solutions in pressurised cells, the temperature can be varied in a very broad range. Many fundamental electrochemical data have been obtained in this medium. Thermodynamic quantities such as activity coefficients of ions [252], equilibrium double-layer capacity [261], zeta potential of metals [233], potential-pH diagrams [206] or properties of the palladium–hydrogen electrode were determined [262]. Exotic systems, e.g. the "solvation" of rare earth atoms in liquid gallium [234], have been studied. Main research interests in subcritical aqueous solution were focused on the kinetics, reaction mechanism and transport properties.

Many processes of practical interest are kinetically controlled and strongly affected by temperature. Anodic oxidation of organic substances has been investigated like the reaction of benzene at a lead dioxide electrode [225], of methanol at Pt alloy electrodes [263] and the degradation of organic pollutants [265]. Fixation of carbon dioxide is a process of eminent importance, since excess electric energy from wind power stations can be used to generate liquid fuels by reducing CO_2. An electrochemical variant of this process has been done in high-pressure cells [264].

Energy conversion as well as energy storage under participation of electrochemical processes has been mentioned [175, 176]. Such methods are not restricted to open cells. In autoclave cells, promising procedures have been performed where hydrogen is generated electrolytically at high temperature [266, 267].

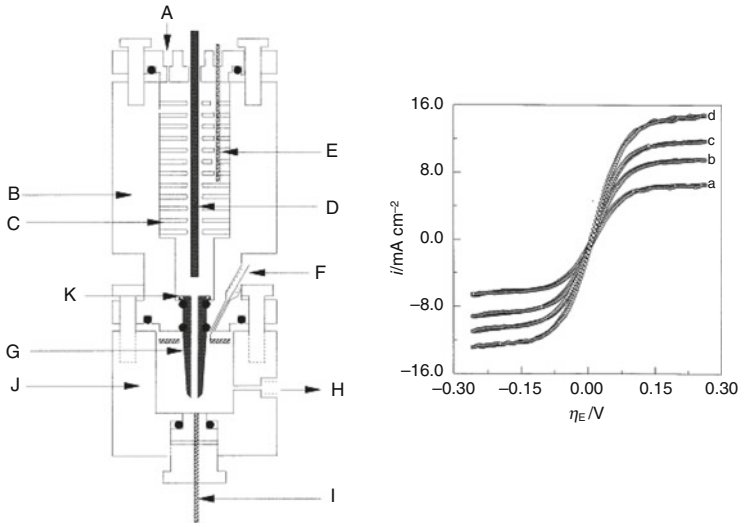

Fig. 3.9 *Left*: High-temperature–high-pressure electrochemical wall-tube cell: (A) inlet, (B) pre-cell, (C) mixing dishes, (D) platinum resistor, (E) reference electrode, (F) counter electrode, (G) zircaloy nozzle, (H) outlet, (I) working electrode, (J) cell and (K) zircaloy rings. *Right*: Typical voltammograms in Fe^{3+}/Fe^{2+} 1 mM in 0.2 M Na_2SO_4 (pH 1.5) on a platinum electrode at 85 °C. Sweep rate 50 mV s^{-1}, H: 0.264 cm, d: 0.204 cm and $r_e = 0.05$ cm. Flow rates: (a) 4, (b) 8, (c) 12 and (d) 20 cm^3 min^{-1}. From [259], with permission

Elementary processes of water electrolysis at mercury [268–271] and at platinum [272] electrodes have also been studied in autoclaved aqueous solution. Diffusion coefficients [235, 236] and transfer coefficients [273] have been determined in pressurised aqueous medium. The influence of the phenomenon of thermodiffusion (Soret effect) was followed [217]. This effect generally plays a role if regions of different temperature inside a homogeneous electrolyte phase occur. This is not typical for isothermal systems considered here. In non-isothermal cells (see later below), it should be taken into account.

3.2.3 *Electrochemistry in Supercritical Fluids*

As mentioned above, electrochemistry in supercritical fluids [210–212, 216, 218–221, 223, 224, 226–231, 239–241, 262, 274–285] not generally means high-temperature electrochemistry. It depends on the critical temperature, which might be lower than room temperature for many gases. Critical temperature is an inherent constituent of the critical point of materials. Thus, the quantity temperature has to be considered carefully; consequently, the subject can be considered to belong to the field of thermoelectrochemistry. Anyway, working with supercritical fluids is one of the most amazing and promising new fields of current chemistry. In many applications of practical interest, supercritical gases like carbon dioxide proved to

be useful, e.g. for extraction procedures, in supercritical chromatography. As a consequence, such fluids are interesting for electrochemists as well [227, 229–231, 239–241, 262, 274–285], e.g. to design electrochemical detectors. Generally, the widely unknown redox chemistry in such fluids has been worthwhile to be investigated. Even if there is no drastic change of properties when going from liquid to gaseous phase, it was amazing to see that gases can function as solvents. With acetonitrile, the passage from liquid to supercritical electrochemistry is easy [229, 230]. Voltammograms of organic compounds in both phases do not differ markedly. Fluorocarbons like difluoromethane or tetrafluoroethane are quite interesting to be studied by supercritical electrochemistry [276, 278, 280, 282–285]. Their critical temperature is generally low and they can be handled easily. The electrochemical window can be very broad, e.g. 9 V with 1,1,1,2-tetrafluoroethane [276], as seen in Fig. 3.10. Exotic reactions like oxidation of xenon and of cesium ion are reported there as well. A non-classical solvent for electrochemical experiments is supercritical carbon dioxide [275, 277, 279] in which hydrophobic electrolytes can be dissolved to give conducting media. Electrochemical studies have been done also in supercritical ammonia [231] and in supercritical sulphur dioxide [227]. In supercritical mixtures of carbon dioxide with classical solvents like methanol [274], extremely powerful chemical reaction paths become available. In carbon dioxide/tetrafluoroethylene, the electrochemical reduction of CO_2 results in oxalate [281].

The supercritical state of water is the most extreme one of common solvents. Its critical temperature T_C is 374 °C and the critical pressure is 22,059 MPa. The properties of liquid and supercritical fluid states are quite different. Supercritical water, e.g., is less polar than liquid water and a solvent for hydrophobic substances. It can be expected that electrochemistry in supercritical water would provide useful information about natural hydrothermal processes, e.g. oxide formation [218]. The majority of research papers, however, were focused on analytical investigations, preferably potentiometric pH measurement [210–212, 216, 219, 220, 253]. The chemistry of different redox couples has been studied as well [223, 224, 226,

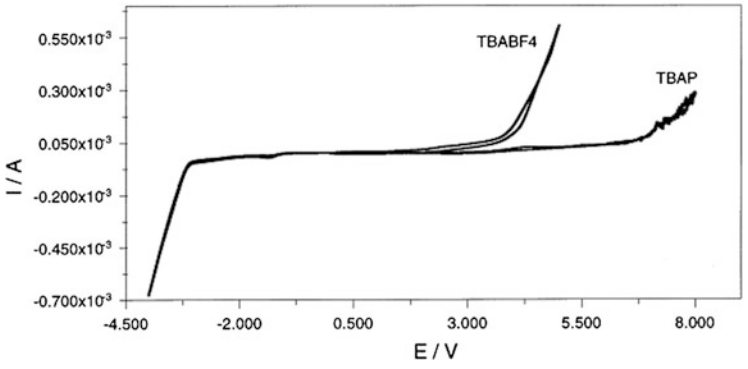

Fig. 3.10 Voltammograms of supercritical tetrafluoroethane with two supporting electrolytes. Conditions:temperature 25 °C, pressure 10 bar. Platinum electrode. Sweep rate 100 mV s^{-1}. From [276], with permission

228]. Corrosion also was a subject of investigation [221] with respect to nuclear power plants.

3.3 Sonoelectrochemistry

In sonoelectrochemistry, electrodes are exposed to strong ultrasound. An ultrasound transducer (so-called *ultrasonic horn*) is introduced, preferably opposite to the electrode. There are also proposals where the electrode itself acts as ultrasonic transducer, a *sonoelectrode*. Sonoelectrochemistry is not a part of thermoelectrochemistry, but temperature effects make up a big part of the actions caused in a sonicated cell. Thereby, the subject may be considered to be some kind of an interlink on the way to modern thermoelectrochemistry. Some arrangements and results are depicted in Fig. 3.11.

By means of power ultrasound, typically in the frequency region between 20 and 100 kHz, energy is pumped into an electrochemical cell. This high density energy causes extensive effects. Most of them are connected to the phenomenon of *cavitation*. Cavitation means formation of vacuum bubbles inside the solution caused by fast movement of the ultrasonic transducer. When the bubbles collapse, local temperature can be drastically increased; even exotic states of matter may be generated like gas plasma. As a result, transport processes are strongly enhanced, the electrode surface is cleaned and activated continuously, high-energy

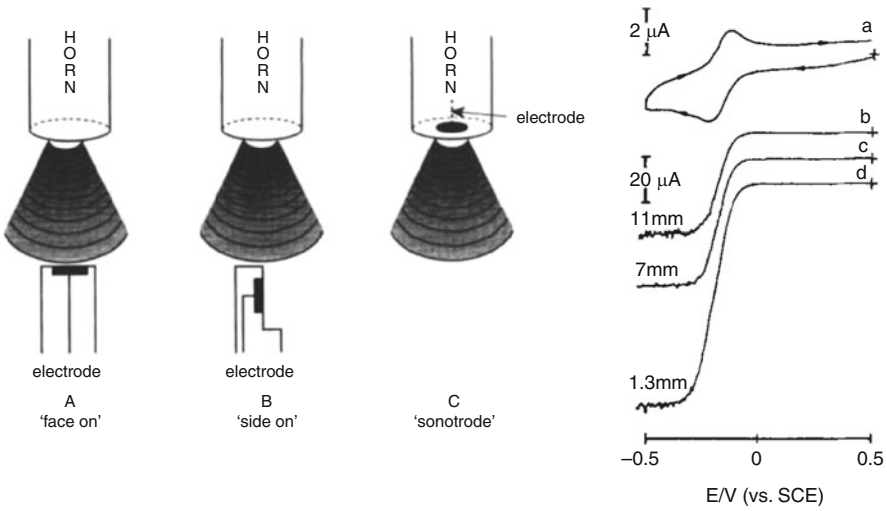

Fig. 3.11 *Left*: Three types of electrode geometries in sonoelectrochemistry. *Right*: Voltammograms for the reduction of 0.23 mM $Ru(NH_3)^{3+}$ in aqueous 0.1 M KC1 obtained at 22 °C using a 2 mm diameter Pt electrode under (a) silent conditions (scan rate 50 mV s^{-1}), (b–d) in the presence of ultrasound (scan rate 20 mV s^{-1}, 20 kHz, 30 W cm^{-1}). From [291], with permission

intermediates like radicals are formed by cavitation and reaction rate as well as the reaction pathway is mediated [288]. In sonicated cells, it cannot be distinguished clearly between mechanical and thermal effects.

In organic synthesis, sonication has a long tradition. Ultrasound in electrochemistry has been introduced as a means to enhance convection in coulometric cells [286, 287]. Most important application became Anal Chem [288, 289]. Very popular was electrochemical stripping analysis [290], since in this case the action of ultrasound can be restricted to the electrochemical trace accumulation, where no interaction between power sound and sensitive signal measurement has to be suspected.

The complex ultrasound effects in electrochemical cells have been discussed in some more fundamental publications [291–295].

Prominent applications of sonoelectrochemistry are electroplating [296], since very smooth layers have been generated this way, furthermore production of nanomaterials, nanoparticles and very fine metallic powders [297–299]. Among the latest achievements was sonoelectrochemical generation of quantum dots [300].

Interesting results have been achieved with electropolymerisation, preferably for conducting polymer layers [301–303].

Waste degradation is an important field of sonochemistry. It has been combined with electrochemical processes [304].

Electrodes in sonicated cells have to withstand very harsh conditions. It is no wonder that boron-doped diamond electrodes found broad application [289, 305].

Sonoelectrochemistry has provided valuable information about processes at locally heated places close to electrode surface. On the other hand, it is not easy to distinguish between mechanical attack and thermal effects. Consequently, theoretical description is not perfect till now. Heated electrodes could provide more precise information about phenomena at very hot electrode surfaces, since, in principle, a strongly heated electrode tip or electrode wire might be made a model of a cavity with an inbuilt electrochemical probe.

3.4 Electrochemical Calorimetry

A very important chapter of thermoelectrochemistry is electrochemical calorimetry. Here, clearly the quantity temperature is considered to be an independent variable. In calorimetry, temperature is not varied or imposed arbitrarily to excite or affect electrochemical reactions, but spontaneous temperature changes are recorded in the course of a reaction. The reason is to follow the heat transport processes in an electrochemical cell. A well-defined theoretical fundament on thermodynamic basis exists since the 1960s [306–308].

Traditional electrochemical calorimetry does not differ markedly from other kinds of traditional chemical calorimetric methods. The electrochemical cell is put into calorimetric bombs or thermally isolated containers, respectively [309–312]. With a cell containing two compartments of identical composition, the

reversible heat of a reaction ($T \cdot \Delta_R S$) has been determined under isothermal conditions [310]. Later, many similar arrangements have been used, e.g. [104, 311]. More recently, complete commercial batteries, e.g. lithium cells, have been studied to test the thermal behaviour under practical conditions. The modern technique of accelerated rate calorimetry has been utilised frequently [312]. Composition of electrodes, especially of the $LiFePO_4$ anode, is a very important question in the development of lithium batteries. Interest in thermal behaviour of such electrodes has brought about a large number of papers dealing with calorimetry. The vast majority of investigations have been done with commercial calorimetric equipment. Commercial button cells often have been studied in microcalorimeters [313]. Generally, microcalorimeters are of growing interest [314–318]. Microcalorimeters allow a more dynamic work but nevertheless they keep in the frame of classical thermoelectrochemistry.

The interest in modern chemical energy sources is representing in a growing number of papers, where the internal processes in batteries are modelled and the theoretical models are compared with experimental calorimetric results [319–324]. Models have been established also for thermal behaviour of fuel cells, e.g. the PEMFC [131]. Large capacity "electrochemical capacitors" also were subject of modelling [325]. With modern electrode materials, there is not a clear distinction between pure physical capacitive charging and electrochemical energy storage. Thus, capacitors including intercalation processes at the electrodes in many cases can be considered to be electrochemical cells as well.

Often, the term "calorimetric" appears in papers dealing with solid state materials used to compose battery electrodes. A frequently applied analytical method is differential scan calorimetry. This method belongs to the arsenal of thermal analysis. It is similar to differential thermal analysis. Such techniques are useful to characterise solid state materials, but they are not electrochemical.

The work discussed till this point belongs to classical thermoelectrochemistry. A very important step is done, however, when in situ calorimetric methods are considered. In situ calorimetry means, that temperature changes are recorded in the course of a reaction, as close as possible to the investigated electrode surface. If the thermal inertness of the temperature sensor is low, fast changes can be followed, and temperature can be recorded as a time function. Methods with such characteristics can be considered to be methods of modern thermoelectrochemistry.

The origin of in situ electrochemical calorimetry dates back to the middle of last century [326–328]. Already in first papers, temperature changes at single electrodes have been measured preferably by means of semiconductor thermistors. This remained the most popular technology till today [326–342]. Oxidic semiconductor thermistors are robust and can be isolated easily by covering with thin layers of glass and similar materials. They endure high temperatures, generally up to the melting point of their contact leads. Their high temperature sensitivity allows the measurement of tiny temperature differences. A close contact between the electrode and the thermistor is very important. Commercially available thermistor probes in the form of small bulbs were protected by an insulating layer, and the working electrode wire was wound around the thermistor [331, 332]. Also, graphite hollow

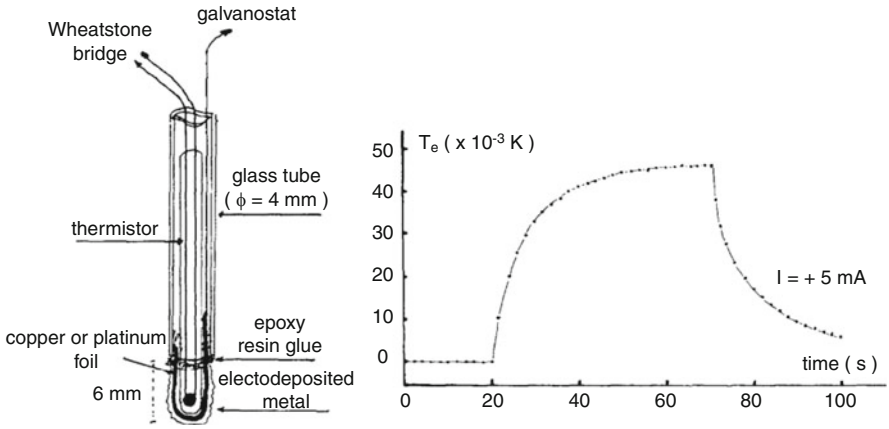

Fig. 3.12 *Left*: Thermistor electrode. *Right*: Temperature change at the electrode for copper oxidation with 5 mA anodic current. From [338], with permission

cylinders in close contact to a thermistor have been used [333, 334]. Heat exchange of reactions of adhering solid crystals were determined by such arrangements. Thermistor probes covered by thick electrode layers of copper [335, 336], silver [337] or platinum [338] proved also to be useful (Fig. 3.12). A similar solution is thermistors glued to platinum foils [339, 340]. Flat thermistor structures with metallic foil back [329] as well as thick-film technology-made structures have been covered by platinised platinum to form calorimetric devices [341, 342]. They allowed the determination of the adsorption heat of hydrogen and oxygen at platinum surfaces. Instead of thermistors, pyroelectric foils carrying electrode layers have been used for calorimetry in situ [343–347]. Such foils are made of polyvinylidene difluoride (PVDF). In the course of their fabrication, the foils are exposed to a special mechanical treatment in a strong electric field. This way, a polar material is formed, which transforms thermal effects into electric signals. Low heat capacity of such structures is useful if fast temperature changes have to be followed. Layers of nickel [343] and of platinum [344, 345] have been studied, and the heat exchange even of a submonolayer conversion [346] has been determined. Reversible and irreversible heat partitions could be separated this way [347]. A typical arrangement is depicted in Fig. 3.13. An interesting approach in electrochemical calorimetry was application of "acoustic thermometry" [348]. A very thin electrode can be excited to emit acoustic waves if an AC electrolysis current generates sine wave heating at the electrode surface.

In situ electrochemical calorimetry generally makes use of thermometers which are closely connected with the electrode surface studied. This way, single electrode properties can be determined. Cells with electrode-thermometer units are non-isothermal cells where temperature differences between working and reference electrodes are encountered. Their thermal behaviour is similar to that of cells with electrodes which are heated by external devices. Consequently, all the effects characteristic for non-isothermal cells (e.g. the Soret effect) have to be considered.

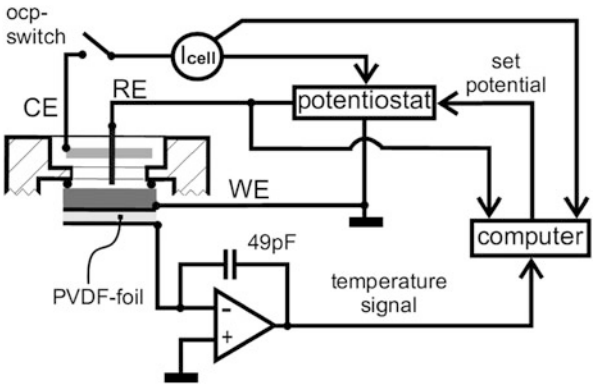

Fig. 3.13 Electronic circuit of an in situ calorimetric cell on the basis of metallised PVDF foil. The pyroelectric signal is collected at the backside of the metallised PVDF foil, referenced to the WE. The electrochemical cell current I_{cell} is measured at the CE. The cell can be electrically switched off by the computer-controlled ocp-switch. *RE* reference electrode, *CE* counter electrode. From [316], with permission

In most cases, the temperature differences generated by electrolysis are low and their influence can be neglected.

3.5 Miscellaneous

There are some miscellaneous thermoelectrochemical applications which cannot be classified to fit in one of the subchapters above. Some examples will be discussed here.

In [349], with a special kind of organic electronics, an irreversible electrochemical process is utilised to record the "temperature history" of packages or containers which might contain goods that perish if exposed to higher temperature. The printed circuit made of organic electronic materials is covered by an electrolyte layer consisting of polyethylene glycol with LiF_3CSO_3. Ionic conductivity of the electrolyte depends on temperature and controls the reaction rate of an electrochemical reaction, in this case an overoxidation of the conducting polymer PEDOT. The propagating overoxidation front can be determined by conductivity changes. This way, a picture of the "temperature history" is obtained. Large numbers of such devices can be manufactured since the technology is cheap enough to be used for temperature supervision of ordinary packages.

References

1. Cavalleri O, Kind H, Bittner AM, Kern K (1998) Langmuir 14:7292–7297
2. Nikolic ND, Pavlovic LJ, Pavlovic MG, Popov KI (2007) J Serbian Chem Soc 72:1369–1381

3. Yu JX, Wang L, Su L, Ai XP, Yang HX (2003) J Electrochem Soc 150:C19–C23
4. Goux A, Pauporte T, Chivot J, Lincot D (2005) Electrochim Acta 50:2239–2248
5. Zhang QB, Hua YX, Dong TG, Zhou DG (2009) J Appl Electrochem 39:1207–1216
6. Abou-Krisha MM, Assaf FH, El-Naby SA (2009) J Solid State Electrochem 13:879–885
7. Saitou M, Oshiro S, Hossain SMA (2008) J Appl Electrochem 38:309–313
8. Salvador BR, Jilberto PF, Marcelo JL, Jacqueline CS, Rodrigo EA (2008) J Chil Chem Soc 53:1429–1432
9. Garcia-Torres J, Valles E, Gomez E (2010) Electrochim Acta 55:5760–5767
10. Mendoza-Huizar LH, Rios-Reyes CH (2012) J Solid State Electrochem 16:2899–2906
11. Koh JL, Teh LK, Romanato F, Wong CC (2007) J Electrochem Soc 154:D300–D303
12. Aerts T, De Graeve I, Terryn H (2009) Electrochem Commun 11:2292–2295
13. Gabrielli C, Keddam M, Maurin G, Perrot H, Rosset R, Zidoune M (1996) J Electroanal Chem 412:189–193
14. Liu G, Tang ZY, Xu Q, Li CS (2008) J Inorg Mater 23:291–294
15. Khudolozhkin VO, Avchenko OV, Aleksandrov IA, Kuchma AS (2002) Geochem Int 40: 1013–1020
16. Fu JL, Gao DQ, Xu Y, Xue D (2008) Electrochim Acta 53:5464–5468
17. Lukaszewski M, Hubkowska K, Czerwinski A (2011) J Electroanal Chem 651:131–142
18. Park G, Gunawardhana N, Nakamura H, Lee YS, Yoshio M (2012) J Power Sourc 199: 293–299
19. Santos JS, Matos R, Trivinho-Strixino F, Pereira EC (2007) Electrochim Acta 53:644–649
20. Schmidt TJ, Ross PN, Markovic NM (2001) J Phys Chem B 105:12082–12086
21. Prado C, Wilkins SJ, Gründler P, Marken F, Compton RG (2003) Electroanalysis 15: 1011–1016
22. Musameh MM, Kachoosangi RT, Compton RG (2008) Analyst 133:133–138
23. El Abedin SZ, Saad AY, Farag HK, Borisenko N, Liu QX, Endres F (2007) Electrochim Acta 52:2746–2754
24. Kondo H, Matsumiya M, Tsunashima K, Kodama S (2012) Electrochim Acta 66:313–319
25. Cifuentes L, Casas JM, Simpson J (2008) Chem Eng Sci 63:1117–1130
26. Aaboubi O, Housni A (2012) J Electroanal Chem 677:63–68
27. Hwang SS, Kim JS (2002) Corrosion 58:392–398
28. Galal A, Atta NF, Al-Hassan MHS (2005) Mater Chem Phys 89:28–37
29. Li DG, Zhou GS (2008) Acta Chim Sin 66:617–620
30. Nie XH, Li XG, Du CW, Cheng YF (2009) J Appl Electrochem 39:277–282
31. Shiratori K, Nobusada K (2008) J Phys Chem A 112:10681–10688
32. Smets N, Van Damme S, De Wilde D, Weyns G, Deconinck J (2008) J Appl Electrochem 38:551–560
33. Silkin SA, Pasinkovskii EA, Petrenko VI, Dikusar AI (2012) Surf Eng Appl Electrochem 48:1–10
34. Deconinck D, Van Damme S, Deconinck J (2012) Electrochim Acta 60:321–328
35. Mills EJ (1877) Proc Roy Soc London 26:504
36. Bouty E (1879) J Physique 8:289, 341
37. Lange E, König FO (1932) Elektrochemie der Phasengrenzen. In: Wien W, Harms F (eds) Handbuch der Experimentalphysik, vol 12-2. Akadem. Verlagsgesellschaft, Leipzig, pp 327–353
38. Debethune AJ, Licht TS, Swendeman N (1959) J Electrochem Soc 106:616–625
39. Salvi GR, Debethune AJ (1961) J Electrochem Soc 108:672–676
40. Garcia-Araez N, Climent V, Feliu JM (2012) Russ J Electrochem 48:271–280
41. Faita G, Longhi P, Mussini T (1967) J Electrochem Soc 114:340
42. Conway BE, Wilkinson DP (1993) Electrochim Acta 38:997–1013
43. Odukoya A, Naterer GF (2011) Int J Hydrogen Energy 36:11345–11352
44. Hills GJ, Payne R (1965) Trans Faraday Soc 61:326–349

45. Lopez-Perez G, Andreu R, Gonzalez-Arjona D, Calvente JJ, Molero M (2003) J Electroanal Chem 552:247–259
46. Damaskin BB (2006) Russ J Electrochem 42:615–619
47. Szabo K, Mika J (1991) Acta Chim Hung 128:195–205
48. Dinan T, Stimming U (1986) J Electrochem Soc 133:2662–2663
49. Hamelin A, Doubova L, Stoicoviciu L, Trasatti S (1988) J Electroanal Chem 244:133–145
50. Trasatti S (1991) Electrochim Acta 36:1657–1658
51. Silva F, Sottomayor MJ, Martins A (1993) J Electroanal Chem 360:199–210
52. Popov A, Dimitrov N, Naneva R, Vitanov T (1994) J Electroanal Chem 376:97–100
53. Kastening B, Hahn M, Kremeskotter J (1994) J Electroanal Chem 374:159–166
54. Kastening B, Hahn M, Rabanus B, Heins M, zumFelde U (1997) Electrochim Acta 42: 2789–2799
55. Taniguchi M, Tashima D, Otsubo M (2007) 2007 Annual report conference on electrical insulation and dielectric phenomena, pp 396–399
56. Zhou WJ, Zhao DD, Xu MW, Xu CL, Li HL (2008) Electrochim Acta 53:7210–7219
57. Raleigh DO (1974) J Electrochem Soc 121:639–645
58. Lietzke MH, Stoughton RW (1963) J Phys Chem 67:2573
59. Wachter R, Barthel J (1971) Ber Bunsen Ges Phys Chem 75:1134
60. Barthel J, Gores HJ, Schmeer G (1979) Ber Bunsen Ges Phys Chem 83:911–920
61. Wachter R, Barthel J (1979) Ber Bunsen Ges Phys Chem 83:634–642
62. Barthel J, Stroder U, Iberl L, Hammer H (1982) Ber Bunsen Ges Phys Chem 86:636–645
63. Barthel J (1979) Ber Bunsen Ges Phys Chem 83:252–257
64. Barthel J, Gores HJ, Carlier P, Feuerlein F, Utz M (1983) Ber Bunsen Ges Phys Chem 87:436–443
65. Barthel J, Gerber R, Gores HJ (1984) Ber Bunsen Ges Phys Chem 88:616–622
66. Khokhlov VA, Smirnov MV (1979) J Appl Chem USSR 52:1454–1456
67. Nagy Z, Hung NC, Yonco RM (1989) J Electrochem Soc 136:895–896
68. Gosavi S, Gao YQ, Marcus RA (2001) J Electroanal Chem 500:71–77
69. Mostany J, Scharifker BR, Saavedra K, Borras C (2008) Russ J Electrochem 44:652–658
70. Wendt H, Plzak V (1983) Electrochim Acta 28:27–34
71. Schmidt TJ, Ross PN, Markovic NM (2002) J Electroanal Chem 524:252–260
72. Amadelli R, Maldotti A, Molinari A, Danilov FI, Velichenko AB (2002) J Electroanal Chem 534:1–12
73. Park SM, Ho S, Aruliah S, Weber MF, Ward CA, Venter RD, Srinivasan S (1986) J Electrochem Soc 133:1641–1649
74. Schmidt TJ, Stamenkovic V, Ross PN, Markovic NM (2003) PCCP 5:400–406
75. Zhang L, Song CJ, Zhang JJ, Wang HJ, Wilkinson DP (2005) J Electrochem Soc 152: A2421–A2426
76. Lee SK, Pyun SI, Lee SJ, Jung KN (2007) Electrochim Acta 53:740–751
77. Song C, Zhang L, Zhang J, Wilkinson DP, Baker R (2007) Fuel Cells 7:9–15
78. Dhar HP, Christner LG, Kush AK (1986) J Electroanal Chem 213:161–167
79. Jaszay T, Caprani A, Priem F, Frayret JP (1988) Electrochim Acta 33:1093–1100
80. Schmidt TJ, Grgur BN, Markovic NM, Rose PN (2001) J Electroanal Chem 500:36–43
81. Kardash D, Korzeniewski C, Markovic N (2001) J Electroanal Chem 500:518–523
82. Lei JL, Luo JL (2002) PCCP 4:1206–1210
83. Miller B, Chen AC (2005) Electrochim Acta 50:2203–2212
84. Suski L, Ruggiero M (1999) Electrochem Sol State Lett 2:579–582
85. Jiang JH, Kucernak AR (2001) Electrochim Acta 46:3445–3456
86. Grafov BM (2010) Russ J Electrochem 46:239–242
87. Churikov AV (2001) Russ J Electrochem 37:176–186
88. Bilal BA, Tributsch H (1998) J Appl Electrochem 28:1073–1081
89. Inzelt G, Lang G (1991) Electrochim Acta 36:1355–1361
90. Dubois D, Moninot G, Kutner W, Jones MT, Kadish KM (1992) J Phys Chem 96:7137–7145

91. Xu YH, Chen CP, Wang QD, Chen LX (2001) Int J Hydrogen Energy 26:1177–1181
92. Wang Y, Rogers EI, Compton RG (2010) J Electroanal Chem 648:15–19
93. Liu HJ, Xu Q, Yan CW, Cao YZ, Qiao YL (2011) Int J Electrochem Sci 6:3483–3496
94. Gu WB, Wang CY (2000) J Electrochem Soc 147:2910–2922
95. Kalu EE, Nwoga TT, Srinivasan V, Weidner JW (2001) J Power Sourc 92:163–167
96. Wu QD, Liu S, Li L, Yan TY, Gao XP (2009) J Power Sourc 186:521–527
97. Lu DS, Li WS, Tan CL, Huang QM (2011) Electrochim Acta 56:4540–4543
98. Shim J, Kostecki R, Richardson T, Song X, Striebel KA (2002) J Power Sourc 112:222–230
99. Somasundaram K, Birgersson E, Mujumdar AS (2012) J Power Sourc 203:84–96
100. Lanz P, Sommer H, Schulz-Dobrick M, Novak P (2013) Electrochim Acta 93:114–119
101. Yoon T, Park S, Mun J, Ryu JH, Choi W, Kang YS, Park JH, Oh SM (2012) J Power Sourc 215:312–316
102. Song LB, Li XH, Wang ZX, Xiong XH, Xiao ZL, Zhang F (2012) Int J Electrochem Sci 7: 6571–6579
103. Feng XM, Ai XP, Yang HX (2004) Electrochem Commun 6:1021–1024
104. Huang Q, Yan MM, Jiang ZY (2006) J Power Sourc 156:541–546
105. Koltypin M, Aurbach D, Nazar L, Ellis B (2007) J Power Sourc 174:1241–1250
106. He XM, Pu WH, Ren JU, Wang L, Wang JL, Jiang CY, Wan CR (2008) Ionics 14:335–337
107. Huang H, Wang C, Zhang WK, Gan YP, Kang L (2008) J Power Sourc 184:583–588
108. Ku JH, Jung YS, Lee KT, Kim CH, Oh SM (2009) J Electrochem Soc 156:A688–A693
109. Maccario M, Croguennec L, Le Cras F, Delmas C (2008) J Power Sourc 183:411–417
110. Mun J, Jung YS, Yim T, Lee HY, Kim HJ, Kim YG, Oh SM (2009) J Power Sourc 194: 1068–1074
111. Utsunomiya T, Hatozaki O, Yoshimoto N, Egashira M, Morita M (2011) J Power Sourc 196: 8598–8603
112. Levi MD, Wang C, Aurbach D, Chvoj Z (2004) J Electroanal Chem 562:187–203
113. Silva F, Gomes C, Figueiredo M, Costa R, Martins A, Pereira CM (2008) J Electroanal Chem 622:153–160
114. Karthikeyan DK, Sikha G, White RE (2008) J Power Sourc 185:1398–1407
115. Lai W, Ciucci F (2010) Electrochim Acta 56:531–542
116. Novak P, Inganas O (1988) J Electrochem Soc 135:2485–2490
117. Mohamed NS, Arof AK (2004) J Power Sourc 132:229–234
118. Shajan XS (2012) Ionics 18:737–745
119. Matsumoto M, Uno T, Kubo M, Itoh T (2013) Ionics 19:615–622
120. Kotobuki M, Suzuki Y, Munakata H, Kanamura K, Sato Y, Yamamoto K, Yoshida T (2011) Electrochemistry 79:464–466
121. Mcbreen J, Ogrady WE, Richter R (1984) J Electrochem Soc 131:1215–1216
122. Burke LD, Hurley LM (2000) J Solid State Electrochem 4:353–362
123. Chen YX, Li MF, Liao LW, Xu J, Ye S (2009) Electrochem Commun 11:1434–1436
124. Mahapatra SS, Dutta A, Datta J (2010) Electrochim Acta 55:9097–9104
125. Guillen-Villafuerte O, Garcia G, Guil-Lopez R, Nieto E, Rodriguez JL, Fierro JLG, Pastor E (2013) J Power Sourc 231:163–172
126. Williams M, Horita T, Yamagi K, Sakai N, Yokokawa H (2009) J Fuel Cell Sci Technol 6
127. Lee CY, Huang RD (2012) Int J Hydrogen Energy 37:3459–3465
128. Dam VAT, de Bruijn FA (2007) J Electrochem Soc 154:B494–B499
129. Maranzana G, Lottin O, Colinart T, Chupin S, Didierjean S (2008) J Power Sourc 180: 748–754
130. Lindstrom RW, Kortsdottir K, Wesselmark M, Oyarce A, Lagergren C, Lindbergh G (2010) J Electrochem Soc 157:B1795–B1801
131. Burheim O, Kjelstrup S, Pharoah JG, Vie PJS, Moller-Holst S (2011) Electrochim Acta 56: 3248–3257
132. Thomas A, Maranzana G, Didierjean S, Dillet J, Lottin O (2013) J Electrochem Soc 160: F191–F204

133. Chiang LK, Liu HC, Shiu YH, Lee CH, Lee RY (2008) Renew Energy 33:2580–2588
134. Huang TJ, Huang MC (2008) J Power Sourc 175:473–481
135. Nicolella C, Reverberi AP, Carpanese P, Viviani M, Barbucci A (2008) J Fuel Cell Sci Technol 5
136. Wang XH, Huang H, Holme T, Tian X, Prinz FB (2008) J Power Sourc 175:75–81
137. Zheng F, Chen Y (2008) J Materials Sci 43:2058–2065
138. Shao L, Wang SR, Qian JQ, Xue YJ, Liu RZ (2011) Solid Oxide Fuel Cells 12 (Sofc Xii) 35:721–726
139. Ni M (2011) Int J Hydrogen Energy 36:3153–3166
140. Park J, Li PW, Bae J (2012) Int J Hydrogen Energy 37:8532–8555
141. Palcut M, Mikkelsen L, Neufeld K, Chen M, Knibbe R, Hendriksen PV (2012) Int J Hydrogen Energy 37:14501–14510
142. Pereira JRS, Rajesh S, Figueiredo FML, Marques FMB (2013) Electrochim Acta 90:71–79
143. Rohnke M, Falk M, Huber AK, Janek J (2013) J Power Sourc 221:97–107
144. Fletcher SI, Sillars FB, Carter RC, Cruden AJ, Mirzaeian M, Hudson NE, Parkinson JA, Hall PJ (2010) J Power Sourc 195:7484–7488
145. Wang JG, Yang Y, Huang ZH, Kang FY (2013) J Power Sourc 224:86–92
146. Tahar NB, Savall A (2009) Electrochim Acta 55:465–469
147. Tahar NB, Savall A (2011) J Appl Electrochem 41:983–989
148. Kulikova LN, Fateev VN, Rusanov VD (1998) Russ J Electrochem 34:306–309
149. Dall'Antonia LH, Tremiliosi-Filho G, Jerkiewicz G (2001) J Electroanal Chem 502:72–81
150. Sugimoto W, Ohta T, Yokoshima K, Takasu Y (2007) Electrochemistry 75:645–648
151. Kim DJ, Kwon HC, Kim HP (2008) Corrosion Sci 50:1221–1227
152. Finklea HO, Ravenscroft MS, Snider DA (1993) Langmuir 9:223–227
153. Han Y, Uosaki K (2008) Electrochim Acta 53:6196–6201
154. Kamat PV, Karkhanavala MD, Moorthy PN (1979) J Appl Phys 50:4228–4230
155. Dulal SMSI, Yun HJ, Shin CB, Kim CK (2007) Electrochim Acta 53:934–943
156. D'Ajello PCT, Pasa AA, Munford ML, Schervenski AQ (2008) Electrochim Acta 53: 3156–3165
157. Inamdar AI, Mujawar SH, Barman SR, Bhosale PN, Patil PS (2008) Semicond Sci Technol 23:085013
158. Cabilio NR, Omanovic S, Roscoe SG (2000) Langmuir 16:8480–8488
159. Rhoten MC, Burgess JD, Hawkridge FM (2000) Electrochim Acta 45:2855–2860
160. Bak E, Donten M, Stojek Z (2008) Electrochem Commun 10:1074–1077
161. Stene S (1930) Rec Trav Chim Pays-Bas 49:1133–1145
162. Tsuruta T, Macdonald DD (1982) J Electrochem Soc 129:1221–1225
163. Ulmer GC, Manna MF, Grandstaff DE, Vicenzi EP, Barnes HL, Lvov SN, Zhou X, Ulyanov SM (2000) Appl Mineral 1 and 2:79–82
164. van Staveren DR, Bothe E, Weyhermuller T, Metzler-Nolte N (2001) Chem Commun 131–132
165. Fontanesi C, Andreoli R, Benedetti L, Giovanardi R, Ferrarini P (2003) Coll Czech Chem Commun 68:1407–1419
166. Zen JM, Hsu CT, Hsu YL, Sue JW, Conte ED (2004) Anal Chem 76:4251–4255
167. Streeter I, Giovanelli D, Wildgoose GG, Lawrence NS, Jiang L, Jones TGJ, Compton RG (2004) Electroanalysis 16:1205–1210
168. Yang GC, Yu LB, Jia JB, Zhao ZB (2012) J Solid State Electrochem 16:1363–1368
169. Berney H, West J, Haefele E, Alderman J, Lane W, Collins JK (2000) Sens Actuat B Chem 68:100–108
170. Cai CX, Ju HX, Chen HY (1995) Electrochim Acta 40:1109–1112
171. Liu XJ, Huang YX, Zhang WJ, Fan GF, Fan CH, Li GX (2005) Langmuir 21:375–378
172. Chandra A, Pandey RN, Srivastava ON, Prasad G (1991) Semicond Sci Technol 6:137–140
173. Salazar PF, Kumar S, Cola BA (2012) J Electrochem Soc 159:B483–B488
174. Styczynski S, Ciszewski A, Solopa W (2006) Przemysl Chemiczny 85:1234–1236

175. Licht S (2011) STEP (Solar Thermal Electrochemical Production) of energetic molecules: a synergy of photovoltaics and solar thermal to form a new, higher efficiency solar energy process
176. Licht S, Chitayat O, Bergmann H, Dick A, Ayub H, Ghosh S (2010) Int J Hydrogen Energy 35:10867–10882
177. Baltruschat H (2004) J Am Soc Mass Spectrom 15:1693–1706
178. Löffler T, Bussar R, Xiao X, Ernst S, Baltruschat H (2009) J Electroanal Chem 629:1–14
179. Chojak Halseid M, Jusys Z, Behm RJ (2010) J Electroanal Chem 644:103–109
180. Sun S, Heinen M, Jusys Z, Behm RJ (2012) J Power Sourc 204:1–13
181. Diao GW, Zhang ZX (1999) Chin J Anal Chem 27:732–736
182. Burstein GT, Moloney JJ (2004) Electrochem Commun 6:1037–1041
183. Wildgoose GG, Giovanelli D, Lawrence NS, Compton RG (2004) Electroanalysis 16: 421–433
184. Zhang W, Charles EA, Congleton J (2004) Chem Res Chin Univ 20:494–500
185. Gründler P (2007) Chemical sensors. Springer, Berlin, pp 156–158
186. Fergus JW (2008) Sens Actuat B Chem 134:1034–1041
187. Chevallier L, Traversa E, Di Bartolomeo E (2010) J Electrochem Soc 157:J386–J391
188. Yang JC, Spirig JV, Karweik D, Routbort JL, Singh D, Dutta PK (2008) Sens Actuat B Chem 131:448–454
189. Ueda T, Okawa H, Takahashi S (2013) Electrochemistry 81:74–76
190. Yang JC, Dutta PK (2010) Sens Actuat B Chem 143:459–463
191. Matsumura H, Nakamura N, Yohda M, Ohno H (2007) Electrochem Commun 9:361–364
192. Scharifker BR, Zelenay P, Bockris JO (1987) J Electrochem Soc 134:2714–2725
193. Appleby AJ (1970) J Electrochem Soc 117:1159
194. Appleby AJ (1970) J Electrochem Soc 117:328
195. Borodzinski JJ, Galus Z (1982) J Electroanal Chem 135:221–241
196. Borodzinski JJ, Galus Z (1985) J Electroanal Chem 183:261–276
197. Sanchez S, Lambertin D, Cowache P, Picard GS, Fradejas MRB, Castrillejo Y (1999) High Temp Mater Process 3:91–103
198. Fastner U, Steck T, Pascual A, Fafilek G, Nauer GE (2008) J Alloys Comp 452:32–35
199. Hab AI (2007) Mater Sci 43:383–397
200. Elshina LA, Kudyakov VY, Malkov VB, Elshin AN (2008) Glass Phys Chem 34:617–622
201. Novoselova AV, Khokhlov VA, Shishkin VY (2001) Russ J Appl Chem 74:1672–1677
202. Novoselova AV, Khokhlov VA, Shishkin VY (2003) Russ J Phys Chem 77:S119–S124
203. Tian LF, Wen MF, Li LY, Chen J (2009) Electrochim Acta 54:7313–7317
204. Shkurankov A, Endres F, Freyland W (2002) Rev Sci Instrum 73:102–107
205. Macdonald DD, Scott AC, Wentrcek P (1979) J Electrochem Soc 126:908–911
206. Macdonald DD, Bartlett RW (1979) J Metals 31:127
207. Hettiarachchi S, Macdonald DD (1984) J Electrochem Soc 131:2206–2207
208. Hettiarachchi S, Kedzierzawski P, Macdonald DD (1985) J Electrochem Soc 132:1866–1870
209. Hettiarachchi S, Macdonald DD (1987) J Electrochem Soc 134:1307–1308
210. Macdonald DD, Hettiarachchi S, Lenhart SJ (1987) J Electrochem Soc 134:C423
211. Hettiarachchi S, Makela K, Song H, Macdonald DD (1992) J Electrochem Soc 139:L3–L4
212. Macdonald DD, Hettiarachchi S, Song H, Makela K, Emerson R, Benhaim M (1992) J Solution Chem 21:849–881
213. Kriksunov LB, Macdonald DD (1994) Sens Actuat B Chem 22:201–204
214. Kriksunov LB, Macdonald DD, Millett PJ (1994) J Electrochem Soc 141:3002–3005
215. Biswas R, Lvov SN, Ahmad Z, Macdonald DD (1997) Proceedings of the symposium on electrode materials and processes for energy conversion and storage IV 97:340–353
216. Eklund K, Lvov SN, Macdonald DD (1997) J Electroanal Chem 437:99–110
217. Engelhardt GR, Lvov SN, Macdonald DD (1997) J Electroanal Chem 429:193–201
218. Lvov SN, Macdonald DD (1997) Proceedings of the ninth international conference on high temperature materials chemistry 97:472–479

219. Lvov SN, Macdonald DD (1997) Proceedings of the ninth international conference on high temperature materials chemistry 97:746–754
220. Lvov SN, Gao H, Kouznetsov D, Balachov I, Macdonald DD (1998) Fluid Phase Equilibria 151:515–523
221. Lvov SN, Zhou XY, Wei X, Ulyanov SM, Macdonald DD (1999) Abstr Papers Am Chem Soc 218:129
222. Ai JH, Chen YZ, Urquidi-Macdonald M, Macdonald DD (2007) J Electrochem Soc 154: C43–C51
223. Flarsheim WM, Tsou YM, Trachtenberg I, Johnston KP, Bard AJ (1986) J Phys Chem 90: 3857–3862
224. Mcdonald AC, Fan FRF, Bard AJ (1986) J Phys Chem 90:196–202
225. Bard AJ, Flarsheim WM, Johnston KP (1988) J Electrochem Soc 135:1939–1944
226. Flarsheim WM, Bard AJ, Johnston KP (1989) J Phys Chem 93:4234–4242
227. Cabrera CR, Garcia E, Bard AJ (1989) J Electroanal Chem 260:457–460
228. Liu CY, Snyder SR, Bard AJ (1997) J Phys Chem B 101:1180–1185
229. Crooks RM, Bard AJ (1988) J Electroanal Chem 243:117–131
230. Cabrera CR, Bard AJ (1989) J Electroanal Chem 273:147–160
231. Crooks RM, Bard AJ (1988) J Electroanal Chem 240:253–279
232. Edenboro BW, Robins RG (1969) Electrochim Acta 14:1285
233. Jayaweera P, Hettiarachchi S, Ocken H (1994) Colloids Surfaces A 85:19–27
234. Delpech S, Picard G, Finne J, Walle E, Conocar O, Laplace A, Lacquement J (2008) Nucl Technol 163:373–381
235. Lipkin AG, Gusev BA, Efimov AA (1992) Zashchita Metallov 692–694
236. Trevani LN, Calvo E, Corti HR (2000) Electrochem Commun 2:312–316
237. Niedrach LW (1982) J Electrochem Soc 129:1445–1449
238. Yasuda M, Fukumoto K, Ogata Y, Hine F (1988) J Electrochem Soc 135:2982–2987
239. Watanabe Y, Kain V, Kobayashi M (2002) JSME Int J A Sol Mech Mater Eng 45:476–480
240. Arganis-Juarez CR, Malo JM, Uruchurtu J (2007) Nucl Eng Des 237:2283–2291
241. Shintani D, Ishida T, Fukutsuka T, Matsuo Y, Sugie Y (2008) Corrosion 64:607–612
242. Kuzin BL, Beresnev SM, Osinkin DA, Bogdanovich NM, Kotov YA, Bagazeev AV (2010) Russ J Electrochem 46:278–284
243. Guan YC, Han KN (1996) J Electrochem Soc 143:1875–1880
244. Yeh TK, Chien YC, Wang BY, Tsai CH (2008) Corrosion Sci 50:2327–2337
245. Ramanathanan S, Karthikeyan A, Govindarajan SA, Kirsch PD (2008) J Vacuum Sci Technol B 26:L33–L35
246. Munoz-Rojas D, Leriche JB, Delacourt C, Poizot P, Palacin MR, Tarascon JM (2007) Electrochem Commun 9:708–712
247. Aklalouch M, Amarilla JM, Rojas RM, Saadoune I, Rojo JM (2008) J Power Sourc 185: 501–511
248. Lu XC, Li GS, Kim JY, Lemmon JP, Sprenkle VL, Yang ZG (2012) J Power Sourc 215: 288–295
249. Bokach D, de la Fuente JLG, Tsypkin M, Ochal P, Endsjo IC, Tunold R, Sunde S, Seland F (2011) Fuel Cells 11:735–744
250. Wildgoose GG, Giovanelli D, Klymenko EV, Lawrence NS, Jiang L, Jones TGJ, Compton RG (2004) Electroanalysis 16:337–344
251. Zhang RH, Zhang XT, Hu SM (2013) Sens Actuat B Chem 177:163–171
252. Bogaerts WF, Vanhaute AA (1984) J Electrochem Soc 131:68–72
253. Lvov SN, Zhou XY, Ulyanov SM, Bandura AV (2000) Chem Geol 167:105–115
254. Lietzke MH, Stoughton RW (1953) J Am Chem Soc 75:5226–5227
255. Lvov SN, Macdonald DD (1996) J Electroanal Chem 403:25–30
256. Bosch RW, Bogaerts WF, Zheng JH (2003) Corrosion 59:162–171
257. Tsionskii VM, Kriksunov LB (1988) Instrum Exp Techn 31:259–260

258. Wildgoose GG, Lawrence NS, Coles BA, Jiang L, Jones TGJ, Compton RG (2003) PCCP 5:4219–4225
259. Trevani LN, Calvo E, Corti HR (1997) J Chem Soc Faraday Trans 93:4319–4326
260. Tachibana K (2004) Electrochemistry 72:720–721
261. Kriksunov LB, Semenikhin OA, Bunakova LV (1993) Electrochim Acta 38:1761–1768
262. Nagy Z, Yonco RM (1986) J Electrochem Soc 133:2232–2235
263. Wakabayashi N, Uchida H, Watanabe M (2002) Electrochem Sol State Lett 5:E62–E65
264. Bandi A, Specht M, Weimer T, Schaber K (1995) Energy Convers Manag 36:899–902
265. Zhou MH, Lei LC, Dai QZ (2007) Chem Commun 2645–2647
266. Andress RJ, Martin LL (2010) Int J Hydrogen Energy 35:958–965
267. Lee MS, Koo IG, Kim JH, Lee WM (2009) Int J Hydrogen Energy 34:40–47
268. Tsionskii VM, Kriksunov LB (1986) J Electroanal Chem 204:131–140
269. Kriksunov LB, Krishtalik LI, Tsionskii VM (1989) Sov Electrochem 25:614–617
270. Kriksunov LB, Krishtalik LI (1993) J Electroanal Chem 354:99–103
271. Tsionskii VM, Kriksunov LB, Krishtalik LI (1991) Electrochim Acta 36:411–419
272. Kriksunov LB, Bunakova LV, Zabusova SE, Krishtalik LI (1994) Electrochim Acta 39: 137–142
273. Tsionskii VM, Krishtalik LI, Kriksunov LB (1988) Electrochim Acta 33:623–630
274. Dombro RA, Prentice GA, Mchugh MA (1988) J Electrochem Soc 135:2219–2223
275. Abbott AP, Harper JC (1996) J Chem Soc Faraday Trans 92:3895–3898
276. Abbott AP, Eardley CA, Harper JC, Hope EG (1998) J Electroanal Chem 457:1–4
277. Abbott AP, Harper JC (1998) Energy Electrochem Process Cleaner Environ 97:83–86
278. Abbott AP, Eardley CA (1999) J Phys Chem B 103:6157–6159
279. Abbott AP, Harper JC (1999) PCCP 1:839–841
280. Abbott AP, Eardley CA (2000) J Phys Chem B 104:9351–9355
281. Abbott AP, Eardley CA (2000) J Phys Chem B 104:775–779
282. Goldfarb DL, Corti HR (2000) Electrochem Commun 2:663–670
283. Abbott AP, Eardley CA, Scheirer JE (2001) PCCP 3:3722–3726
284. Abbott AP, Durling NE (2001) PCCP 3:579–582
285. Abbott AP, Corr S, Durling NE, Hope EG (2002) J Chem Eng Data 47:900–905
286. Bard AJ (1963) Anal Chem 35:1125–1128
287. Mason TJ, Lorimer JP, Walton DJ (1990) Ultrasonics 28:333–337
288. Compton RG, Eklund JC, Page SD, Sanders GHW, Booth J (1994) J Phys Chem 98: 12410–12414
289. Banks CE, Compton RG (2004) Analyst 129:678–683
290. Gründler P (2008) Curr Anal Chem 4:263–270
291. Compton RG, Eklund JC, Marken F (1997) Electroanalysis 9:509–522
292. Del Campo FJ, Coles BA, Marken F, Compton RG, Cordemans E (1999) Ultrasonics Sonochem 6:189–197
293. Gonzalez-Garcia J, Esclapez MD, Bonete P, Hernandez YV, Garreton LG, Saez V (2010) Ultrasonics 50:318–322
294. Klima J (2011) Ultrasonics 51:202–209
295. Ramachandran R, Saraswathi R (2011) Russ J Electrochem 47:15–25
296. Chiba A (1999) Electrochemistry 67:930–934
297. Gedanken A (2004) Ultrasonics Sonochem 11:47–55
298. Saez V, Mason TJ (2009) Molecules 14:4284–4299
299. Zin V, Campadello E, Zanella A, Brunelli K, Dabala M (2010) Metallurgia Italiana 29–37
300. Shi JJ, Wang S, He TT, Abdel-Halim ES, Zhu JJ (2014) Ultrasonics Sonochem 21:493–498
301. Reyman D, Guereca E, Herrasti P (2007) Ultrasonics Sonochem 14:653–660
302. Atobe M, Ishikawa K, Asami R, Fuchigami T (2009) Angew Chem Int Ed 48:6069–6072
303. Taouil AE, Lallemand F, Hallez L, Hihn JY (2010) Electrochim Acta 55:9137–9145
304. Garbellini GS, Salazar-Banda GR, Avaca LA (2008) Quimica Nova 31:123–133
305. Compton RG, Foord JS, Marken F (2003) Electroanalysis 15:1349–1363

306. Vetter KJ (1961) Elektrochemische Kinetik. Springer, Berlin
307. Agar JN (1963) Thermogalvanic cells. In: Delahay P (ed) Advances in electrochemistry and electrochemical engineering. Interscience Publishers, London, pp 31–121
308. Boudeville P, Tallec A (1988) Thermochim Acta 126:221–234
309. Lange E, Hesse T (1933) Z Elektrochem 39:374–384
310. Sherfey JM (1963) J Electrochem Soc 110:213–221
311. Fang Z, Wang SF, Zhang ZH, Qiu GZ (2008) Thermochim Acta 473:40–44
312. Ishikawa H, Mendoza O, Sone Y, Umeda M (2012) J Power Sourc 198:236–242
313. Song LB, Li XH, Wang ZX, Guo HJ, Xiao ZL, Zhang F, Peng SJ (2013) Electrochim Acta 90: 461–467
314. Zhang HZ, Zhang PM, Fang Z (1995) J Therm Anal 45:151–156
315. Mostany J, Scharifker BR (1997) Electrochim Acta 42:291–301
316. Etzel KD, Bickel KR, Schuster R (2010) Rev Sci Instrum 81:034101–034108
317. Etzel KD, Bickel KR, Schuster R (2010) ChemPhysChem 11:1416–1424
318. Fang Z, Wang S, Zhang Z (2011) J Therm Anal Calorim 106:937–943
319. Hellwig C, Sorgel S, Bessler WG (2011) Batteries energy technol (general) – 219th ECS Meeting 35:215–228
320. Nieto N, Diaz L, Gastelurrutia J, Alava I, Blanco F, Ramos JC, Rivas A (2013) J Electrochem Soc 160:A212–A217
321. Christensen J, Cook D, Albertus P (2013) J Electrochem Soc 160:A2258–A2267
322. Catherino HA (2013) J Power Sourc 239:505–512
323. Bazinski SJ, Wang X (2014) J Electrochem Soc 161:A168–A175
324. Bandhauer TM, Garimella S, Fuller TF (2014) J Power Sourc 247:618–628
325. Miller JR (2006) Electrochim Acta 52:1703–1708
326. Holmes HF, Joncich MJ (1959) Anal Chem 31:28–32
327. Holmes HF, Joncich MJ (1960) Anal Chem 32:1251–1253
328. Graves BB (1972) Anal Chem 44:993–1002
329. Spritzer MS (1975) Thermoelectrochemistry – thermal studies at electrode surfaces. Abstr Papers Am Chem Soc 169:105
330. Cooke SL, Graves BB (1968) Chem Instrum 1:119
331. Tamamushi R (1973) J Electroanal Chem 45:500–503
332. Tamamushi R (1975) J Electroanal Chem 65:263–273
333. Soto MB, Kubsch G, Scholz F (2002) J Electroanal Chem 528:18–26
334. Soto MB, Scholz F (2002) J Electroanal Chem 528:27–32
335. Ozeki T, Watanabe I, Ikeda S (1979) J Electroanal Chem 96:117–121
336. Ozeki T, Watanabe I, Ikeda S (1983) J Electroanal Chem 152:41–54
337. Ozeki T, Ogawa N, Aikawa K, Watanabe I, Ikeda S (1983) J Electroanal Chem 145:53–65
338. Boudeville P (1994) Inorg Chim Acta 226:69–78
339. Wang H, Wang D, Li B, Sun S (1995) J Electroanal Chem 392:13–19
340. Wang H, Wang D, Li B, Sun S (1995) J Electroanal Chem 392:21–25
341. Shibata S, Sumino MP, Yamada A (1985) J Electroanal Chem 193:123–134
342. Shibata S, Sumino MP (1985) J Electroanal Chem 193:135–143
343. Jiang Z, Xiang Y, Wang J (1991) J Electroanal Chem 316:199–209
344. Jiang Z, Zhang W, Huang X (1994) J Electroanal Chem 367:293–296
345. Jiang ZY, Zhang J, Dong LJ, Zhuang JH (1999) J Electroanal Chem 469:1–10
346. Schuster R, Rosch R, Timm AE (2007) Z Phys Chem 221:1479–1491
347. Bickel KR, Etzel KD, Halka V, Schuster R (2013) Electrochim Acta 112:801–812
348. Decker F, Fracastoro-Decker M, Cella N, Vargas H (1990) Electrochim Acta 35:25–26
349. Tehrani P, Engquist I, Robinson ND, Nilsson D, Robertsson M, Berggren M (2010) Electrochim Acta 55:7061–7066

Chapter 4
Modern Thermoelectrochemistry

4.1 Objectives

By definition, modern thermoelectrochemistry has the basic concept of temperature as an independent variable. The intention of this branch of science has been expressed by the following comprehensive definition (formulation by L. Dunsch in 2009 [1]):

> Modern thermoelectrochemistry as a branch of electrochemistry is devoted to the influence of the temperature as an independent variable on all charge transfer reactions at condensed interphases.

Following this definition, experimental methods of modern thermoelectrochemistry should allow fast and arbitrary variation of electrode temperature. Also, they should provide measuring techniques to follow small temperature changes occurring at electrode surfaces. This way, the study of electrochemical transients at electrode surfaces as a result of temperature changes (thermal distortions) should be enabled, similar to the classic transient techniques like chronoamperometry where a transient current is recorded as result of a "voltage distortion". Thermal distortions can be imposed in the form of a temperature jump, followed by investigating the relaxation of the electrode surface. Alternatively, "temperature modulation" can be applied, where electrochemical effects are studied as response on periodic temperature variations in the form of sinusoidal or rectangular thermal "waves".

The techniques of modern thermoelectrochemistry should provide ways to impose temperature variations at the place where the interesting processes are occurring, i.e. at the surface of a working electrode and not necessarily at the entire cell volume. Consequences of these characteristics are:

- Main interest of modern thermoelectrochemistry is study of single electrode properties.
- Modern thermoelectrochemistry typically works with non-isothermal cells.

P. Gründler, *In-situ Thermoelectrochemistry*, Monographs in Electrochemistry,
DOI 10.1007/978-3-662-45818-1_4

The term “modern” is appropriate mainly for such techniques which allow to impose fast temperature changes in the form of single pulses or periodic waves. Pure calorimetric methods without thermal excitation are placed somewhere between classic and modern thermoelectrochemistry. Modern techniques should display properties which otherwise would not be accessible.

4.2 Heated Electrodes

To impose a temperature jump, the electrolytic interface either could be heated or could be cooled. Existing contemporary state of the technology does not allow fast and arbitrary cooling; hence the dominant technique of modern electrochemistry is heating. We can study the transient from cold to hot by different methods. The opposite transient, from hot to cold, is available with some methods, but only if a jump from cold to hot is preceding and if the spontaneous cooling down of the interesting interface is running fast. With directly heated thin wire electrodes or with microwave heating, respectively, both transients can be studied this way.

There are two ways to make use of heated electrochemical interfaces. When steep heat pulses are imposed (the so-called *pulse heating*), thermal convection can be ignored within some tenths of a second, so as to work in stagnant solution with the result of attaining very high temperature. Even work in superheated state far above the boiling point is attainable. The alternative is *permanent heating*, which restricts working temperature to values below the boiling point. On the other hand, this variant generates a highly efficient stirring effect with a diffusion layer of constant thickness and with a stable working temperature. The resulting voltammograms are of ideal sigmoidal shape. The different modes of operation have consequences on the electrochemical behaviour, resulting from differences in streaming processes. Details will be discussed in more detail in Chap. 5.

4.2.1 Techniques of Heating

As mentioned above, heating in modern electrochemistry means heating the electrode/electrolyte interface. In order to heat this interesting place, different approaches are available. The electrode material can be heated either, e.g., by laser illumination, by resistive or by inductive heating. Otherwise, instead of the electrode itself, a spot of solution close to the electrode interface may be heated, e.g. by focused microwaves or by resistive electrolyte heating using high-frequency current in parallel to electrolysis current. In both modes of operation, only a very small part of the electrochemical cell is affected by temperature changes, so as to make the latter fast and leave bulk solution free from alterations.

A further classification results from the differentiation between *indirect* or *direct* heating. The former means that “heater” and active electrode area are not identical

but separated by an insulating spacer or something similar. Such arrangements by nature are of somewhat higher thermal inertia compared with devices for direct heating, where no passive intermediate has to be heated up together with the active interface. Maximum heating rates can be achieved only by direct heating.

Among the electrochemical heating techniques discussed here, application of laser pulses or similar techniques working with focused light illumination have disappeared somewhat out of sight, maybe because younger techniques can be run easier and cheaper. The highest degree of perfection and of practicability so far has been achieved with focused microwaves and, even more, with resistive heating of thin metallic wires ("hot-wire electrochemistry"). The latter technology has found broad application during the last years. Thereby, its distinctive features and experimental details will be presented in an own chapter further below (Chap. 6).

4.2.1.1 Heating of Solution Fractions

Miniaturising heated isothermal cells with the ambition to achieve faster heating-up could be considered to be a first step from classical to modern thermoelectrochemistry. This approach obviously does make sense only if the heated solution can be exchanged fast. A practicable design is given with flow-through cells where a certain region of the flowing solution is exposed to electric heaters. An exceptional design has been presented [2], where concentric metal tubes inside a flow-through system formed working and counter electrodes, respectively. A central heater in the form of an internal cylinder was used to heat the flowing solution. Ferrocyanide/ferricyanide solution was electrolysed to study the hydrodynamic conditions. A microelectrode has been included into a tube-sized streaming arrangement which is heated by an external heater in the form of a coil [3]. Figure 4.1 gives an impression of the system. Obviously, it represents a tiny isothermal cell where working temperature can be changed rather fast.

Heated flow-through arrangements also were proposed for high-pressure, high-temperature electrochemistry [3–7]. In such cells, a preheating unit is heating up a certain region of the flowing solution stream before it is reaching the electrolysis compartment containing active electrodes. Devices of this type were used for spectroelectrochemical investigations with Raman spectroscopy at different temperatures [3, 5]. The method could be considered to be the first approach to a thermo-spectroelectrochemistry. Kinetic investigations with similar flow-through cells also were successful, e.g. for kinetics of the Fe^{2+}/Fe^{3+} redox couple [6]. Determination of pH also has been reported [7]. A typical example for cell design is given in Fig. 4.2.

Non-pressurised flow-through cells with outer heating unit have been used to study oxygen reduction [8].

A completely different approach to establish a heated solution region is followed by two techniques which make use of an ordinary electrolysis vessel that is converted to give a non-isothermal cell just by generating a "hot spot" in close vicinity to the electrode-solution interface. The electrode material itself is not

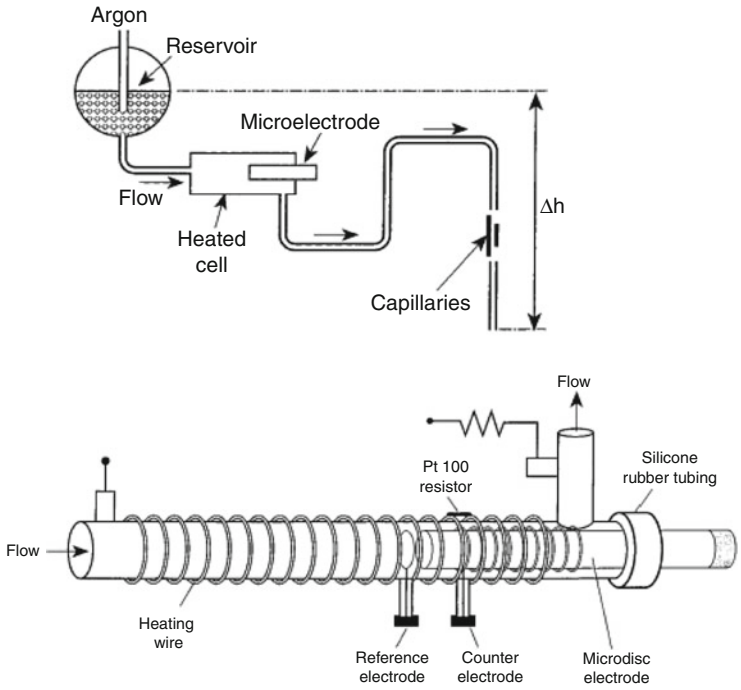

Fig. 4.1 *Top*: Working scheme of a heated flow-through system with microelectrode included. *Bottom*: Design of the instrument (from [3], with permission)

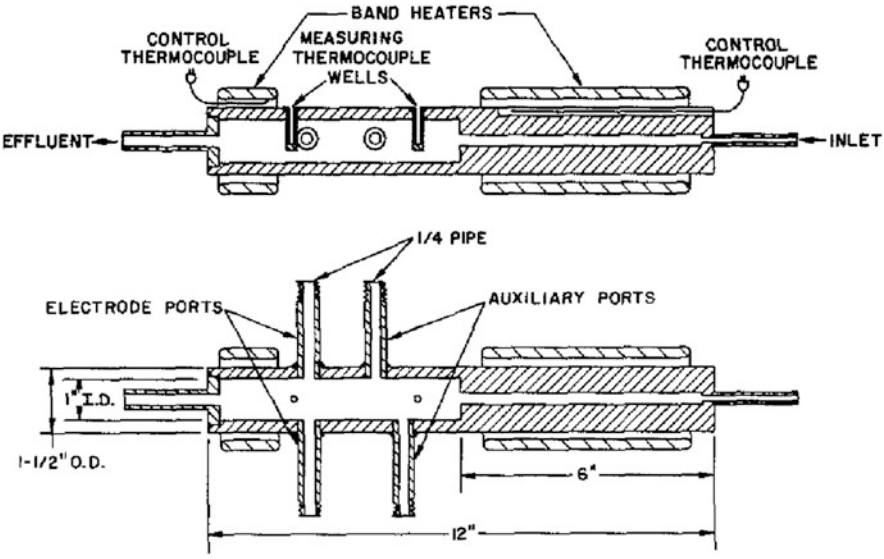

Fig. 4.2 High-temperature/high-pressure flow-through cell. From [6], with permission

heated up, but the active interface assumes increased temperature, probably including an extremely fine part of the metal surface. For proper function of electrochemical processes, indeed micrometre dimensions would be more than sufficient.

Two ways to generate a hot spot have been reported. One of them makes use of focused microwaves in front of a microelectrode; the second one causes ohmic heating of a solution spot in front of a microelectrode by means of high-power, high-frequency current flowing in parallel with the electrolysis current.

Microwave heating is a well-documented, well-developed technology of modern electrochemistry [9–24]. An overview has been given in two reviews [9, 10]. The method has been described first in 1998 by Compton and co-workers [11]. The electrochemical cell is placed inside a microwave oven. As a working electrode, a long wire lead ending in a thin noble metal wire forming at the front side of a microdisk is used. The connection cable of this microelectrode is exposed to the microwave field inside the oven and acts as a kind of antenna. The "antenna" receives the microwave oscillations which leave the metallic part at the solution side acting as a focused energy bundle at this place. As a result, a hot solution spot is formed. This spot is assuming the increased temperature extremely fast, and also the temperature will decrease extremely fast after finishing microwave energy supply. Streaming phenomena in the vicinity of the spot as well as many other characteristics have been described in detail [12, 14]. Extremely strong thermal convection has been described as some kind of "jet boiling" [14]. Local energy concentration allows to work with superheated water as a solvent, like in hot-wire electrochemistry. Unfortunately, there seem to exist some uncertainties with knowledge of the true local temperature. Partially, this may be a consequence that all the bulk solution is located inside the microwave oven and that an uncontrolled warming-up is occurring additionally. It seems reasonable to apply short heating pulses, but in contrast to hot-wire electrochemistry, the strong convection does not allow to make use of a stagnant solution layer. The method probably is not qualified so much for more fundamental studies in electrochemistry. This may be the reason that analytical applications are prevailing so far. Many examples of electrochemical stripping determinations have been reported [15–19]. A typical apparatus is depicted in Fig. 4.3. Characteristics of the method, for continuous as well as for pulsed heating, are sketched in Fig. 4.4. The behaviour with permanent as well as with pulsed heating is shown. The phenomena which are reason for the diagrams given are discussed in more detail in Chap. 5. They are very similar to those with heated wire electrodes.

Examples of stripping analyses with microwave-enhanced voltammetry are trace determination of cadmium [15–17], of lead (deposited as lead dioxide and as elemental lead) [16, 18] and of palladium [19].

Ohmic heating of electrolyte solution as a consequence of electrolysis current is well known and has been utilised casually, e.g. for cooking food [25, 26]. Often, this side effect is undesirable and measures to avoid it are discussed, e.g. when batteries or electrochemical capacitors are charged/discharged [27, 28], and also in technical application of electro-osmosis [29]. The phenomena connected with ohmic heating in traditional cells are investigated [30–32]. Also, it was well

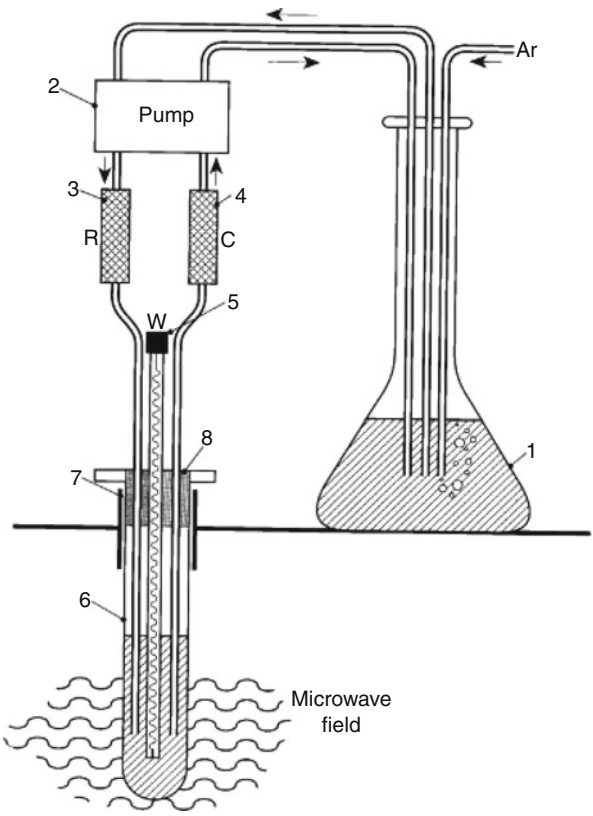

Fig. 4.3 Arrangement for microwave-activated voltammetry. From [15], with permission

known that thermoelectric convection as a result of ohmic heating occurred in studies with asymmetric high-frequency electric fields in electrolyte solutions, which intended to study dielectrophoretic effects [33–35].

Use of ohmic electrolyte heating as a scientific tool was an idea of the later Nobel Prize winner Manfred Eigen. His famous work of kinetic investigations by means of temperature jump started 1954 with heating experiments in electrolyte solutions [36]. Eigen was not interested in chemical processes at the electrode surface, but aimed at kinetic phenomena of ionic reactions occurring in homogeneous solution. Only recently, ohmic solution heating has been rediscovered and efforts have been made to use it intentionally as a tool of modern thermoelectrochemistry. Baranski and co-workers established a method which can be run with low effort [37–40]. The working principle is to send a strong high-power, high-frequency current through a microelectrode disk in admixture with all signal currents. This way, a hot solution spot close to the electrode/electrolyte interface is created similar to spots made by focused microwaves. The working frequency has to be chosen very high, up to gigahertz range. This is presumption to efficiently separate the high-power heating current from low-power electrochemical signals. The electronic equipment, nevertheless, is rather simple and easy to establish with

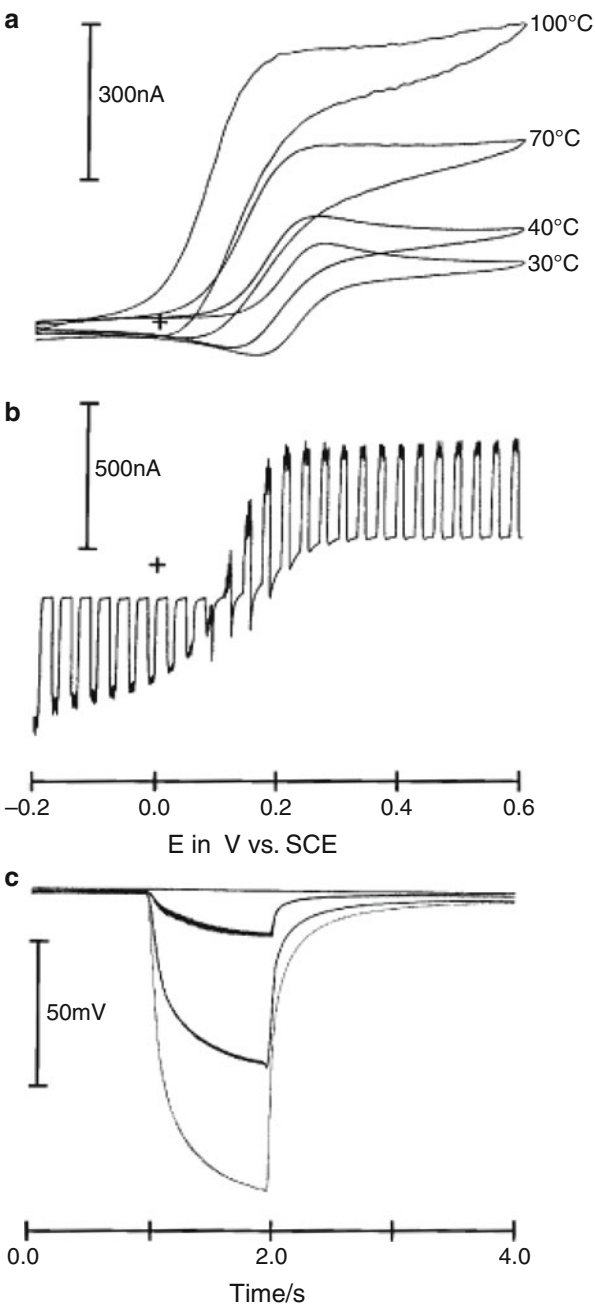

Fig. 4.4 Electrochemical characteristics of microwave-heated solution spot. From [15], with permission

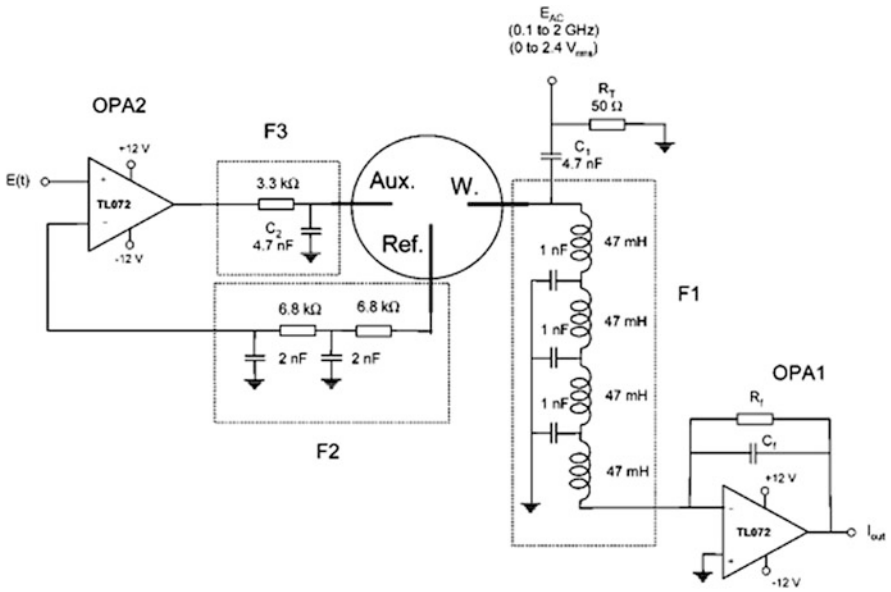

Fig. 4.5 Electronic set-up for generation of a hot solution spot by high-frequency heating current in parallel to electrolysis current. From [37], with permission

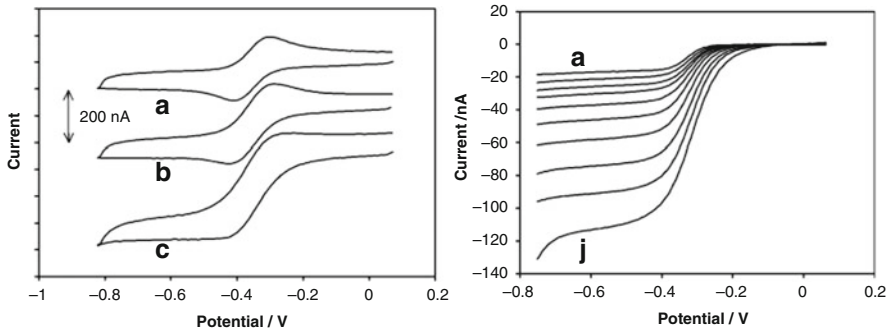

Fig. 4.6 *Left*: Changes in cyclic voltammograms caused by a superimposed sinusoidal waveform at frequency 200 MHz. AC amplitudes in V_{rms}: (a) 0, (b) 1.62 and (c) 2.3. *Right*: Changes in steady-state voltammograms caused by a superimposed sinusoidal waveform at frequency 150 MHz. AC amplitudes in V_{rms}: (a) 0, (b) 0.79, (c) 1.01, (d) 1.13, (e) 1.28,(f) 1.44, (g) 1.62, (h) 1.82, (i) 2.05 and (j) 2.31. Solution: 0.01 M $Ru(NH_3)_6^{3+}$, 2.5 M $(NH_4)_2SO_4$ and 1 M NH_3. Working electrode: Au disk, 12.5 μm in radius; sweep rate, 0.02 V/s. From [37], with permission

low cost (see Fig. 4.5). The results are impressing. Voltammograms and other electrochemical functions are similar to results of microwave voltammetry and to voltammetry with hot-wire electrochemistry (Fig. 4.6). Pulsed as well as continuous heating has been reported. Dielectrophoretic phenomena caused by the heating AC as well as other side effects have been discussed. Meanwhile, a well-founded

theoretical basis of the method has been established [39]; however, no practical application has been reported so far. The method has been refined in direction of a valuable diagnostic tool to study fundamental phenomena like dielectric relaxation of water at ultrahigh frequencies and of faradaic rectification effects (the latter as a method for indirect estimation of electrode impedance). With this orientation, less powerful AC current has been imposed. In such studies, not heating of solution was desired, but a variety of other effects caused by overlaid high-frequency current [41].

4.2.1.2 Heating of the Electrode Body

At present, altogether four ways are existing to heat an electrode body in situ:

- Heating a disk-shaped electrode by illumination with laser or focused light beams
- Electric heating by an external heater (indirect electric heating)
- Electric heating (ohmic or Joule heating) of the electrode body by an imposed heating current (direct electric heating)
- Inductive heating of the electrode body by an external high-frequency field

Heating by Laser or by Focused Tungsten Light

Apart from two single papers dealing with an early variant of direct electric heating [42, 43], the oldest way to heat up electrodes in situ has been laser illumination. Indeed, modern thermoelectrochemistry starts with laser-activated methods. Meanwhile, a large number of papers have been published [44–112], although during last years the output has decreased.

Laser beams can be directed to an electrode disk either from the rear (beam does not cross the solution) or from the electrolyte side. The former case obviously will generate exclusively thermal effects, whereas the latter may bring about photoelectrochemical as well as thermoelectrochemical phenomena. Only a few experiments may be assigned clearly to photoelectrochemistry, as with studies of photoelectron emission [46–48]. Often, a clear distinction is difficult. In 1985, Konovalov and Raitsimring differentiated the contributions of both effects in their experiments with short time laser pulses [49]. By far the most laser applications aimed at thermal effects on electrochemical processes.

Laser illumination of electrodes as a thermoelectrochemical method dates back to 1975 [50], when Barker and Gardner applied pulsed diode laser light to implement thermal modulation as a new method. That time, many authors experimented with different modulation techniques in order to separate useful signal from noise. A scheme of the instrument of Barker and Gardner is given in Fig. 4.7. When periodic heat pulses in the form of a square wave function are imposed at the electrode interface, thermal changes of the electrode processes result in periodic

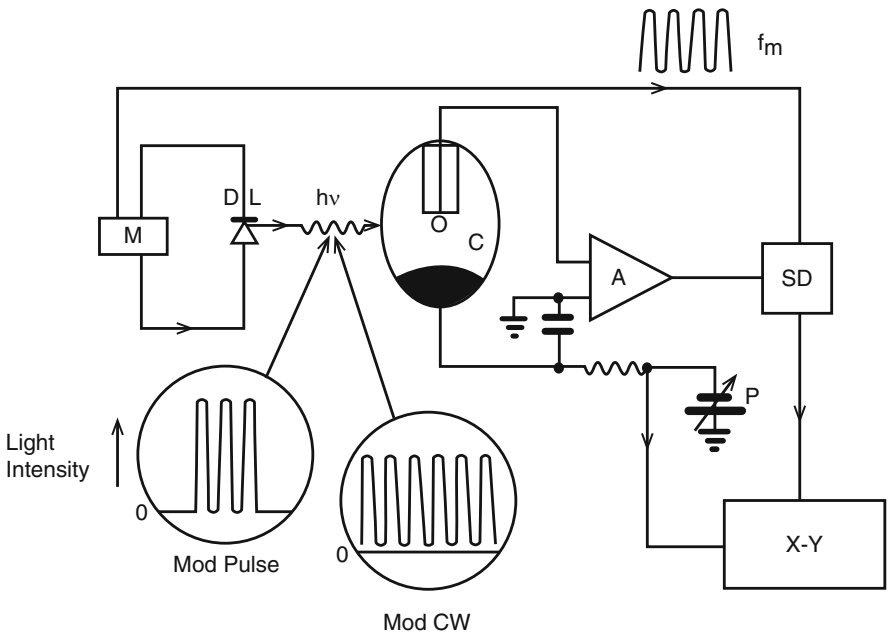

Fig. 4.7 Thermal laser modulation of Hg electrode. (M) Modulator for diode laser DL, (C) electrolysis cell, (A) f_m amplifier, (SD) synchronous detector for signals of frequency f_m, (P) polarising voltage, (X-Y) pen recorder. From [50], with permission

oscillations of electrochemical quantities which can be separated by electronic means. It is not a problem to do this separation in a phase-selective manner. This way, the (aperiodic) electrochemical noise is separated efficiently from signals which clearly can be ascribed to pure electrode processes.

After the pioneering work of Barker and Gardner, the interest in thermal modulation weakened. Beginning in the eighties of the last century, the method became revitalised in conjunction with growing interest in electrochemical kinetics [51–64]. In 1983, Miller re-established a thermal laser modulation technique [51] which was applied to rotating-disk electrodes during the following years [55]. The scheme of an improved arrangement is given in Fig. 4.8. Electrodes were illuminated from the rear side by laser pulses with frequencies of 1 till 30 Hz. This way, pure thermal effects were acting. Since rotating disk electrodes are hydrodynamic systems, the overlapping of mechanical streaming phenomena with thermal convection results in highly complex streaming conditions [52, 53]. The authors considered the influence of thermodiffusion (Soret effect) [54]. They presented a comprehensive theoretical treatment of reversible redox couple behaviour [55]. Many of their insights have been verified later by hot-wire electrochemistry and also partially by laser-activated voltammetry.

Thermal modulation turned out to be a valuable tool of modern thermoelectrochemistry. Instead of lasers, focused light of a tungsten lamp has been applied to

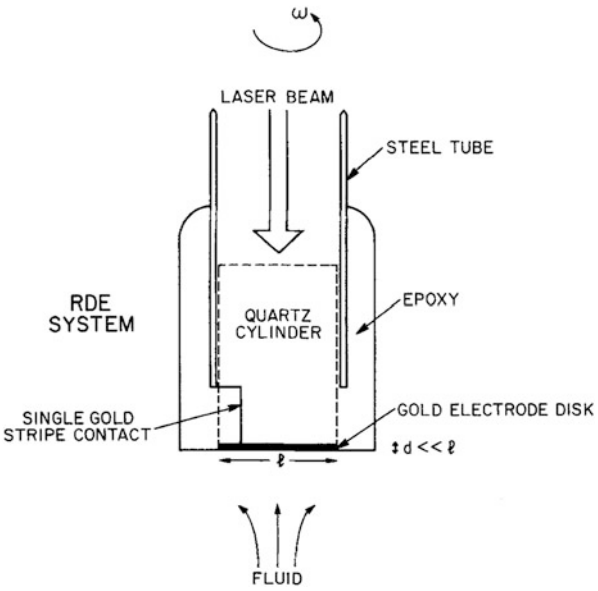

Fig. 4.8 Thermal modulation of an RDE (from [53], with permission)

determine the activation energy of electrochemical processes [56, 57], as well as thermal effects on the limiting current of reversible processes at platinum electrodes [58].

An outstanding example for laser application was investigation of the interface between two immiscible liquids. The scheme of an arrangement is shown in Fig. 4.9. For such systems, laser heating seems to be the only existing way to perform thermoelectrochemical experiments. Ion-transfer entropy across the interface has been determined successfully [59]. For theoretical interpretation of the oscillations caused by thermal modulation, Olivier et al. introduced the term "thermoelectrochemical impedance" [60]. A comprehensive treatment of this term has been given by Rotenberg [61, 62]. The activation energy of the diffusion process has been determined [61], and the studies have been extended to the interface conducting polymer/electrolyte solution [63]. By means of an oscillating IR diode, Aaboubi et al. studied the complex overlapping phenomena at the limiting current region of a vertically oriented electrode and proposed a special transfer function [64].

Instead of continuous modulation, single thermal pulses have been imposed by laser beams. This can be seen as a continuation and an expansion of the temperature-jump technique which had been introduced to study kinetics of ionic processes [36]. The method has found application preferably with single-crystal electrodes [65–70]. Many fundamental quantities have been determined, among them the potential of zero charge (E_{pzc}) of Au(111) [65], the potential of maximum entropy [66, 70], the process of hydrogen adsorption at platinum surfaces [67, 68] and the entropy of double-layer formation [69]. This quantity also has been

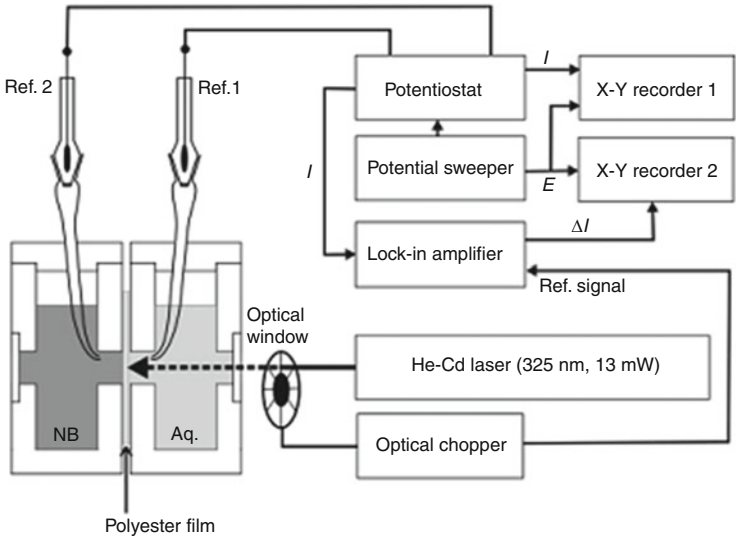

Fig. 4.9 Laser-activated temperature-modulated voltammetry at an interface between immiscible liquids. From [59], with permission

determined for polycrystalline electrodes [71–73]. The implications of the Soret effect at such electrodes have been studied by means of the temperature-jump technique [74–76]. An interesting approach was to apply the technique for determination of solid-state properties in conducting polymers. The temperature jump is generating an electrochemical thermocouple effect which contains information about the nature of carriers (either electrons or holes [77].

A large number of papers dealing with laser-induced temperature jumps were addressed to heterogeneous rate constants in electrochemical kinetics [78–83]. Heterogeneous rate processes have been studied [78], as well as double-layer formation at glassy carbon electrodes [79]. Superfast electrode reactions [80] and short-lived intermediates at electrode surfaces [81, 82] were the subject of investigations. Anodic silver oxidation in the presence of different anions has been studied [83, 84].

Adsorption phenomena were followed by temperature-jump techniques [85–87], and layers of surface-attached species have been analysed [88–91]. Surface modification by gold nanoparticles [89] and by self-assembled monolayers at gold surfaces [90, 91] has been the subject of investigations.

Electrochemical methods of analysis (electroanalysis) have made progress by laser-assisted techniques [44, 92–94]. They were useful to detect ascorbic acid at a carbon electrode in flow injection [44]. Capabilities of pulsed laser beam illumination of gold and platinum disk electrodes were tested with the well-known redox couples toluidine blue, iodide, ferricyanide, ruthenium hexammine and ferrocene (see Fig. 4.10) [92]. Laser-activated voltammetry proved useful for selective removal of impurities from glassy carbon- and boron-doped diamond surfaces [93].

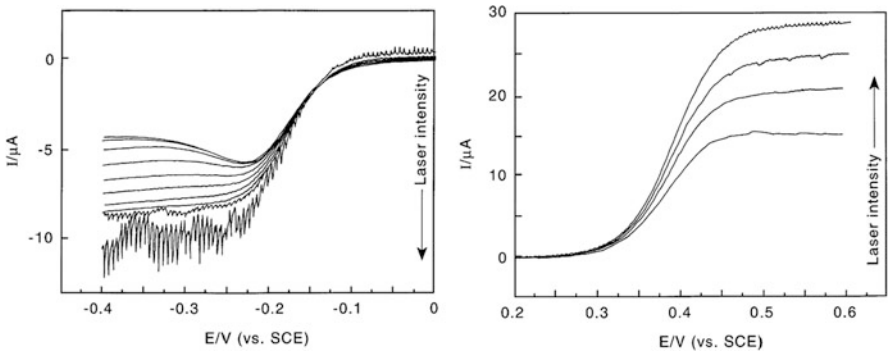

Fig. 4.10 Linear sweep voltammograms (5 mV s^{-1}) at a 1 mm diameter platinum disk electrode subjected to increasing laser intensity (*left*: 0–1.2 W cm^{-2}; *right*: 0–0.8 W cm^{-2}). *Left*: Ru $(NH_3)_6Cl_3$ in 0.1 M KCl; *right*: ferrocene/0.1 M TBAH in acetonitrile. From [92], with permission

Several effects of pulsed lasers at electrode surfaces were studied to find optimum conditions for electroanalytical chemistry [94].

Industrial electroplating processes have been improved by means of laser irradiation [95–102]. Enhancement of plating has been discussed as resulting from acceleration of charge transfer rate, potential changes and thermal stirring effects [95, 96]. Copper plating on different substrates was found to be enhanced by laser application [97, 98]. Laser pulses which strongly interacted with hydrodynamic conditions had a remarkable effect on nucleation and growth of zinc electrodeposits [99, 100]. By means of focused laser beams, maskless surface patterns were generated [101]. Nickel electrodeposition has been discussed [102]. Laser treatment of electrodes has been studied with further industrial electrochemical processes like hydrogen evolution on nickel electrodes [103] and etching of manganese-zinc ferrites in KOH induced by a focused laser beam [104].

An important task of laser activation was cleaning of electrode surfaces in situ [45]. By means of high-power laser beams, organic residues, adsorptive layers and other contaminations have been removed successfully [105–109]. Such treatment procedures proved useful mainly for carbonaceous surfaces [105–108], but also metallic electrodes have been treated by strong lasers, even till plastic deformation occurred [109].

Indirect Electric Heating

Electric heating of electrodes by means of an external heater (indirect electric heating) highly simplifies apparatus in comparison to laser heating. It is advantageous that there is no mutual interference between heating and measuring circuits. Hence, heating can be done by direct current. On the other hand, there is introduced an additional barrier between heater and active electrode surface with the consequence of higher thermal inertia. The insulating layer should be made of material

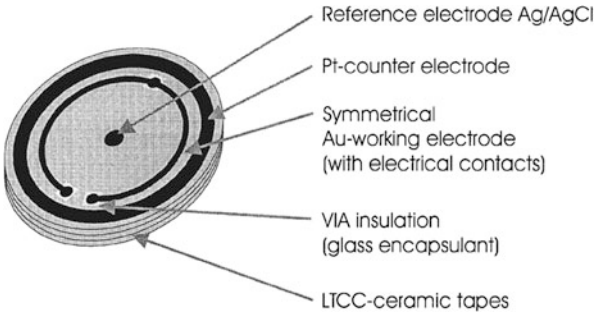

Fig. 4.11 LTCC sensor with indirect heating of a Pt electrode. "VIA" means a conducting hole through a thin ceramic plate. From [114], with permission

with high thermal conductivity. Ceramic materials are preferred. Harima and Aoyagui in 1976 proposed an arrangement consisting of a thin aluminium foil as the heater in close contact with a thin mylar foil carrying a gold film as active electrode [110, 111]. The authors presented a theoretical treatment of transient processes following a rapid temperature perturbation [110], but an experimental application has not been published. Indirect heating of large electrodes was used to study slow processes [112]. An indirectly heated iron disk electrode was used to study thermal calcium carbonate scaling by means of electrochemical impedance studies [113].

Later, indirect electrode heating was rediscovered when a technology of microelectronics has proved useful, namely the *Low-Temperature Cofired Ceramics* (LTCC) [114–119] (Fig. 4.11). In this technique, stacks of thin ceramic plates containing screen-printed patterns are interconnected by vertical holes filled with conducting material (so-called VIAs). Indirectly heated electrodes have been designed with platinum heaters and gold electrodes at the surface. On this basis, a variety of biosensors, among them such with different enzyme layers, have been designed and tested successfully [116–119]. Alternative indirect electrode heating has been proposed based on polysilicon layers [120] and on CMOS structures [121]. With indirectly heated LTCC sensors, rather fast temperature change can be achieved. This gave rise to do experiments with the new thermoelectrochemical technique TPV (temperature pulse voltammetry, see later below), which had been developed originally for hot-wire techniques. Some interesting results for analysis of reactants with sluggish kinetics were obtained, e.g. for nitrogen oxide [114].

Direct Electric Heating: "Hot-Wire Electrochemistry" and "Hot-Layer Electrochemistry"

Joule heating of thin metallic wire electrodes started with some experiments where line frequency was utilised for heating [42, 43]. An important step was the work of Gabrielli and co-workers [122, 123] which heated a 100 µm platinum wire by an

alternating current with a frequency of 250 kHz. The resulting temperature jump of some Kelvin was intended for kinetic studies. The method was useful only for slight temperature changes, since otherwise a strong AC distortion of the electrochemical signal would occur caused by the high-frequency iR drop along the wire. Radio frequency heating of wire electrodes became meaningful when a way had been found to avoid completely this distortion [124]. The principle, sketched in Fig. 4.12, is based on the idea to keep away any AC voltage from the potentiostat working electrode input. It can be assumed that in the frequency region of 100 kHz and more, no substantial faradaic processes will occur. If the working electrode input would be connected "asymmetrically" (like a) in Fig. 4.12), along the wire length, with maximum at the distant wire end, heating current would develop an iR voltage which would be "seen" by the potentiostat input with the result of strong distortion. The first way to compensate for this influence was a symmetric arrangement (like b) in Fig. 4.12) where the working electrode wire is connected to the potentiostat input at the centre between two equal halves of its length. As shown in the figure, now two AC voltage values with opposite sign are "seen" by the working electrode input. This way, the distortion is avoided. Even more elegant is c) in Fig. 4.12, where the electrode wire is not divided, but compensation is made by a bridge arrangement [125]. In this case, protection of potentiostat input is improved further by means of two inductive elements as branches of the bridge. Although direct ohmic heating of thin wires (without isolation between heating and measuring circuits) needs all the precautions described, it is a very powerful method of modern thermoelectrochemistry due to its very short heating-up and cooling-down periods and its inexpensive instrumentation. Experimental details of the technology together with application examples will be given in Chap. 6.

Advantages of direct electrode heating are demonstrated best with heated microwires due to their extremely low heat capacity, the resulting short heating-up period and consequently the chance to do hot-wire electrochemistry above the boiling point without autoclaving. Anyway, when the principle described above had been proven successful for AC distortion compensation, the techniques of direct AC heating have been used not only with thin wires but also with macro structures. Metallic bands made by thin film techniques as well as by screen printing have been tested, also screen-printed carbon electrodes. A special case were heated ITO (indium tin oxide) structures which proved advantageous for electrochemiluminescent studies described further below. Heated carbon paste electrodes have been used also broadly. Paste electrodes can be modified easily by the addition of diverse agents. Examples were pastes made of multi-wall carbon nanotubes modified by agents like ruthenium bipyridyl or by special enzymes. Pastes with ionic liquids as binders also have been used. Application examples of such heated macro structures will be given in the Chap. 6, which is dedicated to the experimental work with electrically heated electrodes.

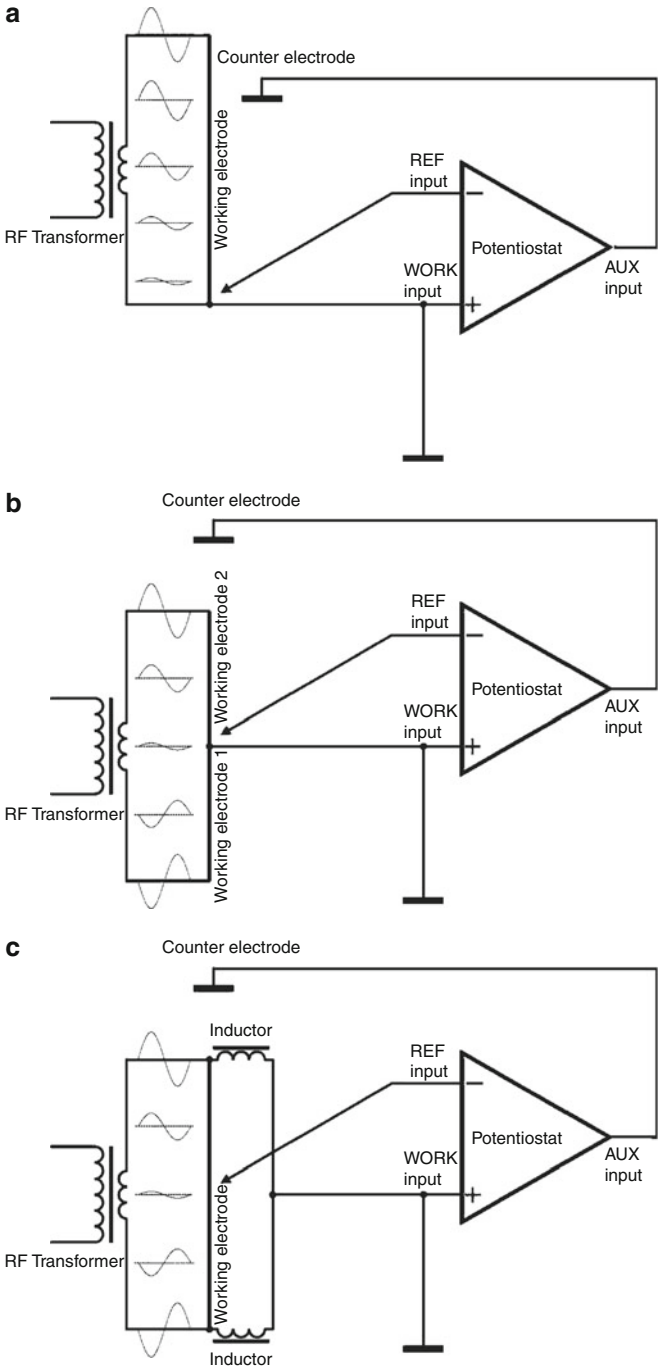

Fig. 4.12 Distortion of potentiostat measuring circuit by AC heating current and its compensation. (**a**) Uncompensated heating (asymmetric arrangement). (**b**) Compensated AC heating (symmetric arrangement). (**c**) Compensated AC heating (bridge arrangement). AC voltage amplitude caused by iR drop of heating current "as seen by the potentiostat" indicated schematically. From [1], with permission

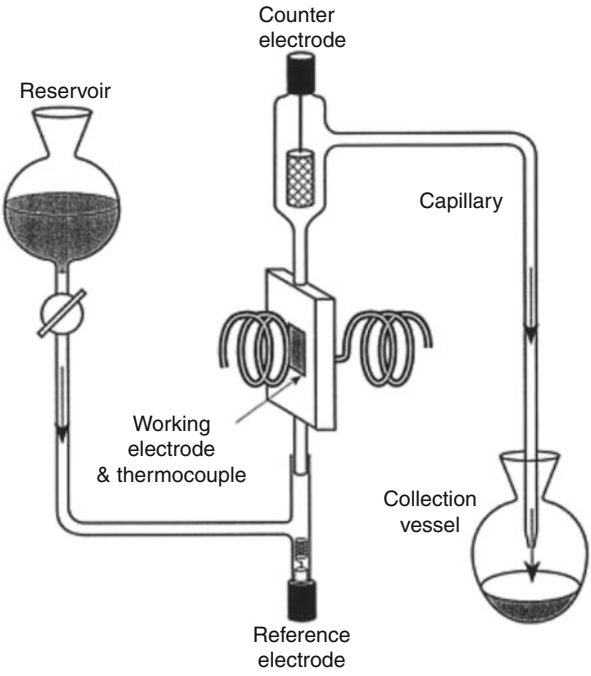

Fig. 4.13 RF-heated electrochemical channel flow system. From [126], with permission

Inductive Heating

As the last method of electrode heating, the inductive heating technique has been mentioned above. Here, eddy currents are induced in metallic electrodes by a strong alternating magnetic field of radio frequency, similar to the action of inductive hot plates on a saucepan. Platinum macroelectrodes have been heated in electrochemical flow-stream cells [126–128], as shown in Fig. 4.13. The method has been tested for analyses of reversible redox couples [126, 127] and of organic redox active compounds [128]. A special advantage is that no galvanic connection exists between heating and measuring circuits.

References

1. Gründler P, Kirbs A, Dunsch L (2009) ChemPhysChem 10:1722–1746
2. Oduoza CF (2004) Chem Eng Process 43:921–928
3. Jacob SR, Hong Q, Coles BA, Compton RG (1999) J Phys Chem B 103:2963–2969
4. Ruther W, Mcmahon JJ, Melendres CA (1986) J Electrochem Soc 133:C304
5. Melendres CA, Mcmahon JJ, Ruther W (1986) J Electroanal Chem 208:175–178
6. Curtiss LA, Halley JW, Hautman J, Hung NC, Nagy Z, Rhee YJ, Yonco RM (1991) J Electrochem Soc 138:2032–2041
7. Lvov SN, Zhou XY, Macdonald DD (1999) J Electroanal Chem 463:146–156

8. Wakabayashi N, Takeichi M, Itagaki M, Uchida H, Watanabe M (2005) J Electroanal Chem 574:339–346
9. Marken F, Sur UK, Coles BA, Compton RG (2006) Electrochim Acta 51:2195
10. Cutress IJ, Marken F, Compton R (2009) Electroanalysis 21:113
11. Compton RG, Coles BA, Marken F (1998) Chem Commun 23:2595
12. Marken F, Tsai YC, Coles BA, Matthews SL, Compton RG (2000) New J Chem 24:653
13. Sur UK, Marken F, Rees N, Coles BA, Compton RG, Seager R (2004) J Electroanal Chem 573:175
14. Ghanem MA, Thompson M, Compton RG, Coles BA, Harvey S, Parker KH, O'Hare D, Marken F (2006) J Phys Chem B 110:17589
15. Marken F, Matthews SL, Compton RG, Coles BA (2000) Electroanalysis 12:267
16. Marken F, Tsai YC, Saterlay AJ, Coles BA, Tibbetts D, Holt K, Goeting CH, Foord JS, Compton RG (2001) J Solid State Electrochem 5:313
17. Tsai YC, Coles BA, Compton RG, Marken F (2001) Electroanalysis 13:639
18. Tsai YC, Coles BA, Holt K, Foord JS, Marken F, Compton RG (2001) Electroanalysis 13:831
19. Ghanem MA, Hanson H, Compton RG, Coles BA, Marken F (2007) Talanta 72:66
20. Ghanem MA, Compton RG, Coles BA, Canals A, Vuorema A, John P, Marken F (2005) Phys Chem Chem Phys 7:3552
21. Ghanem MA, Coles BA, Compton RG, Marken F (2006) Electroanalysis 18:793
22. Ghanem MA, Compton RG, Coles BA, Psillakis E, Kulandainathan MA, Marken F (2007) Electrochim Acta 53:1092
23. Ghanem MA, Compton RG, Coles BA, Canals A, Marken F (2005) Analyst 130:1425
24. Sur UK, Marken F, Coles BA, Compton RG, Dupont J (2004) Chem Commun 24:2816
25. Assiry AM, Sastry SK, Samaranayake C (2003) J Appl Electrochem 33:187
26. Samaranayake P, Sastry SK (2005) J Electroanal Chem 577:125
27. Miller JR (2006) Electrochim Acta 52:1703
28. Srinivasan V, Wang CY (2003) J Electrochem Soc 150:A98
29. Oyanader MA, Arce PE (2008) Lat Am Appl Res 38:147
30. Amatore C, Berthou M, Hebert S (1998) J Electroanal Chem 457:191
31. Bark FH, Kharkats YI, Wedin R (1998) Russ J Electrochem 34:393
32. Kharkats YI, Bark FH, Wedin R (1998) Russ J Electrochem 34:198
33. Ramos A, Morgan H, Green NG, Castellanos A (1998) J Phys D Appl Phys 31:2338
34. Green NG, Ramos A, Gonzalez A, Castellanos A, Morgan H (2001) J Electrostat 53:71
35. Castellanos A, Ramos A, Gonzalez A, Green NG, Morgan H (2003) J Phys D Appl Phys 36: 2584
36. Eigen M (1954) Discuss Faraday Soc 194:17
37. Baranski S (2002) Anal Chem 74:1294
38. Boika A, Baranski AS (2008) Anal Chem 80:7392
39. Boika A, Baranski AS (2011) Electrochim Acta 56:7288
40. Baranski S, Boika A (2012) Anal Chem 84:1353
41. Baranski S, Boika A (2010) Anal Chem 82:8137
42. Ducret L (1961) Comptes Rendus Hebdomadaires des Seances de l Academie des Sciences 252:1948
43. Ducret L, Cornet C (1966) J Electroanal Chem 11:317
44. Ke JH, Tseng HJ, Hsu CT, Chen JC, Muthuraman G, Zen JM (2008) Sens Actuators B 130: 614
45. Akkermans RP, Roberts SL, Marken F, Coles BA, Wilkins SJ, Cooper JA, Woodhouse KE, Compton RG (1999) J Phys Chem B 103:9987
46. Pleskov YV, Rotenberg ZA (1978) J Electroanal Chem 94:1
47. Krivenko G, Kotkin AS, Kurmaz VA (2005) Russ J Electrochem 41:137
48. Krivenko G, Kotkin AS, Kurmaz VA (2005) Russ J Electrochem 41:122
49. Konovalov VV, Raitsimring AM (1985) J Electroanal Chem 195:151
50. Barker GC, Gardner AW (1975) J Electroanal Chem 65:95

51. Miller B (1983) J Electrochem Soc 130:1639
52. Valdes JL, Miller B (1988) J Phys Chem 92:525
53. Valdes JL, Miller B (1988) J Electrochem Soc 135:2223
54. Valdes JL, Miller B (1988) J Phys Chem 92:4483
55. Valdes JL, Miller B (1989) J Phys Chem 93:7275
56. Rotenberg ZA (1993) J Electroanal Chem 345:469
57. Rotenberg ZA (1993) Russ Electrochem 29:941
58. Rotenberg ZA, Dribinskii AV, Lukovtsev VP (1999) Russ J Electrochem 35:395
59. Hinoue T, Ikeda E, Watariguchi S, Kibune Y (2007) Anal Chem 79:291
60. Olivier A, Merienne E, Chopart JP, Aaboubi O (1992) Electrochim Acta 37:1945
61. Rotenberg ZA (1997) Electrochim Acta 42:793
62. Rotenberg ZA (1997) Russ J Electrochem 33:221
63. Rotenberg ZA (2001) Russ J Electrochem 37:113
64. Aaboubi O, Citti I, Chopart JP, Gabrielli C, Olivier A, Tribollet B (2000) J Electrochem Soc 147:3808
65. Climent V, Coles BA, Compton RG (2001) J Phys Chem B 105:10669
66. Climent V, Coles BA, Compton RG (2002) J Phys Chem B 106:5258
67. Climent V, Coles BA, Compton RG (2002) J Phys Chem B 106:5988
68. Garcia-Araez N, Climent V, Feliu JM (2012) Russ J Electrochem 48:271
69. Climent V, Coles BA, Compton RG, Feliu JM (2004) J Electroanal Chem 561:157
70. Climent V, Garcia-Araez N, Compton RG, Feliu JM (2006) J Phys Chem B 110:21092
71. Benderskii VA, Velichko GI (1982) J Electroanal Chem 140:1
72. Benderskii VA, Velichko GI, Kreitus IV (1984) J Electroanal Chem 181:1
73. Benderskii VA, Velichko GI (1984) Sov Electrochem 20:316
74. Smalley JF, Macfarquhar RA, Feldberg SW (1988) Abstracts of Papers of the American Chemical Society 196:121
75. Smalley JF, Macfarquhar RA, Feldberg SW (1988) J Electroanal Chem 256:21
76. Valdes JL, Miller B (1988) J Electrochem Soc 135:C160
77. Geng L, Rubinstein I, Smalley JF, Feldberg SW (1988) Abstracts of Papers of the American Chemical Society 196:47
78. Smalley JF, Krishnan CV, Goldman M, Feldberg SW, Ruzic I (1988) J Electroanal Chem 248:255
79. Jaworski RK, Mccreery RL (1993) J Electrochem Soc 140:1360
80. Benderskii VA, Krivenko AG (1998) Russ J Electrochem 34:1061
81. Benderskii VA (1994) Electrochim Acta 39:1067
82. Bandara A, Kubota J, Onda K, Wada A, Kano SS, Domen K, Hirose C (1998) J Phys Chem B 102:5951
83. Safonov VA, Kiivenko AG, Choba MA (2008) Electrochim Acta 53:4859
84. Safonov VA, Choba MA, Krivenko AG, Manzhos RA, Maksimov YM (2012) Electrochim Acta 61:140
85. Smalley JF, Geng L, Feldberg SW, Rogers LC, Leddy J (1993) J Electroanal Chem 356:181
86. Manzhos RA, Krivenko AG, Podlovchenko BI (2007) Mendeleev Communications 17:258
87. Safonov VA, Choba MA, Krivenko AG, Manzhos RA, Stenina EV, Sviridova LN (2009) Electrochim Acta 54:6499
88. Smalley JF, Newton MD, Feldberg SW (2000) Electrochem Commun 2:832
89. Lowe LB, Brewer SH, Kramer S, Fuierer RR, Qian GG, Agbasi-Porter CO, Moses S, Franzen S, Feldheim DL (2003) J Am Chem Soc 125:14258
90. Smalley JF, Feldberg SW, Newton MD, Chidsey CED (1993) Abstracts of Papers of the American Chemical Society 206:148
91. Smalley JF (2003) Langmuir 19:9284
92. Akkermans RP, Suarez MF, Roberts SL, Qiu FL, Compton RG (1999) Electroanalysis 11: 1191

93. Qiu FL, Compton RG, Marken F, Wilkins SJ, Goeting CH, Foord JS (2000) Anal Chem 72: 2362
94. Brennan JL, Forster RJ (2003) J Phys Chem B 107:9344
95. Puippe JC, Acosta RE, Vongutfeld RJ (1981) J Electrochem Soc 128:2539
96. Vongutfeld RJ, Puippe JC, Acosta RE (1981) Bull Am Phys Soc 26:292
97. Bindra P, Arbach GV, Stimming U (1987) J Electrochem Soc 134:2893
98. Hsiao MC, Wan CC (1991) J Electrochem Soc 138:2273
99. Zouari I, Lapicque F, Calvo M, Cabrera M (1992) J Electrochem Soc 139:2163
100. Zouari I, Calvo M, Lapicque F, Cabrera M (1992) Appl Surf Sci 54:311
101. Zouari I, Pierre C, Lapicque F, Calvo M (1993) J Appl Electrochem 23:863
102. Aaboubi O, Merienne E, Amblard J, Chopart JP, Olivier A (2002) J Electrochem Soc 149: E90
103. Efimov O, Krivenko AG, Benderskii VA (1991) Sov Electrochem 27:401
104. Yung EK, Hussey BW, Gupta A, Romankiw LT (1989) J Electrochem Soc 136:665
105. Hershenhart E, Mccreery RL, Knight RD (1984) Anal Chem 56:2256
106. Poon M, Mccreery RL (1986) Anal Chem 58:2745
107. Poon M, Mccreery RL (1987) Anal Chem 59:1615
108. Rice RJ, Mccreery RL (1991) J Electroanal Chem 310:127
109. Benderskii VA, Efimov IO, Krivenko AG (1991) J Electroanal Chem 315:29
110. Harima Y, Aoyagui S (1976) J Electroanal Chem 69:419
111. Harima Y, Aoyagui S (1977) J Electroanal Chem 81:47
112. Sarac H, Wragg AA, Patrick MA (1993) Electrochim Acta 38:2589
113. Gabrielli C, Keddam M, Maurin G, Perrot H, Rosset R, Zidoune M (1996) J Electroanal Chem 412:189
114. Voss T, Gründler P, Kirbs A, Flechsig GU (1999) Electrochem Commun 1:383
115. Voss T, Kirbs A, Gründler P (2000) Fresenius J Anal Chem 367:320
116. Lau C, Reiter S, Schuhmann W, Gründler P (2004) Anal Bioanal Chem 379:255
117. Lau C, Flechsig GU, Gründler P, Wang J (2005) Anal Chim Acta 554:74
118. Peter J, Reske T, Flechsig GU (2007) Electroanalysis 19:1356
119. Lau C, Borgmann S, Maciejewska M, Ngounou B, Gründler P, Schuhmann W (2007) Biosensors Bioelectronics 22:3014
120. Yang H, Choi CA, Chung KH, Jun CH, Kim YT (2004) Anal Chem 76:1537
121. Trombly N, Mason A (2008) Electron Lett 44:29
122. Gabrielli C, Keddam M, Lizee JF (1983) J Electroanal Chem 148:293
123. Gabrielli C, Tribollet B (1994) J Electrochem Soc 141:1147
124. Gründler P, Zerihun T, Kirbs A, Grabow H (1995) Anal Chim Acta 305:232
125. Wachholz F, Gimsa J, Duwensee H, Grabow H, Gründler P, Flechsig GU (2007) Electroanalysis 19:535
126. Qiu F, Compton R, Coles B, Marken F (2000) J Electroanal Chem 492:150
127. Moorcroft MJ, Lawrence NS, Coles BA, Compton RG, Trevani LN (2001) J Electroanal Chem 506:28
128. Coles BA, Moorcroft MJ, Compton RG (2001) J Electroanal Chem 513:87

Chapter 5
Dynamic Processes in Cells with Heated Electrode–Solution Interfaces

The flow of thermodynamic quantities, preferably entropy, from a heated region to the colder bulk solution, has been discussed in Chap. 2. Thermodynamic quantities cannot be measured directly but have to be calculated. For practical purposes, knowledge of measurable quantities is more interesting. In an electrochemical experiment with heated electrode–solution interfaces, two streams across the interface can be stated, namely heat and matter. Heat is transported since hot and cold zones are in contact, and also to a much lower extent, by reaction heat. Matter is transported as a result of electrochemical processes which give rise to generate or to consume electroactive particles, respectively, as soon as a current is flowing. As a result, two profiles will form near to the interface. We can expect a profile $T = f(x)$, the temperature profile, and $c = f(x)$, the concentration profile. The symbol x denotes the distance from the hottest place. Both profiles can be calculated as given below, and both are very important for the interpretation of electrochemical results in cells with heated interfaces. Knowledge of the profiles can answer important questions, among them the question which maximum temperature can be obtained with a given heating arrangement or the question how the thermal stirring effect is affecting the shape of voltammograms.

It is important to keep in mind that there are differences in behaviour of heated solid electrodes or of heated solution spots close to the electrode. With heated electrodes, heat is streaming as a result of heat conduction from the electrode to solution, whereas in heated solution spots energy may be injected directly into solution, without conduction effects. For profiles at heated solid electrodes, an additional phenomenon has to be considered, namely the existence of adhesion forces between the solid material of the electrode and the molecules of the solvent. This way, a rather complex layer structure can be formed. For heated metallic microwire electrodes, highly efficient calculation methods have been developed. For other methods, there does not exist a comparable theoretical basis.

A very important point is the contribution of solvent properties to the overall behaviour of heated electrodes. There exists a fundamental difference between water and all other common solvents. The surface tension of water is

P. Gründler, *In-situ Thermoelectrochemistry*, Monographs in Electrochemistry,
DOI 10.1007/978-3-662-45818-1_5

extraordinarily high. As a result, formation of vapour bubbles needs considerable activation energy. Consequently, a region with overheated solvent exists for a relatively long time until the boiling process is starting. This special behaviour can be utilised to do experiments in overheated water without any pressurising. With non-aqueous solvent, a similar chance generally does not exist. With such solvents, heated solution layers with temperature above the boiling point are difficult to obtain, even for short-time measurements.

5.1 Temperature Profile and Concentration Profiles

As mentioned above, two similar transport phenomena may take place on a heated electrode, namely:

1. Heat transfer—the transport of thermal energy from a body with higher temperature (the electrode) to another body with lower temperature (the electrolyte solution)
2. Diffusion of particles from regions with higher concentration to regions with lower concentration

Typically, heated electrodes do not assume temperature values high enough to initiate remarkable heat transfer by thermal *radiation* within the timescale and under the conditions considered here. The remaining processes, *conduction* and *convection*, must be accounted for. It can be shown that the effects of the partial processes mentioned may be calculated individually if their differing timescales are considered. In a short time interval after start of heating, conduction is predominant due to the fact that convection will start delayed as a consequence of solvent molecules' inertia. It will be shown that the end of the "conduction period" (heat transported inside a nearly stagnant fluid) and its transition into a "convection period" can be clearly distinguished following the progress of electrolytic current. This way, heat transfer at heated thin wires has been calculated satisfactorily. Many other principles ruling the behaviour of heated interfaces have been discovered with heated thin wire experiments, i.e. with *hot-wire electrochemistry*. Many considerations hold true for all kinds of heated electrode bodies, but possibly not for methods where a hot solution spot is generated close to the tip of a microelectrode.

Transport of *heat by conduction*, and of *matter by diffusion*, follows analogous mathematical principles, namely *Fourier's law of heat conduction* and *Fick's first law of diffusion*. Both are differential equations. If we simplify the problem and start with the one-dimensional form, we consider two ordinary differential equations,

$$\frac{\mathrm{d}Q}{\mathrm{d}t} = -\lambda \frac{\mathrm{d}T}{\mathrm{d}x} \quad \text{Fourier's law} \tag{5.1}$$

$$\frac{dn}{dt} = -D\frac{dc}{dx} \quad \text{Fick's first law of diffusion} \tag{5.2}$$

In the above equations, Q means thermal energy, n the number of moles transferred, t the time, x the distance between electrode surface and a point inside electrolyte, T the temperature and c the concentration of particles taking part in the electrochemical reaction considered. The proportionality constants at the right side of equations are λ the *thermal conductivity* (common unit W cm^{-1} K^{-1}) and D the *diffusion coefficient* (common unit cm^2 s^{-1}). D and λ are considered here to be constants.

If temperature changes at heated wire electrodes are followed continuously, evidence for the existence of a convection-free time period after start of heating can be clearly seen. Actual surface temperature often exhibits a time function like that sketched in Fig. 5.1. It can be explained as follows. Immediately after heating has been started, temperature rises linearly since thermal energy is transferred exclusively by *conduction* into a quiescent solution region. Starting thermal *convection* tends to restrict the slope of temperature rise more and more as a result of increasing "cooling" the wire by convection. Often a current maximum is observed (more expressed with horizontally oriented heated wires) followed by an infinite period with constant temperature. The latter indicates a stationary state where addition of thermal energy from the external source equals the thermal energy transported away from the electrode surface by convection. The duration of the initial time period without convection where heat conduction is the predominating process can be estimated in aqueous solution to be in the range of some tenths of a second. Interestingly, current versus time function during the start period is geometrically similar, independent of heating intensity, and even independent of the wire orientation (vertical or horizontal, respectively). If the curves are scaled to

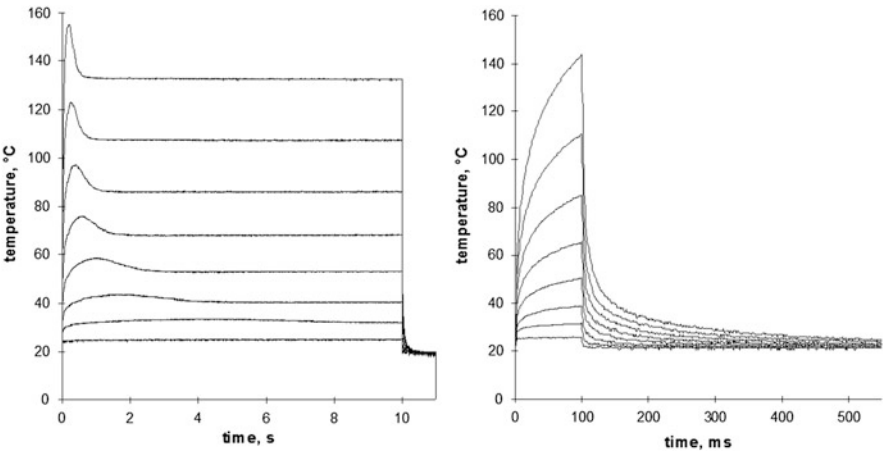

Fig. 5.1 Temperature rise and decay for a horizontally oriented wire electrode (Pt, 25 μm diameter) heated by constant power of different magnitudes. From [1], with permission

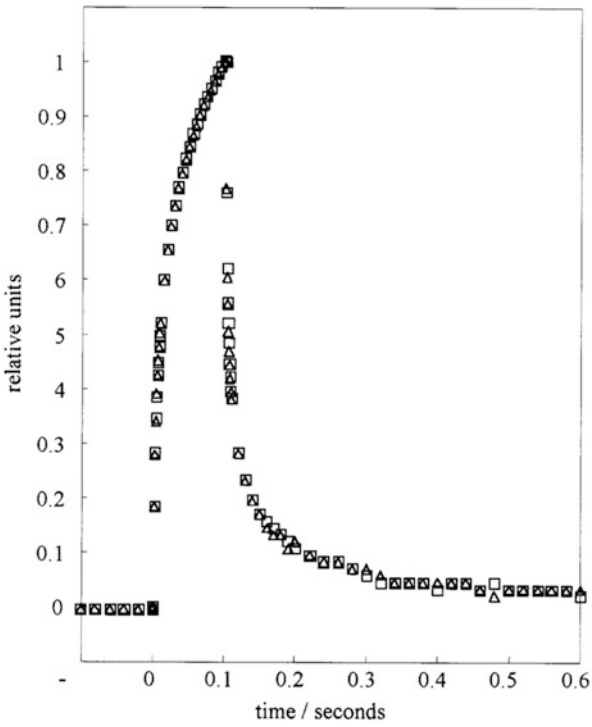

Fig. 5.2 Initial temperature rise and decay during convection-free start period. Platinum wire 25 µm heated by current values 0.1–1 A, resulting in surface temperatures between 22 and 200 °C. Ordinate values are given by fractions of the maximum temperature reached 100 ms after heating start. From [2], with permission

equal amplitude at a given time, they are completely congruent (Fig. 5.2). Insensitivity to orientation is a further indication for the absence of convection in the start period.

Analytical solution of the differential equations given above is not useful or even impossible. The problems of heat transport as well as of particle diffusion can be solved much better by digital simulation. This way, the temperature profiles dT/dx as well as the concentration profiles dc/dx have been calculated for the convection-free period existing at a heated wire electrode of 25 µm in diameter. For this purpose, the solution surrounding the wire is separated in cylindric shells, so as if it would consist of nested valves (Fig. 5.3). The dimensions of individual shells should be small enough to allow utilisation of linear equation forms of heat conduction and of diffusion, respectively. Linear transport of heat or matter into every "ring" as well as away from it is calculated for consecutive short time intervals Δt by means of only two equations:

$$\frac{\Delta Q}{\Delta t} = -k\frac{\Delta T}{\Delta x} \tag{5.3}$$

and

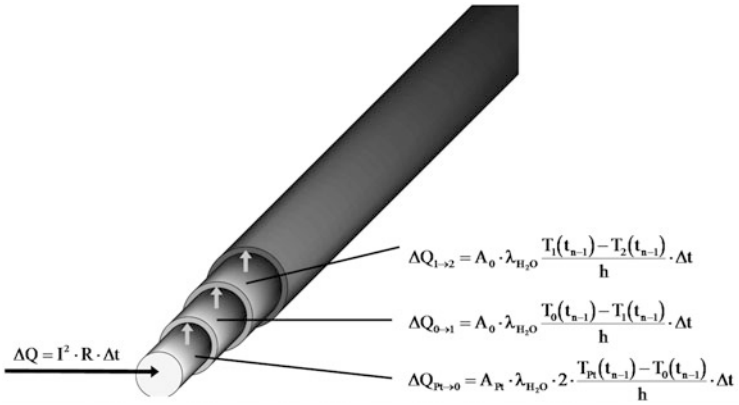

Fig. 5.3 Box model for digital simulation of temperature profile around a heated microwire electrode. From [3], with permission

$$\frac{\Delta n}{\Delta t} = -D\frac{\Delta c}{\Delta x} \tag{5.4}$$

The actual temperature encountered in every individual shell results from the difference between the heat amounts transferred into and out of it. Figure 5.3 illustrates the procedure.

The calculations discussed here can be performed as usual, by means of a program evaluating a series of equations. Alternatively, in the example discussed here, the calculation has been done by means of a spreadsheet calculation table where the consecutive cylindric shells are symbolised by columns. A simple macro initiating consecutive copying one column at the place of the aforegoing one allowed highly efficient simulation even by means of slow PCs. A typical result, plotted in form of three-dimensional graph, is shown in Fig. 5.4. A more detailed description of the applied calculation procedure is given in Appendix A of this book.

The described simulation results can be verified by comparing the calculated temperature for one special place, namely the radius of the heated wire, with the surface temperature values measured by independent methods. Agreement for the given example (platinum wire 25 μm in diameter) was excellent when T was determined by means of temperature-dependent potential shift (see later below).

The calculations confirm the expectation that temperature profiles extend into solution much farther than concentration profiles if reduction or oxidation processes take place at one and the same electrode. A general rule says that the thickness of the temperature profile is about five times that of the concentration profile. All concentration changes occurring at heated electrodes display inside a much thicker zone of increased temperature. This zone is of constant dimensions as soon as the stationary state (see Fig. 5.1) is attained. Consequently, electrochemical reactions take place in a zone of stabilised, well-known temperature, just like in some kind of

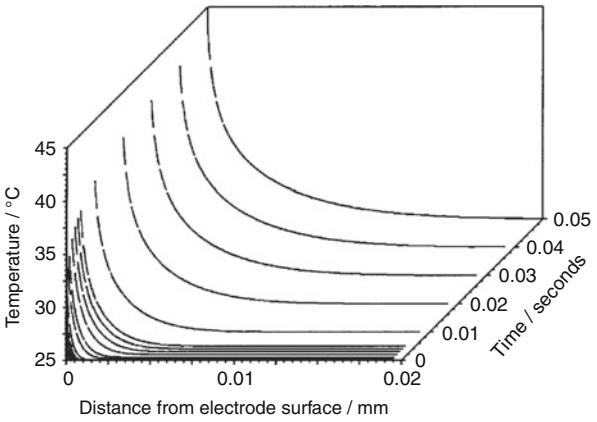

Fig. 5.4 Temperature distribution around a heated wire 25 µm in diameter in aqueous solution. From [2], with permission

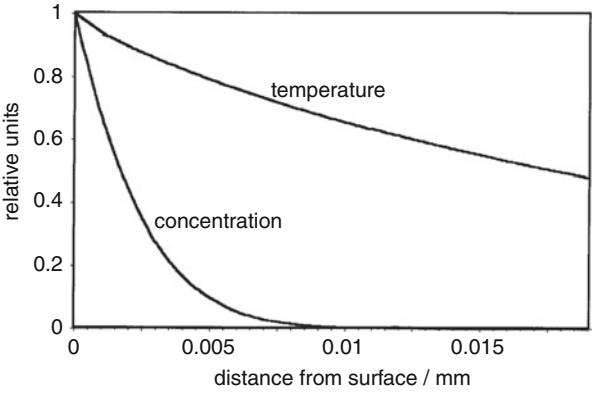

Fig. 5.5 Concentration and temperature profiles after 10 ms of constant current electrolysis at an electrode wire of 25 µm heated by constant electric power. From [2], with permission

micro-thermostat (Fig. 5.5). This special feature of permanently heated microelectrodes will be discussed further in Sect. 6.4 where experiments with permanent heating are described.

5.2 Thermal Convection and Streaming Phenomena

In continuation of the aforegoing discussion, the stationary state at a permanently heated electrode (with focus on cylindric microelectrodes) will be considered. Obviously, we see a near-electrode zone where, caused by heating, the temperature differs from that of bulk solution. Outside this zone, convection is mixing everything, i.e. temperature is approximately ambient, and concentrations are at their initial values (if the volume of bulk solution is large enough to absorb completely any changes emanating from a microelectrode surface).

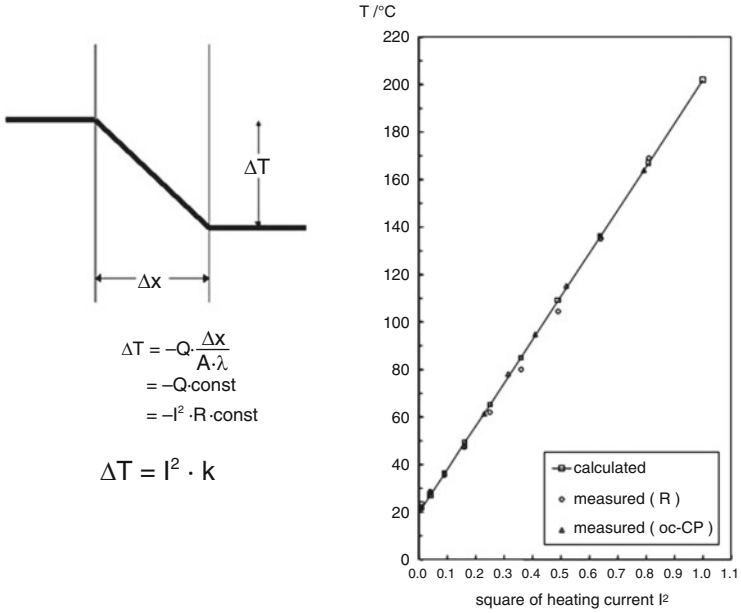

Fig. 5.6 *Left*: Schematic representation of the temperature profile between a heated electrode surface and the constant temperature bulk solution in stationary state. The profile should persist permanently, if thermal energy is added as constant stream (see text). *Right*: Linear function $T = k{\cdot}P = k'{\cdot}I^2$ means constant Δx independent of actual heating conditions. From [4], *left*, and [5], *right*, with permission

Adapting Nernst's considerations which led him to propose the model of the well-known "Nernst diffusion layer", one could expect to find in stationary state a linear temperature profile between heated surface and the boundary marking the end of the increased temperature zone (see Fig. 5.6, left). If heat is added continuously as a constant stream (i.e. with electric heating power $P_{\text{heat}} = \text{const}$), then the sketched profile should persist permanently. The system has reached then the stationary state where heat energy streaming in is equal to the energy streaming out by conduction and convection. This predicted behaviour was verified by heating a wire with constant AC current, i.e. with constant power ($P = I^2{\cdot}R = Q/t = \text{const}$).

Dependence of stationary state electrode temperature on heating power, when displayed in form of a graph T versus I^2 (Fig. 5.6, right), often forms a straight line, i.e. temperature is proportional to the heating power. This is evidence that thickness of the thermal layer Δx_{th} with permanent heating must be more or less constant independent of heating intensity and actual surface temperature. This unexpected finding has been obtained by experiments with heated thin wire electrodes.

As stated above, the layer containing the temperature profile seems to possess a complex substructure. If, at a permanently heated wire electrode, a voltammetric experiment is performed, then, as mentioned above, a constant limiting current is found. It seems that inside the region with $T \neq T_0$ exists a *stagnant layer*, although just at places nearest to the electrode surface should act the strongest forces to cause

convection. The existence of such stagnant solution layer at the electrode surface has been verified experimentally; even its thickness was determined [6]. At present, the electrically heated microwire electrode is the best-studied device, although the insights are valid for electrodes heated by other techniques, and to some extent also for devices where hot solution spots are generated. At a 25 μm platinum wire electrode in aqueous solution, a stagnant layer with thickness of ca. 8 μm has been found. Particles can cross this layer only by diffusion. Evidence for this phenomenon has been achieved by the procedure described in the following. It is based on the fact that at wires of 25 μm, planar as well as cylindric diffusion may occur, depending on the timescale.

A continuously heated wire electrode after a time less than 1 s will assume a stationary state, where the energy added by constant heating current is equal to the heat energy lost into bulk solution by thermal conduction. If cyclic voltammetry is done in this stationary state with very slow scan rate, we can assume that the growing diffusion layer (the region where electrolysed constituents either are consumed or generated) has time enough to extend until the boundary of the thermal distribution layer is reached. Consequently, at every time during CV recording with very slow scan rate, a diffusion layer of constant thickness is present. Cyclic voltammograms under these conditions have sigmoidal shape, like, e.g., with a rotating disk electrode (RDE). With faster scan rates, the diffusion layer thickness is no longer constant. The diffusion layer grows into the stagnant layer in the same way as it would be at an electrode in non-stirred isothermal solution. Resulting are the well-known peak-shaped cyclic voltammograms. The shape of voltammograms changing with scan rate is demonstrated in the example given in Fig. 5.7.

Already the form of voltammograms with peak shape shows that there must by some kind of a stagnant layer. More detailed information has been achieved by

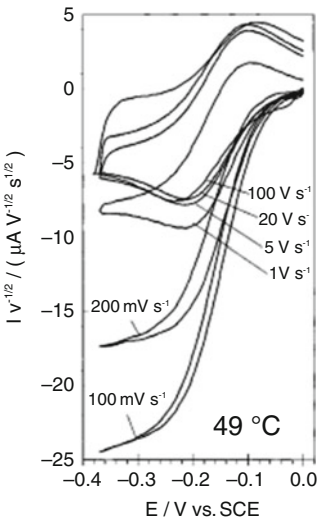

Fig. 5.7 Cyclic voltammograms with different scan rates (100 mV s^{-1} to 100 V s^{-1}) for the reduction of 1 mM $[Ru(NH_3)_6]^{3+}$ in aqueous KCl solution at a continuously heated Pt-wire electrode ($l = 1$ cm, $d = 25$ μm) at 49 °C. From [6], with permission

means of the theory of cylindric diffusion [7]. In the present case, at the start of measurement, thickness of diffusion layer Δx is small compared to electrode radius, i.e. the corresponding diffusion is of planar character and can be described by the classic equation of Randles and Ševčik with Δx as a function of scan rate v:

$$\Delta x(v) = \frac{1}{0.44629(zFv/RTD)^{\frac{1}{2}}} \tag{5.5}$$

with the scan rate v, the gas constant R, the Faraday constant F and the diffusion coefficient D.

As soon as the growing diffusion layer is reaching a critical value with decreasing scan rate, it will no longer be small compared to the wire radius. It cannot be considered to be *planar*, but from this moment it will change more and more to a curved, i.e. *cylindric*, character. Start of cylindric diffusion can be detected by analysing the value of the "apparent diffusion coefficient" $D_{obt} = f(\log v)$. If the classic equation (5.5) will deliver an "exotic" value of D_{obt}, far from reality, obviously cylindric diffusion is predominant. For cylindric diffusion, a modified form of the Randles–Ševčik equation has been derived [7]:

$$I_p = \left(0.44629 + 0.3435\left(r\left(\frac{zFv}{RTD}\right)^{\frac{1}{2}}\right)^{-0.845}\right) \cdot zFAc_{bulk}D\left(\frac{zFv}{RTD}\right) \tag{5.6}$$

with r the wire radius and A the electrode area. Equation (5.6) cannot be solved algebraically to obtain the diffusion coefficient, but the latter can be evaluated from the peak current by means of a simple iteration procedure. The determined D_{obt} under isothermal conditions, i.e. at a non-heated electrode, yields constant values as expected. At a heated electrode the D_{obt} values stay constant as well. If, however, the scan rate is lower than a certain critical value, then D_{obt} shows a sudden increase in the diagram $D_{obt} = f(\log(v))$, as shown in Fig. 5.8. At even lower scan rates, a

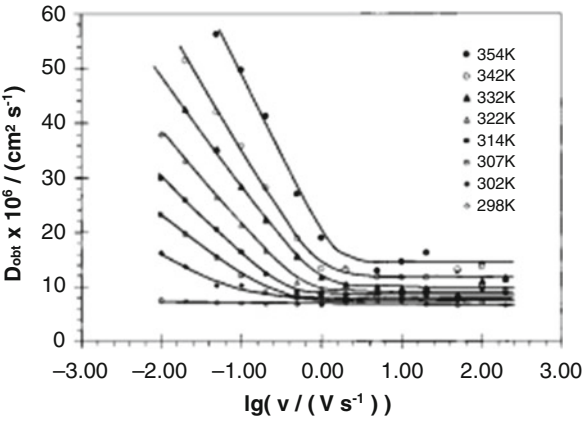

Fig. 5.8 "Obtained" diffusion coefficients D_{obt} from the peak or steady-state currents of cyclic voltammograms with different scan rates (10 mV s^{-1} to 200 V s^{-1}) of 1 mM $[Ru(NH_3)_6]^{3+}$ in aqueous KCl solution (0.1 M) at a continuously heated Pt-wire electrode ($l = 1$ cm, $d = 25$ µm) at different temperatures (25–81 °C). From [6], with permission

limiting current is obtained, and at higher scan rates, peak-shaped current is observed without any influence of the thermal flux.

At higher scan rates, i.e. for a very thin diffusion layer, the real diffusion coefficient D can be expressed as the limiting value of the D_{obt} values for high scan rates $D = \lim_{v\to\infty} D_{\mathrm{obt}}(v)$. From the limiting current at scan rates below the critical value, and the diffusion current at high scan rates, the thickness of the diffusion layer can be evaluated for each temperature at the electrode by means of Eq. (5.7).

$$\Delta x(T) = \frac{zFAc_{\mathrm{bulk}} \lim\limits_{v\to\infty} D_{\mathrm{obt}}(v,T)}{\lim\limits_{v\to 0} I_{\mathrm{lim}}(v,T)} \tag{5.7}$$

So far, it is quite pleasing to have a procedure which allows to determine diffusion coefficient values as well as the thickness of the diffusion layer simply by evaluating one experimental series. It was unexpected, however, to see that the diffusion layer thickness with increasing temperature tends to approach a constant value (Fig. 5.9). This is surprising since the flux is increasing rapidly with temperature, and the real diffusion layer is not even homogeneous.

With increasing electrode surface temperature, the stationary diffusion layer thickness is decreasing very rapidly and reaches a limiting value of about 8 μm at a temperature larger than 20–30 K compared to the bulk temperature. In this region the limiting current is proportional to the real diffusion coefficient. This result has been confirmed by chronoamperometric experiments where the Cottrell decay was evaluated [6].

The existence of a stagnant layer inside the thermal distribution layer was a surprising discovery. It is very meaningful for all practical applications of hot-wire

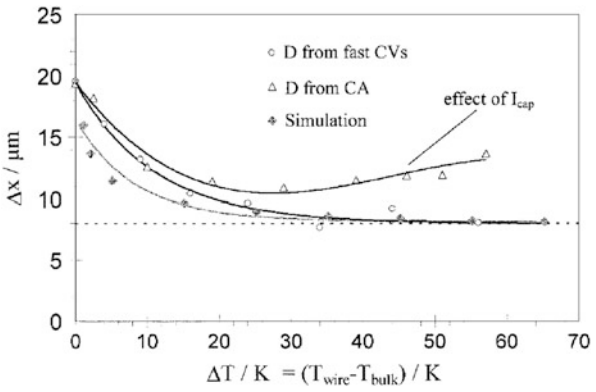

Fig. 5.9 $\Delta x(T)$ calculated from experimental and simulated limiting currents I_{lim} and from the determined diffusion coefficients by fast cyclic voltammetry and short time chronoamperometry and using D (25 °C) $= 6.1 \times 10^{-6}$ cm^2 s^{-1} and $E_{\mathrm{A}} = 14.6$ kJ mol^{-1} (0.151 eV) in case of the simulation, respectively. Experimental techniques applied are cyclic voltammetry (CV) and chronoamperometry (CA). From [6], with permission

electrochemistry. It allows to do analytical determinations in a very convenient way. It is just necessary to choose a low scan rate and to evaluate the resulting sigmoidal voltammograms. Their limiting current is concentration proportional over many decades. On this basis, electrochemical sensors for use in environmental research have been constructed. Electrode heating gives the additional advantage to utilise electrode reactions which are not applicable under room temperature conditions due to their sluggish response. Such methods are useful even for volatile or heat-sensitive constituents since with heated microelectrodes, the bulk solution keeps free from increased temperature. Examples can be found in the next chapter, among them a voltammetric sensor for dissolved oxygen.

5.3 The Complex Layer Structure at a Heated Thin Cylinder Electrode and Consequences for Voltammetry

As mentioned above, for thin microwire electrodes there exists a well-established theoretical basis. As a summary of the discussion in the aforegoing Sects. 5.1 and 5.2, we can make the following statements:

- The thermal layer (thermal distribution layer) is of constant thickness. Evidence is given by the experimentally verified strict proportionality between square of heating current and surface temperature (see Sect. 5.2 and Fig. 5.6).
- Inside the thermal layer, a much smaller stagnant liquid layer is found. This layer is of constant thickness. Electroactive particles can cross this layer only by diffusion. The layer is independent of external stirring and independent of actual temperature over a broad range of conditions. For aqueous solutions, thickness of this stagnant layer is ca. 8 μm.
- Voltammograms at heated thin wire electrodes can assume two different shapes. For fast scan rates, cyclic voltammograms have the common peak-shaped form, since their diffusion layer is not of constant thickness, but is growing inside the stagnant solution layer. For very slow scan rates, the diffusion layer always has time enough to grow until the boundary of the stagnant layer has been reached. Consequently, the diffusion layer is always of constant thickness, and sigmoidal curve shape is obtained.

Sigmoidal voltammograms are useful for analytical applications since the constant limiting current can be measured easily and since it is concentration proportional over many decades. This behaviour is desirable for electrochemical sensors. An interesting question is whether the limiting current can be calculated in a similar manner as this is common with traditional voltammetric electrodes (the so-called hydrodynamic electrodes). A prominent hydrodynamic electrode is the RDE. Another well-known type is the famous dropping mercury electrode which has

been the basis of polarography. For the limiting currents, two famous equations have been derived:

$$I_{\mathrm{L}} = 0.620 \cdot z \cdot F \cdot A \cdot c_{\infty} \cdot D^{\frac{2}{3}} \cdot \nu^{-\frac{1}{6}} \cdot \varpi^{\frac{1}{2}} \tag{5.8}$$

Levich equation for the RDE
and

$$\overline{I}_{\mathrm{L}}(t) = 607 \cdot z \cdot c_{\infty} \cdot D^{\frac{1}{2}} \cdot m^{\frac{2}{3}} \cdot \tau^{\frac{1}{6}} \tag{5.9}$$

Ilkovič equation for the dropping mercury electrode

The symbols are A surface area of the rotating disk, c_{∞} bulk concentration, v kinetic viscosity, ω angular rotation rate, m mercury flow rate and τ mercury drop life time.

Both equations provide an expression for the magnitude of the diffusion-limited current. The latter is attained with applied potentials far from equilibrium. For reduction of metallic ions, e.g., this means high cathodic values. Then, the surface concentration of the reduced ion has reached zero and cannot be decreased further by potential variation. In this region, the diffusion layer is of constant thickness. The concentration profile does no longer vary with polarisation potential, since it corresponds to a typical Nernst diffusion layer between $c(\text{surface}) = 0$ and $c(\text{bulk}) = c_{\infty}$. As a result, a constant, strictly concentration proportional limiting current is obtained.

In both equations cited above, the limiting current is expressed as a function of the mechanical "source" of convection, since the diffusion layer thickness Δx is determined by this source. The limiting current is directly proportional to Δx. In the Levich equation, the source of convection is the rotation rate of the electrode axis, ω. In the Ilkovič equation, the corresponding source of convection is a function of mercury flow rate m and drop life time τ, namely the product $m^{\frac{2}{3}} \cdot \tau^{\frac{1}{6}}$. The question is whether for permanently heated electrodes also an equation for the constant limiting current can be derived. As the source for thermal convection, the heating current magnitude can be assumed. The action of this "source", however, is much more complex than just exciting mechanical stirring. Additional to the mechanic forces caused by temperature-dependent density differences, effects on viscosity of the solvent and on the diffusion coefficient of electroactive constituents have to be considered. The desired equation, thereby, can be expected to be not a simple analogue to Levich or Ilkovič equations, respectively.

A good starting point for derivation of an equation $I_{\mathrm{lim}} = f(I_{\mathrm{heat}})$ is the existence of a constant stagnant layer inside the thermal distribution layer. This layer is identical to the diffusion layer for the case of diffusion-limited current. It was shown further above how the thickness of the stagnant layer can be calculated. Furthermore, we know the temperature dependence of the limiting current. It should be identical to the temperature dependence of the diffusion coefficient for the given conditions. For D, an equation of Arrhenius type is valid:

$$D = D^* \exp\left(-\frac{E_A}{RT}\right) \tag{5.10}$$

Indeed, an Arrhenius-type temperature dependence was verified experimentally for different electroactive species. For the current density $j_{lim} = I_{lim}/A$ follows:

$$j_{lim} = \frac{D^* \cdot zF \cdot c_\infty}{\Delta x_{diff}} \exp\left(-\frac{E_A}{RT}\right) \tag{5.11}$$

with Δx_{diff} thickness of the diffusion layer.

For j_{lim} as a function of the heating current i_{heat} we will get

$$\begin{aligned} j_{lim} &= D^* \frac{zFc_\infty}{\Delta x_{diff}} \exp\left(-\frac{E_A}{R\left(i_{heat}^2 k_1 + T_\infty\right)}\right) \\ \text{with } k_1 &= \frac{\rho \cdot \Delta x_{th}}{2\pi^2 r^3 \lambda_{sol}} \end{aligned} \tag{5.12}$$

In this equation, Δx_{th} is the thickness of the thermal distribution layer.

By series expansion, the following approximation was found:

$$\begin{aligned} j_{lim} = &\frac{D^* \cdot zF \cdot c_\infty}{\Delta x_{diff}} \exp\left(-\frac{E_A}{RT_\infty}\right) + \frac{D^* \cdot zF \cdot E_A \cdot c_\infty}{\Delta x_{diff} \cdot R \cdot T_\infty^2} \cdot \exp\left(-\frac{E_A}{RT_\infty}\right) \cdot (T - T_\infty) \\ &+ \frac{D^* \cdot zF \cdot c_\infty}{\Delta x_{diff}} \left(\frac{E_A^2}{2R^2 \cdot T_\infty^4} - \frac{E_A}{R \cdot T_\infty^3}\right) \cdot \exp\left(-\frac{E_A}{RT_\infty}\right) \cdot (T - T_\infty)^2 \end{aligned} \tag{5.13}$$

For better handling of the above equation, we may introduce the common values of the variables, and get with $T_\infty = 298$ K and $\Delta T = T - T_\infty$:

$$\begin{aligned} j_{lim} &= 6.6 \times 10^{-3} + 1.16 \times 10^{-4} \cdot \Delta T + 6.31 \times 10^{-7} \cdot (\Delta T)^2 \\ &= A_1 + B_1 \cdot \Delta T + C_1 \cdot (\Delta T)^2 \end{aligned} \tag{5.14}$$

Finally, j_{lim} can be expressed as function of heating current i_{heat}:

$$j_{lim} = A_2 + B_2 \cdot i_{heat}^2 + C_2 \cdot i_{heat}^4 \tag{5.15}$$

Equation (5.15) for heated cylindric wires plays the role which Levich equation does for RDEs. It can be considered to be some kind of a fundamental relationship for heated electrodes. It can be clearly seen that the heating current has a more complex effect than just to excite mechanic agitation.

References

1. Gründler P, Kirbs A, Zerihun T (1996) Analyst 121:1805–1810
2. Gründler P (2000) Fres J Anal Chem 367:324–328
3. Gründler P (1998) Fres J Anal Chem 362:180–183
4. Gründler P, Beckmann A (2004) Anal Bioanal Chem 379:261–265
5. Gründler P, Flechsig GU (2006) Microchim Acta 154:175–189
6. Beckmann A, Coles BA, Compton RG, Gründler P, Marken F, Neudeck A (2000) J Phys Chem B 104:764–769
7. Neudeck A, Dittrich J (1991) J Electroanal Chem 313:37–59

Chapter 6
Working with Electrically Heated Electrodes

Experiments with indirect electrode heating can be done without any special precautions and with all the common equipment available for electrochemical investigations. Additionally, there is necessary only some kind of heating power supply. Commercial units are suitable and even simple line transformers have been utilised. With indirect heating, it does not matter whether DC or low frequency AC is applied.

Direct electrode heating requires a medium power radio frequency supply and the compensation circuitry described. Otherwise, huge AC distortions would occur in the measuring circuit. Somewhat higher are the requirements for pulse heating which allows high-temperature electrochemistry. In this case, the heating current must be triggered by the electrolysis circuitry where normally a potentiostat is located. Some commercial instruments allow such triggering within their measuring sequences. They can be completed then by a simple AC heating unit which contains an input for trigger signals. Alternatively, special instrumentation has been proposed which contain modules for electrochemical measurements as well as for AC heating. In this case, a dedicated software solution is important. An example will be mentioned below and further described in Appendix B.

Direct electric heating has been applied with a large variety of electrode designs including flat structures, heated paste reservoirs, etc. Some of them are *macro*electrodes which normally are restricted to *permanent heating* experiments. The familiar term "hot-wire electrochemistry" traditionally is used preferentially for experiments with *pulsed heating* where *micro*electrodes are in use.

6.1 Heated Wires (Hot-Wire Electrochemistry)

This chapter is dedicated explicitly to the "hot-wire electrochemistry", since, at present, it represents the only fully developed technique in the inventory of modern thermoelectrochemistry. It has found its way into the analytical laboratory. Also,

P. Gründler, *In-situ Thermoelectrochemistry*, Monographs in Electrochemistry,
DOI 10.1007/978-3-662-45818-1_6

seemingly it played the role of some kind of catalyst to restart further development of older methods like laser activation of electrodes and establishment of alternative techniques like microwave electrochemistry.

Some of the technical characteristics of hot-wire electrochemistry have been summarised in several papers with experimental orientation [1–6]. The term "Hot-Wire Electrochemistry" became familiar after it had been mentioned first in a scientific discussion.

6.1.1 *Heated Microwires and Their Virtual "Absurd" Characteristics*

There are good reasons for the preference of thin noble metal wires with diameter in the sub-millimetre range in hot-wire electrochemistry. Early contributions date back to 1983 [7]. Experiments with non-metallic electrode materials were not very successful. Glassy carbon fibres are not sufficiently inert to heat them in electrolyte solution; furthermore, their higher specific resistivity does not meet the requirements of direct heating by alternating current. To achieve a sufficient temperature, heating AC amplitude must be high. Consequently, a large iR drop is generated which might cause electrolytic processes as well as strong AC distortions in the measuring circuitry. To counteract, electrode wires with larger diameter would be necessary. Such electrodes are not characterised by the extraordinary properties of microelectrodes.

Noble metal wires can be handled manually without special precautions down to a diameter of ca. 25 μm. Platinum and gold wires of such diameter have been proven and tested successfully to be used as hot-wire electrodes. Their resistance should be in the range of some ohms altogether. With an overall resistance too low, the electric contacts would become a more and more detrimental factor. On the other hand, too high resistance means too large values of the iR drop generated along the heated wire by AC current. At a platinum wire of 25 μm diameter and of usual length, iR peak voltage drop less than ±5 V would appear. Such value keeps within the acceptable range where its capacitive distortions inside the electrolyte can be compensated for. If we would use a ten times longer platinum wire, the iR drop would increase to inacceptable values. With gold wires of equal dimension, when heated to give equal temperature, the iR drop is lower, hence the effect of contact resistance is somewhat increased.

Heated 25 μm wire electrodes exhibit a set of characteristics that appear preposterous to common sense and seem to contradict everyday experience:

(a) Metallic 25 μm wires can be heated to 500 °C in free air without damage of contacts and insulating materials at their ends.
(b) The surrounding supporting electrolyte solution does not make up a bypass for heating alternating current. It does not act as a parallel resistor taking away substantial part of heating energy.

(c) As mentioned above, close to the electrode surface, a thin stagnant layer exists. Particles can cross this layer only by diffusion. It is free of convection although moving forces caused by density gradients are maximum in this region.

Item (a) can be explained by the very low heat capacity of thin metallic wires. If a completely mounted wire is heated in air (as a cleaning operation described below), an appropriate AC current will induce red glow at the wire exposed, whereas the wire part covered by ordinary insulating material keeps cool. The difference in heat conductivities between air and solid or polymer insulation materials is sufficient to bring about this behaviour.

Supporting electrolyte solutions, although of considerable electric conductivity, does not really act as a bypass for heating current [item (b)]. This can be explained by means of a model sketched in Fig. 6.1.

In the model symbolised by the circuit in Fig. 6.1, the solution resistance is divided into "boxes" which are represented by a stack of rings formed by "slicing" thin cylindric shells surrounding the electrode wire. The resulting ring segments are volume elements and also resistance elements, which can be calculated individually [3]. This way, streamlines of the flowing AC current are available. The cross section of the solution resistor network bypassing the metallic wire is not uniform, but has a maximum in the middle of the wire length. Otherwise, its overall resistance is determined mainly by the wire ends, where the conducting solution elements are extremely small.

Including item (c), the stagnant solution layer in contact with the heated electrode surface, we can state that cylindric microelectrode properties in combination with heat distribution and streaming processes reveal some surprising characteristics which have been utilised in hot-wire electrochemistry much more than this has been done in common applications before.

6.1.2 Design of Experiments

6.1.2.1 Electrodes and Cells

Platinum and gold wires 25 μm in diameter proved to be the optimum basis for manufacturing hot-wire electrodes. They are robust enough to be handled manually and thick enough to be visible without using a microscope. Their resistance keeps in the range below 20 Ω for moderate length (Table 6.1). The resistance of 2.5 cm pieces, which are common in experimental practice, would amount to 5.35 Ω for platinum and to 1.12 Ω for gold, respectively. When heated to reach just ca. 100 °C in water as an example, power of ca. 2.2 W is necessary. Neglecting the temperature-dependent resistivity change, at the platinum wire we need a heating

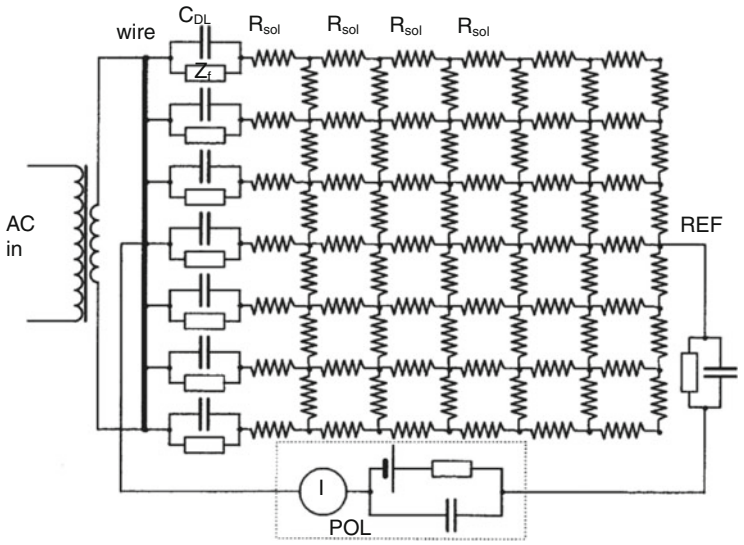

Fig. 6.1 Symbolic equivalent circuit of an electrode wire heated and polarised inside solution. Resistor and capacitor symbols drawn stand for elements of differential size: C_{DL} double layer capacity elements along the wire length, Z_f faradaic impedance elements, R_{sol} solution resistance elements inside bulk solution. REF symbolises the reference and counter electrodes in common, and POL the polarisation and current measuring circuit. From [3], with permission

Table 6.1 Resistance of platinum and gold wires 25 μm in diameter

Pt wire	Au wire
214.0 Ω m^{-1}	44.63 Ω m^{-1}

voltage amplitude of 3.5 V_{rms}, and at the gold wire 1.57 V_{rms}, respectively. Between the outer ends of the wires versus working electrode input of a potentiostat, instantaneous voltage peaks of 4.95 V, or of 2.22 V, respectively, would appear, however with opposite sign at different ends. The potentiostat, consequently, would not take notice of such signals, since they are compensated by the circuits depicted in Fig. 4.12. However, local radio frequency current, of mainly capacitive character, through solution in parallel to the heated wire can be expected. There is evidence that the magnitude of such currents is small and that they do not bring about any detectable faradaic effects. This situation would not hold true with wires of much higher resistance, i.e. with very long 25 μm platinum, or with thin wires made of carbonaceous materials. In this case, very high peak voltage amplitudes would result if the necessary heating power has to be achieved. Such conditions might cause additional distortion effects resulting, e.g. from *faradaic rectification*.

Different heated wire carriers have been designed. Among them, types based on printed board material (glass fibre/epoxy with 35 μm copper plate) proved to be the most versatile. A well tried and tested design is depicted in Fig. 6.2. Copper patterns

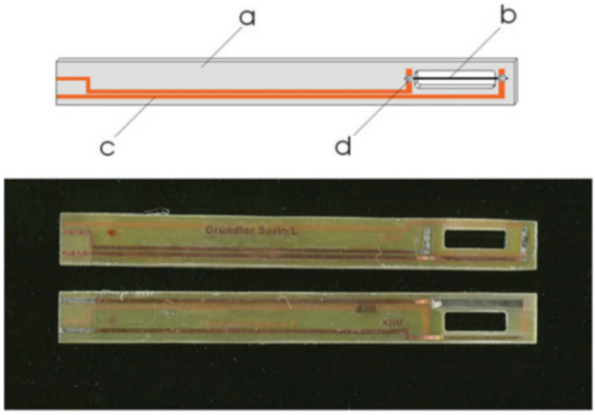

Fig. 6.2 Working electrode design with 25 µm metallic wires. *Top*: schematic representation: (a) Printed board carrier, (b) heated wire, (c) copper leads, (d) solder points. *Bottom*: front side carrying the heated wire and rear side with etched patterns forming counter (gold plated) and reference electrodes (silver plated and chloridised), respectively

made by common photolithographic procedures act as electric contacts for the wire, or for external connectors, respectively. Also, it proved useful to shape additional electrodes at the rear side. In the example given, a copper lead was gold plated to form the counter electrode. A silver plated and chloridised copper stripe served as pseudo-reference electrode. Insulation of all the metallic parts which should not be exposed to solution has been a problem which required long time to be solved. In particular, the electric contact between conductor and heated wire should not lose its sealing action when exposed to temperature variation by the electrode wire. Mixtures of polyethylene or polypropylene with paraffin proved partially useful since their beginning melting process did not damage tightening. Unfortunately, such mixtures are not useful for many non-aqueous solvents. Finally the problem was solved when some sorts of hot-melt adhesives proved useful. Such materials are found in the gluing layer at ordinary laminating pouches, and also in hot-melt glue sticks available in hardware stores. Their chemical composition differs, but very often ethylene-vinyl acetate copolymers (EVA) are in use. This material keeps stable in water and in various non-polar solvents. Even nitrobenzene as a solvent did not attack EVA seals. The carrier of laminating foils normally is made of polyethylene terephthalate. Such foils do not contain polyethylene, although this could be supposed. The plastic belongs to the family of polyesters. It tolerates increased temperature and is stable versus many organic solvents. The electrode family sketched in Fig. 6.2 was manufactured simply by application of a laminating foil cover, which means “ironing” the printed board material stripe by means of an ordinary electric iron. For fabrication of higher numbers, a somewhat altered hot laminator proved useful. Use of laminating foils in electrochemistry has been described first by Neudeck [8]. The laminate insulation has been tested successfully in tetrahydrofurane, chloroform, dichloromethane, acetonitrile and nitrobenzene.

The laminating process can be successful with printed board material support only if the surface, especially the contact between conductor and heated wire, is flat

Fig. 6.3 Miniature cell for electrode stripes like shown in Fig. 6.2. For Explanation, see text

enough to be covered by the gluing layer at the contact side of laminating foil. In most cases, by hot-air soldering, a useful flat contact could be made. With gold wires, the process is difficult, since gold is soluble in many soldering alloys. Alternatively, some sorts of conducting pastes proved useful for making temperature stable electric connections.

Combination electrode stripes as proposed above can be used in every common electrochemical cells, either with its integrated counter and reference electrodes, or with an external reference electrode. For use with non-aqueous solvents, some precautions are necessary. Figure 6.3 shows a miniature cell of 5 ml volume, consisting of a 10 mm-thick-walled centrifuge tube. The completed electrode stripe is carried by a PTFE plug which is fitted by a gas-tight silicon rubber sleeve. The electrode stripe also is sealed by a gas-tight rubber sleeve. In- and outlets of purging gas are capillary openings fitted with hollow needles. To avoid warming up of the low volume cell content, the cell can be placed in a larger thermostatted container. The food plate of the device contained a permanent magnet which allowed safe placement on a steel plate, e.g. inside a common Faraday cage.

Like in any other branch of electrochemistry, surface treatment of the electrodes is highly important. Common surface treatment techniques generally start with mechanic polishing by diamond or alumina suspensions, etc. Of course, such abrasive techniques are not applicable to 25 μm metallic wires and useful alternatives had to be found.

Two standard treatment procedures have been developed. Both are applicable to the completely mounted wires on glass fibre/epoxy support or the like:

Platinum wires are soaked in 0.5 M sulphuric acid for 1 min, then washed with water, dried cautiously by filter paper, and finally annealed at open air where the temperature is risen to 500 °C by electric heating for 2 min.

Gold wire electrodes are electrolysed in 0.5 M sulphuric acid containing 10 mmol/l chloride for 30 s, then washed, dried and annealed by 500 °C at open air for 2 min.

Platinum and gold are different in specific resistivity, thereby different heating current is necessary to obtain a sufficiently correct average temperature of 500 °C at open atmosphere. For this purpose, a little, somewhat modified Wheatstone bridge proved useful. The bridge is dimensioned such a way that it would be in equilibrium just if the heated wire has assumed 500 °C. To reach this state, the bridge voltage is varied till the wire resistor has the appropriate resistivity, and equilibrium is reached. In later practice, instead of a bridge, a stabilised heating current was applied. Platinum wires reach 500 °C with ca. 270 mA, gold wires of equal dimensions with 470 mA. Current spikes that might occur when the heating current is switched in have to be avoided strictly; otherwise the wires will explode readily. Also, gas bubbles in contact with the wire should be avoided.

6.1.2.2 Electronics

The basic configuration of hot-wire electrochemistry is simple. Every commercial potentiostat can be combined with a high frequency heating unit to form the actual bridge circuit which had been outlined schematically in Fig. 4.12c.

In Fig. 6.4, a typical hot-wire measuring station is depicted. Every ordinary potentiostat can be used, if only continuous heating is desired. For pulse heating, the RF generator should be triggered at well-defined instants in the course of a measurement. In this case, a digital potentiostat is advantageous. Digital potentiostats are used to generate their voltammetric exciting signals not as continuous waveforms by means of classic analogue electronics. Instead they make use of digital programming, i.e. by combining rectangular voltage pulses. The voltammetric ramp, e.g. is substituted by a high resolution voltage staircase. Digital instruments do not have a problem to send trigger signals at precisely defined moments in the course of a measuring sequence. A pulse heating unit must be capable of processing trigger signals in order to fast switching of the heating AC current.

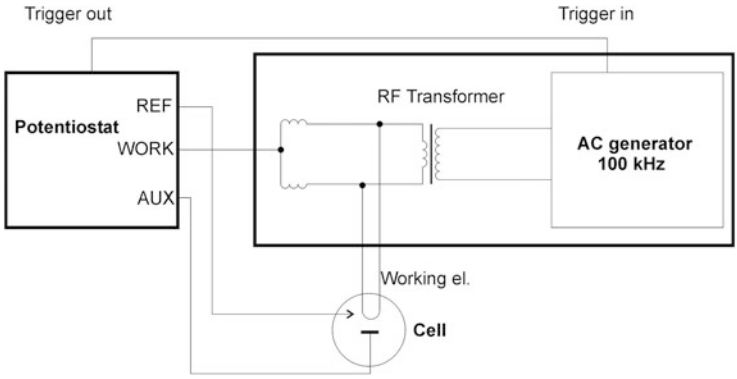

Fig. 6.4 Combination of an RF heating unit (framed arrangement, *right*) with a common potentiostat (*left*) to form a hot-wire electrochemical device. The triggering facility is necessary only for pulse heating. Potentiostat inputs: *REF* reference electrode, *WORK* working electrode, *AUX* auxiliary (counter) electrode

The heating radio frequency (normally 100 kHz) is imposed on the heated wire by means of a transformer (*RF transformer* in Fig. 6.4). This way it is ensured that only pure alternating current, without traces of direct current, will flow. Otherwise, a dc polarisation at the wire would happen which could not be filtered out. The heated wire (*Working el*. in Fig. 6.4) is directly connected with the highly sensitive working electrode input (WORK) of the potentiostat. Interaction by heating AC is avoided by the bridge arrangement shown in the above figure, where the WORK input ends between two commensurate resistors which go to the ends of the wire electrode. The resulting compensation function is brought to perfection when inductive resistors are used instead of ohmic resistors, as shown in the figure. Their resistivity is very high in the RF frequency range, but low with slower signal changes as usual in electrochemistry. The unit named AC generator must be capable of rather high power radio frequency current, up to ca. 3 W. A well-tested arrangement is the combination of a miniature 100 kHz generator with an RF power amplifier. Commercially available audio power amplifiers normally have a frequency limit in the lower radio frequency range. On the other hand, power requirement is never driven here to full power capacity; thereby commercial audio amplifiers are useful. Good results have been obtained with a fixed frequency, adjustable amplitude 100 kHz sine wave generator, combined with a cheap audio frequency power amplifier based on an integrated circuit. First commercial "heating boxes" for thermoelectrochemistry are on the market [9], but home construction is not really a problem if the principles mentioned above are met. Only making the inductive elements (RF transformer and inductive bridge) requires some knowledge of electric fundamentals.

As mentioned above, there are no special demands on the potentiostat, unless pulsed heating is desired. In principle, it should be possible to connect an ordinary analogue potentiostat with a digital-to-analogue converter (DAC) controlled by a

normal PC. The latter should generate digital waveforms which are feeding the DAC. Also, the PC could be used to receive measurement results from the potentiostat analogue output via an analogue-to-digital converter in order to evaluate and finally to plot the results. Ordinary PCs cannot work in such modus operandi within their normal operating system, since modern operating systems (like Microsoft Windows) are always busy with lots of background processes. There are, however, specialised measurement software systems which take over the function of the OS if activated. Such systems, e.g. the widespread LabView®, are capable to convert a PC into a hot-wire electrochemistry device. Such solutions are not cheap since, except the expensive software, also special data acquisition cards must be installed. It is a problem also that the resulting system normally is not compatible with other commercial equipment. As a low-cost alternative, a very efficient construction of a home-built thermoelectrochemical instrument made of easily available components is described in Appendix B of this book.

It is not really necessary to construct a complete hot-wire electrochemical system. A heating unit (corresponding to the framed part at the right hand side in Fig. 6.4) has to be combined with a totally programmable potentiostat. Such potentiostats are on the market. As a rule, types which have been tested successfully for use in spectrophotometry are suitable to be used in hot-wire electrochemistry also. As an example, several instruments of the HEKA series (HEKA Dr. Schulze GmbH, Germany) were combined with a heating box built in IFW Dresden. The heating box contained all electric and electronic parts drawn in Fig. 6.4, right hand framed box. HEKA PG390 potentiostat and similar instruments were programmed to perform staircase voltammmetry and other electrochemical methods including new thermoelectrochemical methods described below. Trigger pulses were programmed in the course of measuring sequences at the corresponding points of time. This sort of hot-wire device is optimum and fulfils all requirements. The instrument even could be “misused” by converting it into a high-precision ohmmeter which allowed to follow tiny resistivity changes of a heated wire in-situ in order to follow the wire’s temperature changes. Details are given in the next paragraph dealing with temperature determination.

Till now, there is no dedicated thermoelectrochemical instrument on the market which would allow to perform modern thermo-pulse methods like the temperature-pulse voltammetry. Instead of utilising a commercial programmable potentiostat as described above, completely home-built devices like that described in Appendix B are worthwhile to be considered, since easy to use microcontroller boards became available. In the example in Appendix B, a microcontroller board initiates and controls the virtual measurement sequence, whereas an ordinary PC is collecting and plotting the results via an “animated EXCEL sheet” which also is mimicking a typical control panel. This low-cost arrangement fulfils all requirements even for the most sophisticated modern thermoelectrochemical pulse techniques.

6.1.2.3 Temperature Determination of Heated Wire Electrodes

Knowledge of actual electrode surface temperature is very important. Traditional thermometers are not useful. Dedicated in situ temperature measuring techniques had to be developed. Two principles for in situ temperature determination have been tested extensively and proved useful, namely

(a) following the temperature-dependent electrode potential shift, either by measuring an open-circuit potential or alternatively by measuring the voltammetric half-wave potential
(b) following the temperature-dependent resistivity change of the heated wire itself, where the latter is used then as some kind of *resistive thermometer*.

The "potentiometric" T measurement (item (a), see above), i.e. utilising the temperature coefficient of the standard potential of reversible redox couples, is the reference method, since the actual temperature of the exposed electrode surface alone is determined. By means of open-circuit potentiometry, the temperature rise and its decay during heating-up and cooling-down periods can be followed continuously. In the early period of hot-wire electrochemistry, temperature-time diagrams provided valuable information about the structure of the heat distribution layer surrounding the electrode and about streaming phenomena inside this layer. Unfortunately, there is a serious drawback. For open circuit continuous T recording, a reversible redox couple is necessary of which must be available both partners (reduced as well as oxidised form) that should be stable in solution under ordinary conditions. The temperature coefficient of the potential should be as high as possible. For aqueous solution, all conditions are fulfilled reasonably by the couple ferrocyanide/ferricyanide with $dE/dT = -1.6$ mV K^{-1}. For non-aqueous solutions, unfortunately it proved difficult to find appropriate couples. A further problem encountered frequently with open-circuit potentiometry is slow equilibration of the indicated potential. The surface of the heated electrode thereby has to be cleaned very carefully. Most efficient proved the final annealing at 500 °C.

The potentiometric T determination is done commonly in an extra experiment in a cell containing all constituents of interest, preferably the supporting electrolyte in equal concentration as with the solution for which electrode temperature is desired, and additionally both partners of the reversible redox system in equal concentration, e.g. ferro/ferricyanide 2–5 mM each. Every commercial electrochemical instrument capable of high-impedance voltage recording can be used. Triggering is not necessary; the heating circuit can be switched manually after potential recording has been started. As a result, pictures of the type shown in Fig. 5.1 are obtained. Every electrode exemplary must be studied individually since small deviations in length or in further properties are unavoidable. The plots $T = f(\text{time})$ depend on wire orientation. Vertical wires show a less expressed temperature maximum when convection is starting.

Table 6.2 Reversible redox couples with high values of $\Delta E^{\theta}/\Delta T$ in non-aqueous solvents

Couple	Solvent/Supp. electrolyte	ΔS J mol^{-1} K^{-1}	$\Delta E^{\theta}/\Delta T$ mV K^{-1}	Ref.
$Co(bpy)_3^{3+/2+}$	Water/0.1 M $LiClO_4$	92.1	0.95	[10]
	Formamide/0.1 M $LiClO_4$	117.2	1.21	
	N-Methylformamide/0.1 M $LiClO_4$	157.0	1.63	[10]
	Propylencarbonate/0.1 M $LiClO_4$	192.6	2.00	[10]
	Acetonitrile/0.1 M $LiClO_4$	180.0	1.87	[10]
$Co(phen)_3^{3+/2+}$	Water/0.1 M $LiClO_4$	92.1	0. 5	[10]
	Formamide/0.1 M $LiClO_4$	117.2	1.21	[10]
	N-Methylformamide/0.1 M $LiClO_4$	142.4	1.48	[10]
	Propylencarbonate/0.1 M $LiClO_4$	180.0	1.87	[10]
	Acetonitrile/0.1 M $LiClO_4$	175.9	1.82	[10]
	DMSO/0.1 M $LiClO_4$	198.9	2.06	[10]
	DMF/0.1 M $LiClO_4$	203.1	2.10	[10]
	Nitromethane/0.1 M $LiClO_4$	240.8	2.49	[10]
Ferrocene/ ferricinium	Acetonitrile/0.1 M NBu_4PF_6		0.8	[11]
	Acetonitrile/0.1 M NBu_4PF_6		0.8	[12]

Reversible redox couples useful for potentiometric thermometry in non-aqueous solvents are not easily to find, although there exist some possible candidates (Table 6.2).

As stated above, even the availability of reversible redox couples with high entropy values is not sufficient to do continuous potential recording. The reason is that in many cases only a single partner of the redox system is available, whereas the second one is not stable in solution, or cannot be synthesised. Generating the missing partner by coulometry sometimes was helpful, but often even such procedures did not solve the problem.

If the *potentiometric T determination* does not allow to record temperature changes, the alternative technique, *resistive thermometry* (item (b), see above) will provide curves $T = f(\text{time})$. Unfortunately, the measured values do not completely agree with potentiometric values and have to be corrected as will be explained below.

For continuous recording of resistance, the usual bridge circuit is not useful. Instead, a simple voltage–current procedure can be applied. Either a constant current is imposed and the resulting iR drop is followed or vice versa. Till now, such investigations cannot be done by imposing AC quantities, but have to be done by imposing dc. If voltage is the imposed quantity, and current is measured, the procedure is more realistic since it is comparable to common AC heating practice. This variant requires a highly precise, high power "potentiostat" which must be protected effectively against overload. Current changes in the course of heating

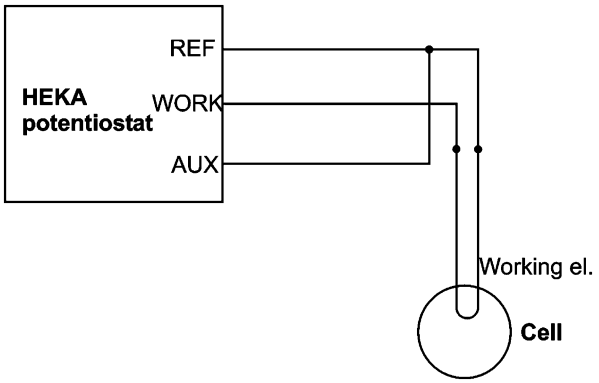

Fig. 6.5 High-precision "ohmmeter" for recording slight temperature-dependent resistivity changes during heating-up and cooling-down periods. A commercial high-precision, high-power potentiostat has been used (HEKA Dr. Schulze GmbH, Germany)

correspond to resistance changes according to Ohm's law. If the "cold resistance" R_{cold} (the resistance for the known value of ambient temperature) is available, ΔT can be calculated easily by evaluating $\Delta R = (R - R_{cold})$. Since R_{cold} for every electrode specimen has its own individual value, the T determination procedure includes measurement of R_{cold}. For that reason, a short sequence with an imposed voltage value in the range of ca. 0.01 V is included. Such values do not generate any detectable heating of the electrode wire. Some commercial potentiostats are capable to be used as a high-precision ohmmeter other than the intended purpose. An example is given in Fig. 6.5.

It must be stated that both methods of T determination have their drawbacks: Open circuit potentiometry suffers from the lack of reversible redox couples with both partners stable in solution. The resistive method, however, does not provide the true temperature of the solution-exposed wire part, since the integral temperature is measured including the wire parts covered by insulating material and connected to larger metallic contacts. The resulting discrepancies in temperature results of both methods have even mislead to the conclusion that sluggishness of potential equilibration might be the reason for larger uncertainties [13]. Although this argumentation later has been disproved, the existing doubts induced the development of a combined technique which allowed continuous recording of the temperature precisely and confidentially. The true electrode surface temperature is determined by means of temperature dependence of voltammetric half-wave potential, whereas the function $\Delta T = f(\text{time})$ is obtained by continuous recording the wire resistance. In other words it means that the resistive temperature–time curve is calibrated by means of $\Delta E_{½}/\Delta T$ for a given point of time. It is sufficient here to have only one partner of the reversible redox couple. Maximum precision for this two-step method has been obtained when the new method TPV (temperature-pulse voltammetry, see Sect. 6.3) was utilised. In Fig. 6.6, examples are given. The irregularity seen in Fig. 6.6 for the heated electrode in dichloromethane is caused by boiling of the solvent. The diverging slopes of the curves result from the different heat conductivities and heat capacities of the solvents.

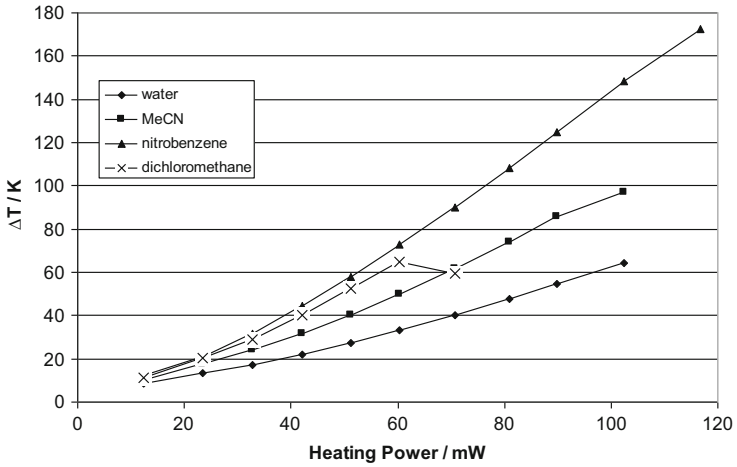

Fig. 6.6 Temperature rise of a 25 µm Pt wire reached at the end of a 10 s heating period in different solvents. For explanation, see text

The temperature variations are calculated by means of the following equation

$$R = R_{\text{cold}}(1 + \beta \cdot \Delta T) \tag{6.1}$$

with the temperature coefficient $\beta = 0.0038\ \text{K}^{-1}$ for platinum

6.2 Heated Macrostructures

All the macrostructures mentioned further above, i.e. thin film and screen printed structures, ITO electrodes and paste electrodes can be heated using all the described techniques of AC distortion compensation and also the methods of temperature determination. Till now, macrostructures throughout were subject to permanent heating only, since fast pulsed heating-up is less useful due to the much higher thermal inertia of the electrodes which are carried by isolating supports.

Examples of experimental work with heated macroelectrodes and of their design will be given in Sect. 6.4.

6.3 New Thermoelectrochemical Methods

6.3.1 Methods with Continuous Electrode Heating

Cyclic voltammetry at continuously heated electrodes does not seem to be a "new method". Nevertheless, voltammograms of this kind reveal information which

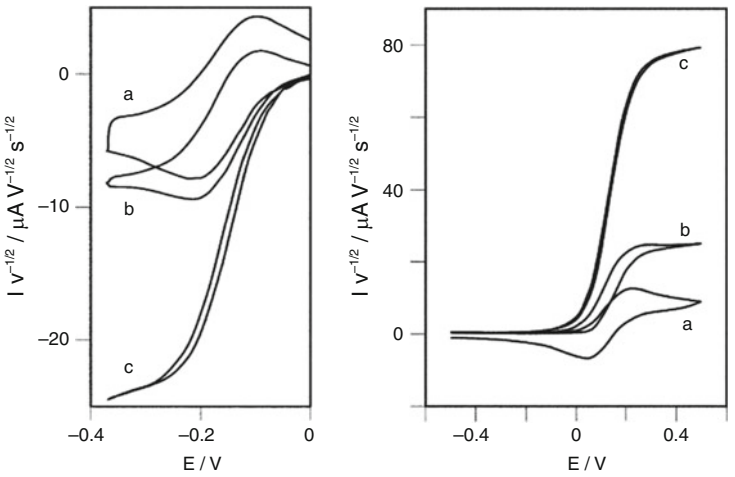

Fig. 6.7 Effect of scan rate on cyclic voltammograms at permanently heated wire electrodes. CVs of reversible redox couples at different scan rates [(a) 20 V/s; (b) 1 V/s; (c) 100 mV/s]. *Left*: $[Ru(NH_3)_6]^{3+}$ (1 mmol/l) in aqueous KCl solution (0.1 mol/l) at a Pt wire 0.25 µm in diameter, reference electrode SCE, temperature 49 °C. *Right*: Ferrocene (2 mmol/l) in DMF with supporting electrolyte tetrabutylammonium fluoroborate (NBu_4BF_4) 0.5 mol/l, temperature 56 °C, reference electrode Ag/0.01 MAg^+//0.1 M NBu_4BF_4/MeCN//0.1 M NBu_4BF_4/DMF. From [14], with permission

could not be obtained by other methods. Two effects are readily identified: (1) for a given heating power, with decreasing scan rate, the voltammograms tend to change their shape from ordinary peak to sigmoidal form (Fig. 6.7); (2) for a given scan rate, with increasing surface temperature, shape of voltammograms tends to go into equal direction (Fig. 6.8). Both effects are based on equal reasons and have been explained in Sect. 5.3. Inside the hot solution layer surrounding the heated electrode, close to surface, a virtually stagnant layer exists with 8 µm thickness in water. Particles can cross this layer merely by diffusion. Reduction or oxidation currents will generate a concentration profile protruding into solution. For very fast scan rates, the thickness of this concentration profile is growing inside the stagnant layer without reaching its boundary. As a result, the ordinary peak-shaped form of a CV in stagnant solution is obtained. In contrary, with very slow scan rates, the concentration profile quickly reaches the boundary of the stagnant layer, and from this instant on, the electrode sees a diffusion layer of constant thickness, like at hydrodynamic electrodes. Result is the typical sigmoidal-shaped voltammogram well known, e.g. from rotating disc electrodes.

For a series of CVs with fixed scan rate, but varied electrode surface temperature, shape of voltammograms changes from classical peak form (without heating) till complete sigmoidal shape (where the increased electrolysis current has driven the concentration profile thickness very fast to the boundary of the stagnant layer, this way generating a diffusion layer of constant thickness).

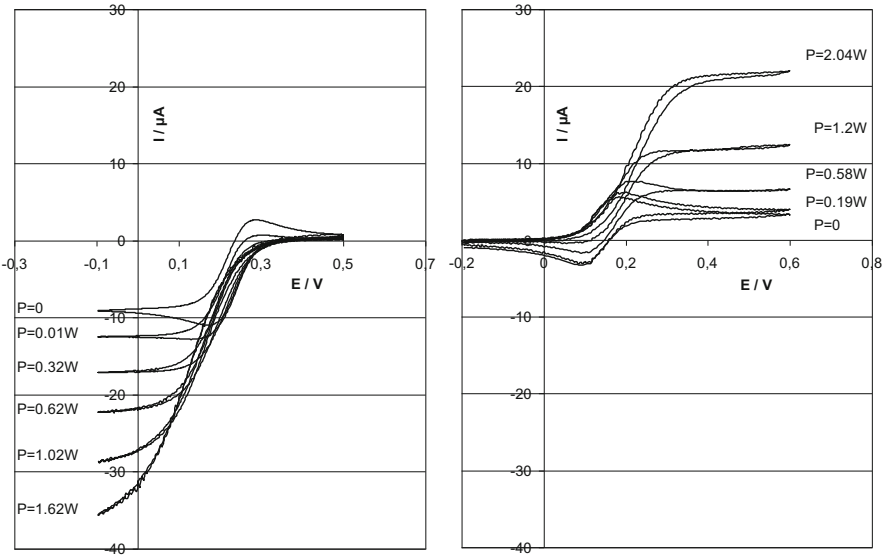

Fig. 6.8 Cyclic voltammograms at heated wires with variable surface temperature. *Left*: Pt electrode 25 µm in $K_3[Fe(CN)_6]$ 2 mmol/l, 0.1 mol/l KCl, *right*: Au electrode 25 µm in ferrocene 1 mmol/l in nitrobenzene/0.1 M NBu_4PF_6. Scan rate 50 mV/s

As stated in Sect. 5.3, evaluation of a series of CVs with varied scan rate using the theory of cylindric diffusion allows to determine both the diffusion coefficient and diffusion layer thickness simultaneously at heated thin wire electrodes.

Sigmoidal voltammograms at permanently heated wire electrodes proved very useful for analytical application since their limiting current can be determined easily. The latter is strictly proportional over some orders of magnitude to bulk concentration of the electrolysed species in solution. An extra benefit is the increased temperature which improves kinetic behaviour. Since temperature is increased only close to the microelectrode, constituents of bulk volume keep unaffected. This proved useful for analysis of dissolved gases and sensitive substances.

Analytical applications of voltammetry at permanently heated electrodes range from determination of dissolved oxygen till DNA hybridisation analysis and include stripping analysis, enzymatic sensors and electrochemiluminescence. Examples will be given later in Sect. 6.4.

6.3.2 Methods with Pulsed Heating

6.3.2.1 Temperature-Pulse Voltammetry (TPV)

With voltammetry at permanently heated electrodes, the long term period in the temperature-time diagram is utilised (see Fig. 5.1, left hand part, period following

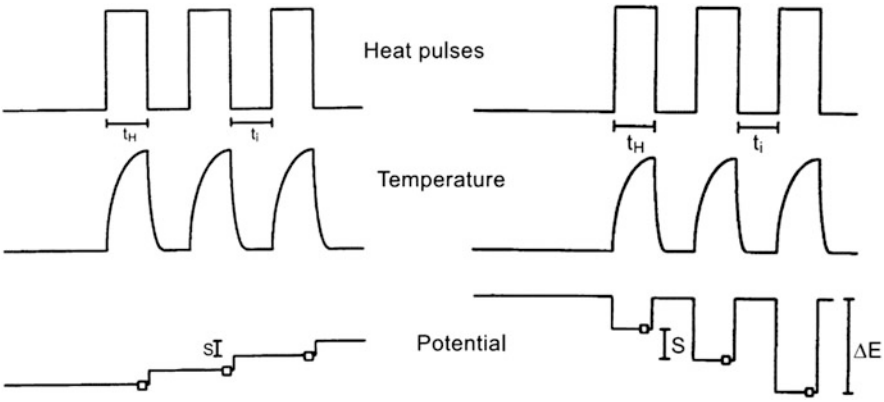

Fig. 6.9 Pulse diagram (schematic) of two temperature-pulse voltammetry variants. *Left*: Staircase mode; *right*: Normal pulse mode. t_H and t_i times of heating pulse cooling-down periods, respectively. *S* potential step amplitude. ΔE potential pulse amplitude in normal pulse mode. From [6], with permission

the *T* maximum). At this time period, a stationary state has been attained which is characterised by stable laminar convection and a constant surface temperature, both depending on heating current magnitude.

Obviously, there must exist also a quite different way to make use of the special features of the heated thin wire electrode. The steep increase of temperature in the diagrams (Fig. 5.1) after heating starts does not vary with wire orientation (horizontal or vertical, respectively), and its geometric shape is independent of heating current magnitude (see Fig. 5.2). When a time of ca. 0.2 s is exceeded, further trend of temperature versus time starts to depend on heating amplitude more and more. Clearly, within the first 100 ms, there exists a convection-free period where *T* might rise very high, possibly beyond the boiling point of surrounding solution. Such considerations became the basis of new thermoelectrochemical methods. The idea behind was to make a series of short current samplings during the convection-free periods. Connecting these instantaneous current values by a line should result in some kind of a *high-temperature voltammogram*. The resulting family of methods was named *temperature-pulse voltammetry* (TPV), [1, 2, 4–6, 15–17] as an analogue of *differential-pulse voltammetry* (DPV). In Fig. 6.9, two variants of TPV are compared by their corresponding pulse diagrams. DPV is an analogue of *TPV in staircase mode* (left diagram in the figure). In DPV as well as staircase-TPV, a potential staircase is imposed the electrode. In DPV, a short square-wave voltage pulse is added. In TPV, a short heat pulse is imposed at every step of the potential staircase, causing the electrode surface temperature to rise first steeply, then with decreasing slope. Near the end of the overlaid pulse signals, electrolysis current is sampled during a very short measuring interval (indicated by □ in the figure). Every current sample, together with its corresponding potential value given by the actual step of the potential staircase, constitutes one single point of the intended

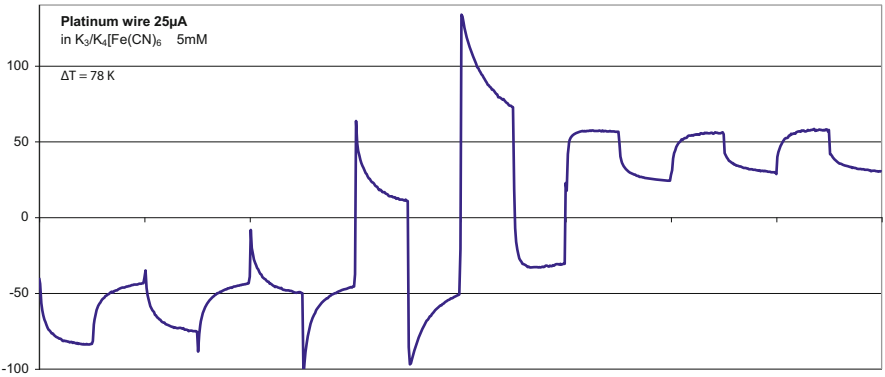

Fig. 6.10 Instantaneous currents with a rough potential staircase for ferricyanide/ferrocyanide 5 mM each in KCl 0.1 M. Overlaid heat pulses generate $\Delta T = 78$ K measured at the end of every pulse. Pt wire electrode 25 µm. Strokes at the abscissa mark potential steps. Cathodic side: left hand. For each step, the current versus time function is drawn. First half of every E step: heating active; second half: heating switched off

temperature-pulse voltammogram (TPV). The second variant, *TPV in normal pulse mode* (right diagram in Fig. 6.9), is an analogue of *normal pulse voltammetry*.

The discussed comparison shows again that potential jumps as well as temperature jumps may change the Free Energy of the electrode reaction in a very similar manner. An important question was the temperature limit which can be reached by TPV. It seemed possible to obtain very high local T values, possibly even to generate supercritical water (or other supercritical solvents). Experimental limits in water have been studied by application of very short heat pulses coupled with very high heating current magnitude up to some amperes for the 25 µm platinum wire. The maximum temperature in water achieved so far was 250 °C for a 5 ms heat pulse [17]. Obviously, under further increased conditions, the boiling process is starting spontaneously without the need of extra condensation nuclei. Supercritical state of water could never be reached experimentally, which was later confirmed by calculation, and that under open cell conditions, it is impossible to achieve it. The reason is that the necessary *critical pressure* cannot be obtained by electrode heating. Indeed, by heating the electrode wire, a pressure wave is generated, but it tends to decay so fast that never all necessary conditions for supercritical water will coincide. Nevertheless, overheated water (the liquid during the metastable state of *boiling retardation*) as a solvent for electrochemical experiments is a quite interesting medium.

In Fig. 6.10, instantaneous variations of electrolysis current are given for a coarse potential staircase with overlaid heat pulses. Diagrams of this type are useful to understand how TPV curves are coming about. The diagrams contain pieces of information according to the variables' potential, current, temperature and time. They are more descriptive than three-dimensional pictures would be, with the variables current, voltage and temperature. Presentations like that one sketched in Fig. 6.10 have some characteristics of spectra, thereby sometimes they have been

named "thermoelectrochemical spectra". In the demonstration example in Fig. 6.10, the abscissa is formed of discrete potential steps. For every potential step, the electrolysis current is plotted as time function. Heat pulses take up half of the potential step duration followed by a cooling-down period filling the rest up to the end of every potential step. What we see is a series of functions $I = f(\text{time})$, half of the step displaying a current rise (heat pulse active) and another half marking the current decay (heat pulse inactive).

Two different types of instantaneous current waveforms can be identified for individual potential steps in Fig. 6.10. The potential step at the left hand side is strongly cathodic; consequently, we see reduction of ferricyanide only. The first half of this potential step starts with heating. As a result of increasing temperature, the reduction current increases. With the following second half (potential is persisting!), the reduction current reaches more or less its original value for ambient temperature. This far-cathodic region is the region of cathodic diffusion-limited electrolysis current. Potential variations (or alternative, temperature induced variation of Free Energy) do not matter markedly in this limiting region. A similar behaviour is found with the last potential step immediate at the right frame of the diagram. Again, we see an increasing current for the first half of the step (heating active), this time the anodic current of ferrocyanide oxidation. This current is decreasing, as expected, during the cooling-down period in the last half of the potential step. As the diagram shows, at the cathodic as well as the anodic limits, where currents are controlled only by diffusion, but not by variations of the imposed potential value, we see low differences between "cold" and "hot" current values. The difference is caused merely by temperature dependence of the diffusion coefficient. But, what is going on in the potential region between cathodic and anodic diffusion limiting?

A quite different behaviour of the electrode can be seen expressively for potential step values close to equilibrium potential. In this region, instantaneous currents are controlled mainly by the temperature-dependent shift of the half-wave potential, i.e. by temperature-dependent variation of Free Energy of the redox reaction. In the example considered here, we study an equimolar mixture of the oxidising and the reducing partners of a reversible couple. The thermal coefficient of potential is negative, i.e. with higher temperature $E_{½}$ is shifted to more negative values. If, e.g. the imposed potential just corresponds to half-wave potential in cold state, heating would cause sharp rise of anodic current, followed by Cottrell decay. With switching to "cold", the current would change its polarity and become cathodic. In other words, in a near-equilibrium potential range we can toggle electrolytic current between anodic and cathodic direction at one and the same imposed potential just by changing the temperature.

The "thermoelectric spectra" mentioned above have been recorded in a more extended way for different species. They played an important role in the early time when hot-wire electrochemistry has been established. Extended pictures like that in Fig. 6.11 allow to understand that TPV curves may assume different shapes dependent on the length of heating-up and cooling-down periods. For heat pulses of very long duration, when actual current rise has ceased, the resulting TPV

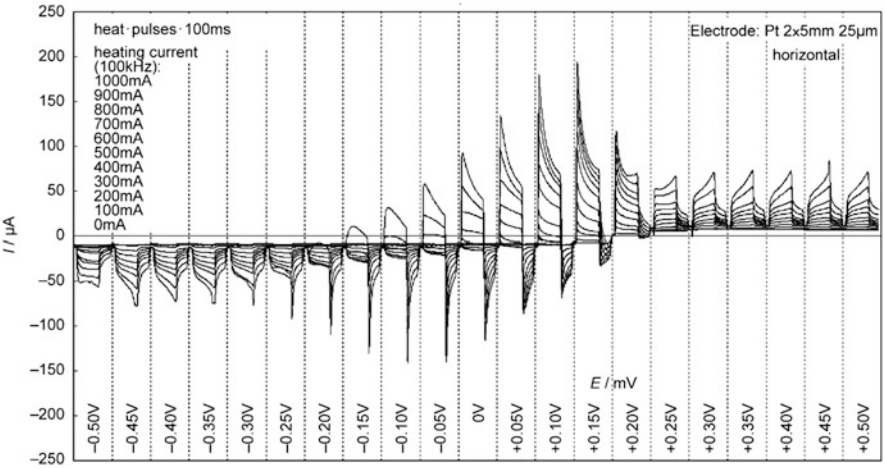

Fig. 6.11 "Thermoelectrochemical spectrum" for ferricyanide/ferrocyanide in KCl 0.1 mol/l. From [18], with permission

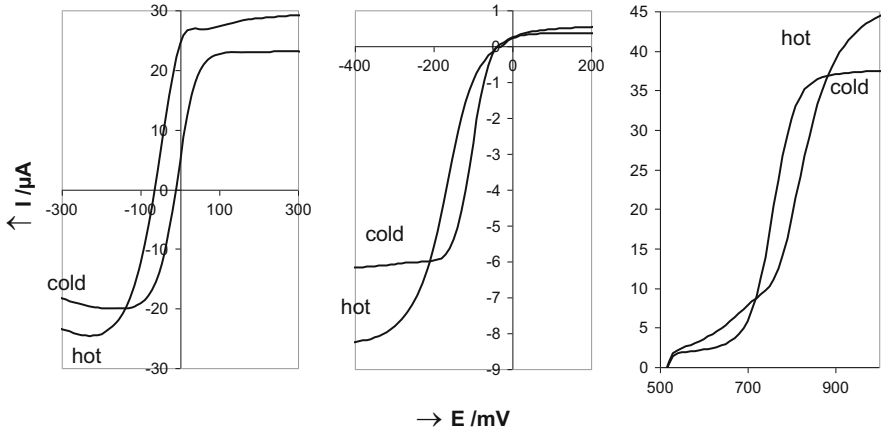

Fig. 6.12 Temperature-pulse voltammograms for reversible couples where the temperature coefficients of potential differ in sign at a platinum wire electrode 25 µm heated with 0.6 W. From *left*: ferricyanide/ferrocyanide 5 mM each in KCl 0.1 M; *centre*: ferricyanide 2 mM in KCl 0.1 M; *right*: ferrocene 2 mM in acetonitrile/NBu_4PF_6 0.1 M. Reference electrodes: *left* and *centre* bare "cold" platinum wire; *right*: Ag/AgCl pseudo-reference electrode. The coefficient $dE_{½}/dT$ for ferricyanide/ferrocyanide is −1.6 mV/K, for ferrocene +0.8 mV/K

assumes sigmoidal shape. This shape also depends on the sign of $dE_{½}/dT$. The examples given in Fig. 6.12 illustrate this relationship. The figure shows how the "hot" voltammogram (characterised by higher current) is shifted toward cathodic potentials for negative temperature coefficient of $E_{½}$ (e.g. for ferri/ferrocyanide), or

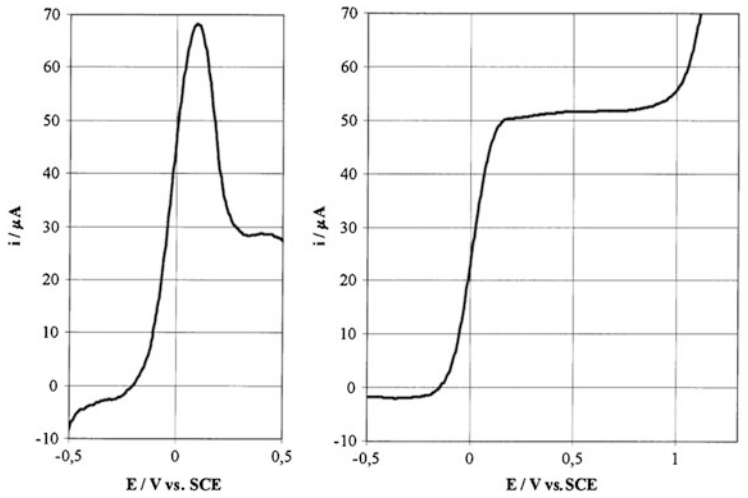

Fig. 6.13 Temperature-pulse voltammograms ("envelope" curve interconnecting current samples of the "hot" curve recorded at the end of each heat pulse) for 5 mM ferricyanide in KCl 0.1 M. *Left*: short pulse 10 ms, *right*: long pulse. From [5], with permission

in direction to anodic potentials for positive temperature coefficient (e.g. for ferrocene/ferricinium).

The current samples used to compose point by point a TPV can be taken at different periods of time along the instantaneous current variation during one single potential step. As mentioned above, the resulting TPV composed of many single current-potential samples assume sigmoidal shape, if the current samples are taken at the end of a long heating pulse where instantaneous current has become nearly constant due to the stationary state existing in this period. This can be understood if we draw an "envelope" connecting all the points at the ends of heating or cooling periods sketched in Figs. 6.10 and 6.11. For long time pulses, as mentioned, the "envelope" will result in sigmoidal shape. For short time pulses, however (e.g. the "envelope" connecting the sharp spikes marking the ends of short heating pulses shown in Fig. 6.11), we see a peak-shaped voltammogram, very similar to a DPV curve, but not symmetric due to the higher current magnitude in the anodic diffusion limited region. The reasons for peak shape formation are equal to those in DPV, i.e. the growing diffusion layer thickness. In Fig. 6.13, both basic shapes of temperature-pulse voltammograms are shown.

TPV diagrams generated with very high resolution (see Fig. 6.14) indeed represent high-temperature voltammograms up to temperature values above boiling point. They do not differ from curves recorded in high-temperature, autoclaved cells, but they are obtained without pressurising. For a more complex chemistry than with reversible redox couples, the TPVs contain much additional information. Examples for thermoelectrochemistry of complex processes will be given in Sect. 6.5.

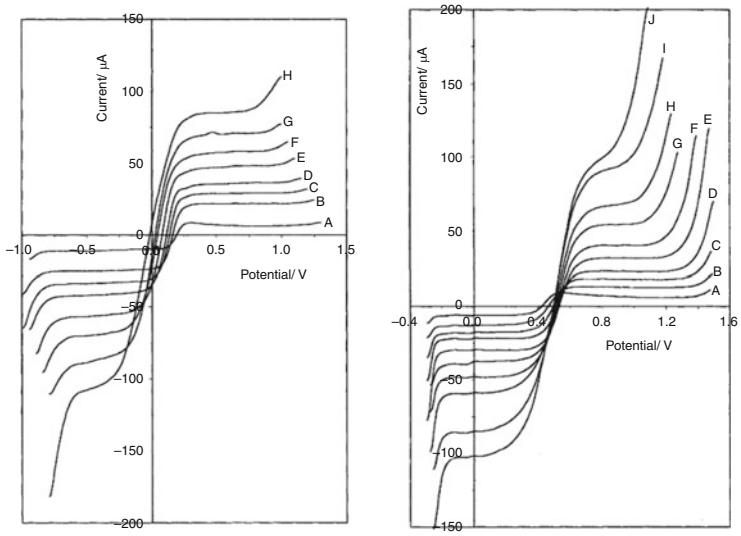

Fig. 6.14 Temperature-pulse voltammograms at Pt electrode 25 µm heated with varied AC amplitudes. Staircase mode, heating pulses 0.1 s. *Left*: Ferricyanide/ferrocyanide 5 mM each in KCl 0.1 M; *right*: Iron(II)/iron(III)sulphate in 0.1 M sulphuric acid. (A) No heating; (B–J) heating magnitude increasing in $0.1\,A_{\mathrm{rms}}$ steps. *Left* starting with $0.3\,A_{\mathrm{rms}}$, *right* starting with $0.1\,A_{\mathrm{rms}}$. From [2], with permission

As mentioned already in Sect. 6.1.2, TPV plays a role in high-precision electrode temperature determination. Like with open circuit potentiometry, only the exposed part of the electrode is evaluated. TPV diagrams similar to the examples shown in Fig. 6.12 illustrate that T can be quantified precisely for every point of time during heating-up and cooling-down periods of an electrode wire just by reading the difference in half-wave potentials of the "cold" and the "hot" TPV. Combining the results with a function $T = f(\text{time})$ continuously recorded by the resistive method, the final outcome is a precise picture of heating and cooling processes containing reliable temperature information at every point.

6.3.2.2 Temperature-Pulse Potentiometry (TPP)

In comparison to voltammetry, with heated potentiometric sensors, advantages are not obvious at first glance. Anyhow, there are chances to tune such sensors in order to achieve higher sensitivity, faster response and better selectivity. Of course, experiments are restricted to all-solid ISEs which can be heated indirectly. An interesting example was presented [19], where a heated copper disc had been modified by an ionophore layer. The slope of the sensor was strongly increased by heating, and the detection limit was decreased by half an order of magnitude.

6.3.2.3 Temperature-Pulse Amperometry (TPA)

Instead of synchronising a potential staircase with repeated heating pulses to perform TPV, a fixed potential may be applied, followed by a thermal pulse which activates the electrode. This is an experimental realisation of the fact that Free Energy of electrodes may be varied arbitrarily either by potential change or alternatively by thermal changes. The fixed potential is chosen such a way that the electrode is inactive (zero current) in non-heated state. With heating, a sharp current rise is generated. If the temperature change is strong enough, the hot electrode can be in limiting current state, and the current signal will be linearly dependent on concentration of the electrolysed component. But also with less strong heating, the resulting current signals typically are concentration proportional. This method, the TPA, has been applied preferably in flowing solution [20–24]. In comparison with classical amperometry, generally a higher sensitivity, a lower detection limit and an improved signal-to-noise ratio are achieved. The reaction rate of substances with sluggish reaction kinetics (e.g. picric acid [21]) is drastically increased, resulting in improved analytical results.

Different types of heated electrodes have been used in TPA, among them gold wires [20], bismuth plated gold wires [23] and gold wires with Nafion-entrapped enzyme [22]. In dependence on pulse duration, the shape of the current pulse signals may vary, between peak shaped for short pulses and more rectangular for longer pulses. The imposed temperature generally was restricted to values below boiling, but there are examples with near-boiling temperature for the shortest pulses tested [21].

Some characteristics of the methods TPP and TPA have been outlined in a review on electrically heated electrodes [24].

6.4 Application Examples with Permanent Heating

6.4.1 Analytical Determinations

At the very beginning of hot-wire electrochemistry, when the technology had proven to be manageable in daily laboratory practice, analytical application attracted notice first. Tiny voltammetric sensors with easily induced thermal convection instead of elaborate machines like rotating disc electrodes seemed attractive for application on-site, e.g. in the natural environment. The chance to overcome sluggish response by means of the intrinsic temperature enhancement was considered to be an additional advantage. Even volatile or delicate solution constituents would be subjects to study since electrode heating does not affect the bulk solution. Stripping analysis with thermal convection was attractive since in this case the heating step and the electrochemical determination process could be separated

[25]. This is the simplest way to avoid that electrochemical measurement would be distorted by heating current.

6.4.1.1 Volatile or Unstable Constituents

Dissolved oxygen in water has been determined at heated platinum wires [26]. Voltammetric signals were improved, and diffusion limited current values could be determined easily by evaluating the sigmoidal voltammograms. The sluggish response of oxygen was overcome since kinetics of reduction has been accelerated. This example had been chosen intentionally in order to demonstrate that increased temperature could be imposed here without affecting the content of a volatile constituent in the bulk solution. Utilisation of increased temperature for accelerating kinetics would be impossible with isothermal cells or half-cells.

Examples of delicate, unstable dissolved analytes with sluggish response were formaldehyde, methanol and formic acid [27]. Their reaction on Pt was not influenced by thermal convection, indicating that the oxidation processes are controlled by surface reactions and not by mass transport. The oxidation current signals were significantly improved at a heated electrode. Oxidation current increments of more than tenfold were obtained for a 56 K temperature rise. Increased temperatures favour the enhancement of the main oxidation reaction as well as the decrease of the overvoltage for the formation of adsorbed reactive OH species on platinum.

6.4.1.2 Stripping Analysis

Stripping applications started with lead determination where the metal traces have been deposited as lead dioxide at the surface of a heated 25 μm platinum wire [28]. Arsenic(V) [29], mercury [30] and different metal traces [31] have been determined at heated gold wires. It has been found that the thermal stirring effect at the 25 μm gold wire was more efficient than the convection at a rotating disc electrode. Heated mercury film electrodes on an iridium base [32] and on screen-printed carbon pattern [33] have been used to determine metallic traces. Surprisingly, the temperature-dependent decrease of hydrogen overvoltage, which is characteristic for mercury electrodes, did not really deteriorate the analysis.

Bismuth electrodes have been proposed as a substitute for mercury electrodes. A bismuth film on the surface of a heated carbon paste electrode indeed proved useful for stripping analysis of lead, cadmium and zinc traces [34]. An example belonging to the next chapter, i.e. analysis of DNA bases at a heated carbon paste electrode after adsorptive accumulation, also can be considered to be a kind of stripping analysis [35].

6.4.2 *Analysis of Bioactive Compounds and Development of Biosensors*

Permanent heating, as a matter of course, keeps restricted to temperature values below boiling point. This was good reason to apply the technique to biosensors. Usually, biologically active substances are dissolved in water, and usually they do not survive temperatures near boiling point or beyond.

At a Pt disc electrode with indirect heating, the important bioactive substance NADH has been determined by voltammetry [36]. Advantageous in this example was efficient cleaning of the platinum surface and better reproducibility of the analysis. By means of heated screen-printed carbon electrodes, residues of the pesticide carbofurane have been determined in water, soil or vegetables [37]. An indirectly heated glassy carbon electrode modified by carbon nanotubes and fibronectin has been used as a cytosensor to detect biologic cells [38]. The catalytic activity of copper electrodes has been enhanced by heating in order to analyse glucose and shikimic acid [39, 40].

6.4.2.1 Adsorptive Accumulation

In many cases, adsorptive accumulation of organic compounds at the electrode surface proved useful to enhance the efficiency of analysis. Accumulation is based on specific adsorption much more than on physical adsorption. The formation of partial chemical bonds is the reason that heating can exhibit a positive effect. With physisorption alone, a negative effect would be suspected since surface coverage tends to decrease with increased temperature.

Thin pencil leads 0.3 mm in diameter have been proposed as heated carbonaceous electrodes. Successful determination of riboflavin [41], rutin [42], flavin adenine dinucleotide [43], silybin [44] and luteolin [45] has been reported. Mostly, direct heating was applied following the principles of hot-wire electrochemistry, but a sensor with indirect heating was proposed also [45].

6.4.2.2 DNA Determination and Hybridisation Analysis

As mentioned above, DNA concentration in an aqueous environment has been determined via adsorptive stripping of its bases [35]. Heated electrodes are preferred for DNA analysis since different steps of these studies have to be done under precise temperature control. Reversible separation of the double helix into two single strands (the so-called de-hybridisation process) as an important precondition for chemical attack of this class of substances, takes place at increased temperatures. Thus, laborious thermostatting is necessary traditionally. Obviously, it is better to choose an increased temperature at the place where it is required for DNA treatment (at the electrode surface), while the solution volume is unaffected.

Heated electrodes were applied to study the interaction of an adsorbed DNA layer with different substrates to follow the temperature dependence of possible DNA damages [46–49].

Hybridisation analysis is the identification of a DNA molecule by means of an immobilised single strand interacting with its complementary strand possibly present in solution. This way, it can be found out whether an organic trace belongs to a biologic species or even an individual. In some respect, hybridisation analysis plays a role similar to the well-known methods of genetic fingerprint.

Electrochemical signals of redox couples can be used for the detection of a hybrid formation (the double helix). DNA hybridisation analysis has been done at heated carbon paste electrodes in combination with magnetic separation steps [50] and at gold/LTCC electrodes [42]. The event of hybridisation can be indicated not only by electrochemical but also by optical detection. Optical detection is done preferably by means of *fluorescence labels* or *fluorescence quenching labels*. Both kinds of detection are performed by means of DNA sequences (oligonucleotides or "oligos") which can be divided into single strands (denaturation or de-hybridisation) by well-defined mild heating. The single DNA strand, which has been labelled in advance by one of the substances mentioned, will show a drastically changed optical response as soon as hybridisation has been occurred, i.e. as soon as the double helix of DNA has been formed. All operations leading finally to hybridisation analysis have to be accommodated by careful thermostatting processes. This was reason to propose heated electrodes where active surfaces can form "micro-thermostats" which may assume temperature values just appropriate for denaturation, hybridisation, etc. Indirect heating in this case proved to be preferable.

Electrochemical indication makes use either of redox labels, which are bound chemically to DNA strands, or of redox active "intercalators". The latter are flat molecules able to intercalate the windings of DNA helix. It has been shown, that the well known, commercially available fluorescence quenching agent dabcyl (p-methyl red) is useful also for hybridisation detection with heated electrodes [51]. It was found that osmium tetroxide in different forms is a most powerful redox label for hybridisation detection, especially at heated electrodes [42, 52–55]. OsO_4 has been used as bipyridyl complex and also bound to a heated gold electrode surface via thiol bridges.

6.4.2.3 Enzyme Sensors

Enzyme molecules immobilised at an electrode surface can be subject to heating only if the enzyme layer is of sufficient thermal stability. A good basis is the technique of entrapment in a polymer layer hardened by pH changes initialised by electrolysis processes. This technique has been invented and perfected by Schuhmann's group [56]. At a first glance, it is not easily to see why temperature changes should be helpful in enzymatic biosensors. Lau et al. have shown, that temperature increase not only enhances reaction rate but also allows easy

distinction of the analyte glucose from generally occurring interferents like ascorbic acid if the different temperature dependence of the voltammetric signals is utilised [57] An even more elegant approach has been worked out to distinguish two or more closely related compounds (e.g. glucose and maltose) when analysed at one and the same enzymatic biosensor [58]. In this example, the differences in mathematical temperature functions of reaction rates are utilised when the temperature of the enzyme electrode was changed by heating.

6.4.3 Detectors for Flow Stream and Electrophoresis

A first example for analysis in flowing streams was a heated gold wire electrode acting as a flow-injection detector, working in temperature-pulse amperometry mode (TPA) [20]. Since the heat pulses were applied at constant potential, the advantages of temperature modulation came into operation, with the result of highly improved detector signal with good signal-to-noise ratio. The TPA is useful to suppress the periodically changing flow rate which is characteristic for flow-stream arrangements [24]. The reason for this improvement is the high intensity of the thermal convection at heated electrodes. The resulting micro-stirring effect exceeds the changes in diffusional transport which would arise from varied solution flow rate.

A microwave-heated platinum disc detector has been used in a capillary-electrophoresis arrangement [59]. A gold disc electrode with indirect electric heating worked as a detector in micro-capillary electrophoresis [60]. Dopamine and catechol were determined successfully. In a similar arrangement, the catalytic activity of copper for detection of shikimic acid and carbohydrates was utilised with an indirectly heated copper disc electrode [40].

Further detector devices worked with heated modified carbon paste electrodes and made use of electrochemiluminescence [61, 62]. Details will be given in next paragraph.

6.4.4 Electrochemiluminescence

In 2006, first time a heated electrode was used to improve the efficiency of an electrochemiluminescent detection system [63]. The $Ru(bpy)_3^{2+}$–ECL and $Ru(bpy)_3^{2+}$–oxalate–ECL systems were used together with a directly heated 25 µm platinum wire electrode. The detection limit of oxalate was found to be decreased by two orders of magnitude if the temperature was increased from 22 °C to 80 °C. The authors emphasise the advantage that temperature is acting at the place where it is necessary, but leaves the dissolved sensitive constituents unaffected. An overview on the system is given in Fig. 6.15. The system was used also for electroluminescence studies with luminol [64] and with lucigenin [65]. In both applications,

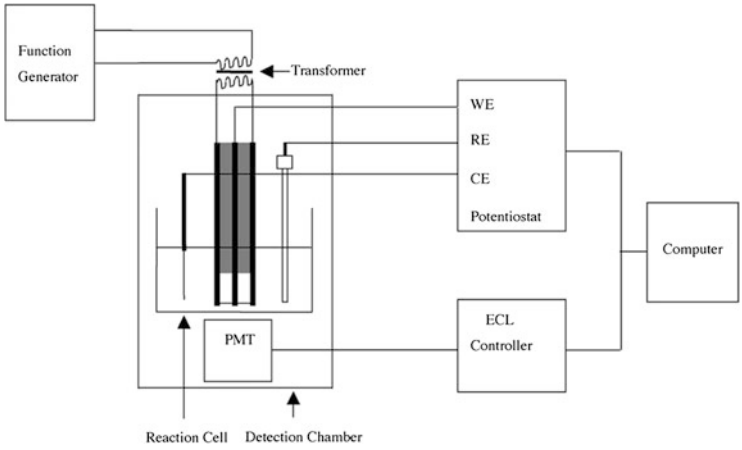

Fig. 6.15 Schematic diagram of an ECL detection system equipped with an electrically heated, temperature controlled cylindrical microelectrode. *WE* working electrode, *RE* reference electrode, *CE* counter electrode, *PMT* photomultiplier. From [63], with permission

a drastic enhancement of results has been achieved with increased electrode surface temperature.

As mentioned above, heated carbon paste electrodes have been utilised to design electroluminescence detectors for micro-capillary electrophoresis [61, 62]. In [62], an unmodified heated carbon paste electrode was used in separation buffer solution with $Ru(bpy)_3^{2+}$ added. $Ru(bpy)_3^{3+}$ was anodically generated and used for detection of triethylamine (TEA) and tri-n-propylamine (TPrA). In [61], the heated electrode consisted of a paste made of multi-wall carbon nanotubes mixed with $Ru(bpy)_3^{2+}$. TPrA was used as coreactant to investigate CE–ECL signals under different conditions. Since $Ru(bpy)_3^{2+}$ was immobilised, the heated electrode acted as an all-solid detector. The analytes were reacting with the electrochemically generated $Ru(bpy)_3^{3+}$, and light was emitted when they were exiting the capillary. Separation and determination of two organophosphate insecticides, acephate and dimethoate, were performed to evaluate the feasibility and reliability of the system. An equal electrode was used to analyse solutions of tripropylamine, in direct way, not as a detector [66]. The MWCNT/$Ru(bpy)_3^{2+}$ paste was applied as a film coated on a carbon paste electrode. In another example of heated carbon paste electrodes, the enzyme xanthine oxidase was immobilised in the paste. The ECL signal of luminol increased when hypoxanthine was added. The system could be used then as a biosensor for hypoxanthine [67].

Pastes made of carbonaceous materials with ionic liquids acted also as heated electrochemiluminescence sensors. A mixture of multi-wall carbon nanotubes with an ionic liquid was used in connection with lucigenine to detect ascorbic acid which influences the luminescence of the latter [68]. Another example was a carbon/ionic liquid paste electrode where N_6-isopentenyl-adenine was detected using its enhancement action on the electrochemiluminescence of ruthenium bipyridyl [69].

In a series of papers, heated indium tin oxide (ITO) electrodes were proposed as carriers for electrochemiluminescent sensors of diverse analytes [70–74]. The system couples the advantages of a heated electrode with the optical transparency property of ITO glass. In [70], H_2O_2/MCLA and TPrA/$Ru(bpy)_3^{2+}$ have been used to test the arrangement which was constructed very similar to the scheme given in Fig. 6.15. In [71], TPrA and colchicine were detected in human serum by means of the ruthenium bipyridyle ECL system. Immobilised xanthine oxidase as a sensor system for hypoxanthine has been mentioned already. It has been used also with a heated ITO electrode [72]. Further examples for electrochemiluminescence detection with heated ITO electrodes were the analysis of N_6-methyladenosine in urine [73] using $Ru(bpy)_3^{2+}$ and finally the ionic-liquid enhanced system luminol-O_2-$BMIPF_6$ [74].

6.5 Application Examples with Pulsed Heating

With pulse heated electrodes, the major application is not chemical analysis, since extraordinary high-temperature values do not seem to be of great advantage for routine analysis. On the other hand, the chance to achieve such high temperatures in an open system, without autoclaving, with cheap and always available instrumentation, was a highly attractive feature for electrochemical research. It opened up ways to utilise overheated liquids as some kind of novel solvents. As an example, overheated water (the metastable medium which is encountered when the well-known effect of *boiling retardation* is occurring) has very interesting properties differing drastically from the water as we know it. Solubility of less polar substances, e.g. is higher. At an early stage of development of hot-wire electrochemistry, there was even hope to make use of supercritical water as a solvent in an open, non pressurised system. Unfortunately, nature does not allow that as explained above. Even now, when ionic liquids have opened up the use of high-temperature electrochemistry in open systems (due to their extremely low vapour pressure), overheated classical solvents are worthwhile to be studied in detail. Future processes, e.g. when the heat waste of nuclear power stations might become subject of direct energy conversion, are examples where very hot water as a solvent cannot be substituted by other media.

Hot-wire electrochemistry with directly pulse-heated microwire electrodes can be considered to be a special branch of high-temperature electrochemistry. It is characterised by two attributes: (1) it can be done with common, generally available instruments and (2) in contrast to classical high-T-electrochemistry, the increased temperature is applied only where it is required, but all other regions of the cell content remain unaffected. These characteristics are of practical, not of fundamental, nature. It means that the results of this technology would be available in most cases also with classical high pressure electrochemical cells.

Pulsed electrode heating till now did not find very broad application. The following examples mark the beginning of a research direction where heated

electrodes are used to study fundamental electrochemical phenomena at which temperature is imposed actively as an independently variable parameter. The examples are not arranged in a hierarchical order, but follow the logics of their more or less accidental development.

6.5.1 *Switched Passive Layers [75]*

Passivating oxide layers are widespread phenomena in electrochemistry. With gold electrodes, this kind of passivation is well studied since it plays an important role for many applications, among them numerous chemical sensors. With anodic polarisation, at gold surfaces in neutral, acid and alkaline solution, different oxide layers are growing. Passivation is caused by the very thin α-oxide layer. This layer can suppress nearly completely electron transfer from and to the electrode surface. This effect has been confirmed for a large variety of redox processes. By means of modern methods of thermoelectrochemistry like TPV, it has been found that temperature has the effect to shift the sharp onset potential of passivation towards more positive values. That is, the passivation is not prevented, but just the passive potential region is changed. Furthermore, it became clear that formation and dissolution of the passive layers are rather fast processes. As a final result, there has been found a way to switch homogeneous reversible reactions on and off just by fast temperature changes at a fixed applied potential [75]. Examples studied were oxidation of ferrocyanide, peroxide and ferrocene carboxylic acid in aqueous solution. Also, the reversible anodic oxidation of gold in presence of chloride ions could be switched thermally. Figure 6.16 shows that, just by fast temperature change, immediately (i.e. within a few milliseconds) the passivation is cancelled so

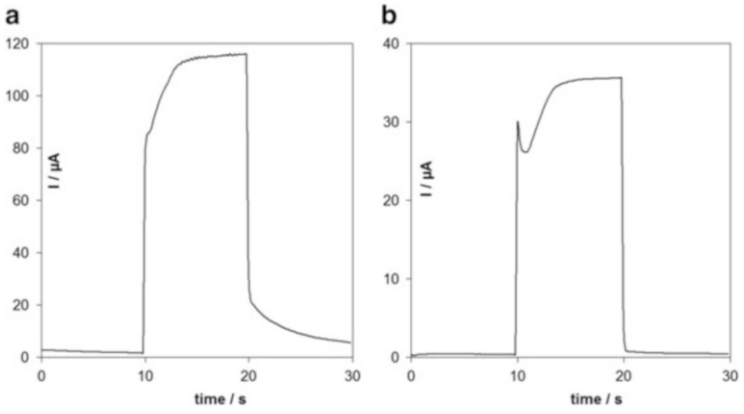

Fig. 6.16 Gold wire electrodes in H_2O_2 5 mM in H_2SO_4 0.5 M, permanently polarised to 960 mV (**a**, *left*); in KCl 5 mM in H_2SO_4 0.5 M, polarised to 1.0 V (**b**, *right*). Each electrode heated up for 10 s (between 10 and 20 s) from room temperature to 62.5 °C. From [75], with permission

that the redox process can proceed as usual. When heating is stopped, temperature decrease and reformation of the passive oxide layer need somewhat longer time to establish, but nevertheless the redox reaction ceases rather fast.

Possible applications of switched passivation might be thermal modulation for improvement of signal-to-noise ratio in analytical chemistry. Also, in other processes a "third party" intervention to stop or activate passivation could be useful.

6.5.2 *Heated Modified Electrodes [76]*

There are not many common surface modification methods which are applicable to heated thin wire electrodes. Among the useful methods, most promising is covalent binding of modification agents at a gold surface. Gold wires with the usual diameter of 25 μm have been modified successfully by binding active agents via disulphide bridges. Such electrodes were subject to mild heating, but results have not been published.

Most widespread modification practice is to spread a certain amount of solution at the electrode surface and to allow to dry. It is a standard technique to prepare electrode surfaces with new, active carbonaceous materials like carbon nanotubes. A suitable surface should be free from uncovered sites. With flat metallic or carbonaceous surfaces, this procedure is useful, but it was not successful with thin wire electrodes. A new modification procedure had to be found. An electrophoretic procedure was used to generate a dense layer of carbon nanotubes at the surface of a gold wire [76]. Single wall carbon nanotubes were suspended in an aqueous solution of the anionic surfactant sodium dodecyl sulphate (SDS). In this suspension, individual nanotubes are covered by a monolayer of the anionic surfactant SDS, which results in a negative surface charge. The wire, which is made positive to attract the negatively charged nanotube molecules, becomes covered by a dense layer of SWCNTs within some minutes. By thermal treatment at 350 °C at air atmosphere (similar to the surface cleaning procedure described in Sect. 6.1.2 dealing with design of experiments), surfactant residues as well as carbonaceous contaminants are burned out, whereas the nanotubes resist this treatment. The resulting layer consists to a high degree of pure nanotubes, as proven by Raman spectroscopy. Such electrodes can be heated in aqueous as well as in different non-aqueous solvents without damage.

Microelectrodes carrying a dense carbon nanotube layer exhibit interesting properties. Their specific double layer capacity is more than 100-fold increased compared to the bare gold surface, with only little difference between fresh, "wet" state and the "dry" state after annealing. Obviously, in "wet" state, each individual nanotube molecule keeps covered by negatively charges surfactant ions. This could be verified by voltammetry where negatively charged redox agents gave only tiny electrolysis current, whereas the current of positively charged redox agents appeared to be higher than the expected, diffusion controlled value.

Heated gold/CNT electrodes were applied in experiments where the role of temperature for the process of inclusion of molecules inside nanotubes has been studied. Results will be published.

6.5.3 *Electropolymerisation [77]*

Polymers and oligomers of thiophene are interesting substances since they play an important role in modern organic semiconductor devices. Thin films produced with α-oligothiophenes were used to manufacture electronic components like organic field effect transistors and organic light emitting diodes. In thermoelectrochemical experiments with α-sexithiophene in nitrobenzene solution, first time the intermediate cation radicals have been detected and characterised by in-situ ESR spectroscopy. By thermoelectrochemistry, the reaction pathway has been found out from the bunch of different possible ways. An interesting side result was the way how formation of thin film semiconducting polymer was occurring at increased temperature. At permanently heated electrodes, apparently no polymer was formed. With pulsed heating in the course of temperature-pulse voltammetry, and in homogeneous solution of increased temperature, polymer films were generated. Obviously, the strong micro-convection (thermal stirring) with permanently heated electrodes blew away the nucleation sites of beginning polymerisation. This can be seen as another evidence for the existence of a "convection free" period of some hundreds of milliseconds after start of the heating process at a 25 μm metallic wire electrode [77]. As a new phenomenon later a strong hysteresis was found with temperature-pulse voltammetry. Forward direction starting with more cathodic potentials, the appearance was completely different from voltammograms found in "backward" direction when the polymer layer had been completed. A "cyclic temperature-pulse voltammetry" has been proposed and appeared to be useful.

References

1. Voss T, Kirbs A, Gründler P (2000) Fres J Anal Chem 367:320–323
2. Gründler P, Kirbs A, Zerihun T (1996) Analyst 121:1805–1810
3. Gründler P (1998) Fres J Anal Chem 362:180–183
4. Gründler P, Kirbs A (1999) Electroanalysis 11:223–228
5. Gründler P (2000) Fres J Anal Chem 367:324–328
6. Gründler P, Flechsig GU (2006) Microchim Acta 154:175–189
7. Gabrielli C, Keddam M, Lizee JF (1983) J Electroanal Chem 148:293–297
8. Neudeck A, Kress L (1997) J Electroanal Chem 437:141–156
9. Gensoric GmbH (2014) Thermalab. Internet Communication. http://www.gensoric.com/Thermalab
10. Sahami S, Weaver MJ (1981) J Electroanal Chem 122:155–170
11. Akkermans RP, Suarez MF, Roberts SL, Qiu FL, Compton RG (1999) Electroanalysis 11:1191–1202

12. Tsierkezos NG (2007) J Solution Chem 36:289–302
13. Gründler P, Dunsch L (2011) J Solid State Electrochem 15:2101–2106
14. Gründler P, Beckmann A (2004) Anal Bioanal Chem 379:261–265
15. Voss T, Gründler P, Kirbs A, Flechsig GU (1999) Electrochem Commun 1:383–388
16. Gründler P, Degenring D (2001) J Electroanal Chem 512:74–82
17. Gründler P, Degenring D (2001) Electroanalysis 13:755–759
18. Gründler P, Kirbs A, Dunsch L (2009) ChemPhysChem 10:1722–1746
19. Chumbimuni-Torres KY, Thammakhet C, Galik M, Calvo-Marzal P, Wu J, Bakker E, Flechsig GU, Wang J (2009) Anal Chem 81:10290–10294
20. Wang J, Jasinski M, Flechsig GU, Gründler P, Tian B (2000) Talanta 50:1205
21. Wachholz F, Biala K, Piekarz M, Flechsig GU (2007) Electrochem Commun 9:2346–2352
22. Tseng TF, Yang YL, Chuang MC, Lou SL, Galik M, Flechsig GU, Wang J (2009) Electrochem Commun 11:1819–1822
23. Jacobsen M, Duwensee H, Wachholz F, Adamovski M, Flechsig GU (2010) Electroanalysis 22:1483–1488
24. Flechsig GU, Walter A (2012) Electroanalysis 24:23–31
25. Gründler P (2008) Current Anal Chem 4:263–270
26. Zerihun T, Gründler P (1996) J Electroanal Chem 404:243–248
27. Zerihun T, Gründler P (1998) J Electroanal Chem 441:57–63
28. Zerihun T, Gründler P (1996) J Electroanal Chem 415:85–88
29. Gründler P, Flechsig GU (1998) Electrochim Acta 43:3451
30. Wang J, Gründler P, Flechsig GU, Jasinski M, Lu JM, Wang JY, Zhao ZQ, Tian BM (1999) Anal Chim Acta 396:33
31. Flechsig GU, Korbut O, Gründler P (2001) Electroanalysis 13:786
32. Jasinski M, Kirbs A, Schmehl M, Gründler P (1999) Electrochem Commun 1:26–28
33. Jasinski M, Gründler P, Flechsig GU, Wang J (2001) Electroanalysis 13:34
34. Flechsig GU, Korbut O, Hocevar SB, Thongngamdee S, Ogorevc B, Gründler P, Wang J (2002) Electroanalysis 14:192
35. Wang J, Gründler P, Flechsig GU, Jasinski M, Rivas G, Sahlin E, Paz JLL (2000) Anal Chem 72:3752
36. Lau C, Flechsig GU, Gründler P, Wang J (2005) Anal Chim Acta 554:74–78
37. Wei H, Sun JJ, Wang YM, Li X, Chen GN (2008) Analyst 133:1619–1624
38. Zhong X, Qian GS, Xu JJ, Chen HY (2010) J Phys Chem C 114:19503–19508
39. Wei H, Sun JJ, Guo L, Li X, Chen GN (2009) Chem Commun 10:2842–2844
40. Chen QZ, Fang YM, Wei H, Huang ZX, Chen GN, Sun JJ (2010) Analyst 135:1124–1130
41. Wu S, Sun J, Lin Z, Wu A, Zeng Y, Guo L, Zhang D, Dai H, Chen G (2007) Electroanalysis 19:2251–2257
42. Wu SH, Sun JJ, Zhang DF, Lin ZB, Nie FH, Qiu HY, Chen GN (2008) Electrochim Acta 53:6596–6601
43. Wu SH, Nie FH, Lin ZB, Dai HM, Zhang DF (2008) Chin J Anal Chem 36:1228–1232
44. Wu SH, Nie FH, Chen QZ, Sun JJ (2011) Anal Chim Acta 687:43–49
45. Wu SH, Zhu BJ, Huang ZX, Sun JJ (2013) Electrochem Commun 28:47–50
46. Korbut O, Buckova M, Tarapcik P, Labuda J, Gründler P (2001) J Electroanal Chem 506:143–148
47. Korbut O, Buckova M, Labuda J, Gründler P (2003) Sensors 3:1–10
48. Wang J, Gründler P (2003) J Electroanal Chem 540:153–157
49. Ferancova A, Adamovski M, Gründler P, Zima J, Barek J, Mattusch J, Wennrich R, Labuda J (2007) Bioelectrochemistry 71:33–37
50. Wang J, Flechsig GU, Erdem A, Korbut O, Gründler P (2004) Electroanalysis 16:928–931
51. Flechsig GU, Peter J, Voss K, Gründler P (2005) Electrochem Commun 7:1059–1065
52. Peter J, Reske T, Flechsig GU (2007) Electroanalysis 19:1356–1361
53. Flechsig GU, Reske T (2007) Anal Chem 79:2125–2130
54. Surkus AE, Flechsig GU (2009) Electroanalysis 21:1119–1123

55. Jacobsen M, Flechsig GU (2013) Electroanalysis 25:373–379
56. Kurzawa C, Hengstenberg A, Schuhmann W (2001) Anal Chem 74:355–361
57. Lau C, Reiter S, Schuhmann W, Gründler P (2004) Anal Bioanal Chem 379:255–260
58. Lau C, Borgmann S, Maciejewska M, Ngounou B, Gründler P, Schuhmann W (2007) Biosens Bioelectron 22:3014
59. Foerster S, Matysik FM, Ghanem MA, Marken F (2006) Analyst 131:1210–1212
60. Wu D, Wu JA, Zhu YH, Xu JJ, Chen HY (2010) Electroanalysis 22:1217–1222
61. Chen Y, Lin Z, Chen J, Sun J, Zhang L, Chen G (2007) J Chromatogr A 1172:84–91
62. Chen Y, Lin Z, Sun J, Chen G (2007) Electrophoresis 28:3250–3259
63. Lin ZY, Sun JJ, Chen JH, Guo L, Chen GN (2006) Anal Chim Acta 564:226–230
64. Lin Z, Sun J, Chen J, Guo L, Chen G (2007) Electrochim Acta 53:1708–1712
65. Lin ZY, Sun JJ, Chen JH, Guo L, Chen GN (2007) Electrochem Commun 9:269–274
66. Lin Z, Sun J, Chen J, Guo L, Chen Y, Chen G (2008) Anal Chem 80:2826–2831
67. Chen YT, Jiang YY, Lin ZY, Sun JJ, Zhang L, Chen GN (2009) J Nanosci Nanotechnol 9:2303–2309
68. Lin ZY, Chen XP, Chen HQ, Qiu B, Chen GN (2009) Electrochem Commun 11:2056–2059
69. Chen YT, Chen X, Lin ZY, Dai H, Qiu B, Sun JJ, Zhang L, Chen GN (2009) Electrochem Commun 11:1142–1145
70. Chen YT, Jiang YY, Lin ZY, Sun JJ, Zhang L, Chen GN (2008) Luminescence 23:63
71. Chen YT, Jiang YY, Lin ZY, Sun JJ, Zhang L, Chen GN (2009) Analyst 134:731–737
72. Chen YT, Qiu B, Jiang YY, Lin ZY, Sun JJ, Zhang L, Chen GN (2009) Electrochem Commun 11:2093–2096
73. Lin ZY, Wang WZ, Jiang YY, Qiu B, Chen GN (2010) Electrochim Acta 56:644–648
74. Chen L, Chi Y, Zheng X, Zhang Y, Chen G (2009) Anal Chem 81:2394–2398
75. Gründler P, Dunsch L (2014) J Solid State Electrochem, doi:10.1007/s10008-014-2482-3
76. Gründler P, Frank O, Kavan L, Dunsch L (2009) ChemPhysChem 10:559–563
77. Haubner K, Gründler P, Dunsch L (2012) J Electroanal Chem 682:72–76

Appendix A: A Calculation Procedure for Temperature Profiles at Heated Wire Electrodes

The calculation procedure presented here is uncommon. Other than usual procedures, where a software program has to be written, here just some knowledge of ordinary spreadsheet handling is necessary. The calculation runs very fast and can be adapted easily to any electrode material or dimension, and any electrolyte solution. As an example, a simple Excel® spreadsheet containing some macros is used. The calculation table with all the macros can be received from the author free of charge.

A heated wire electrode attains a temperature profile with maximum temperature at the surface, and minimum in the bulk solution, sufficiently far from the surface. The surface temperature T_{surf} is not constant, but tends to increase, if heating energy is fed continuously. As a result, the thickness of the temperature profile Δx_{therm} is growing into solution. The profile can be calculated for the simplifying assumption that heat is spreading by conduction alone, without contribution of radiation. This assumption is a good approximation as long as the wire temperature does not exceed that of the bulk solution by more than ca. 100 K.

For calculation of the temperature profile for a given time, Fourier's law of heat conduction (see Chap. 5) has to be solved. In its simplest form, Eq. (A1), it says that the stream of heat energy per time unit, dQ/dt, is proportional to the local temperature profile dT/dx. The proportionality factor is λ, the specific heat conductivity of the surrounding solution, measured in J cm^{-1} s^{-1}. For aqueous solutions, even if they contain supporting electrolyte in common concentration, $\lambda(H_2O) =$ 5.64 mJ cm^{-1} s^{-1} is a good approximation.

$$\frac{dQ}{dt} = -\lambda \frac{dT}{dx} \tag{A1}$$

An ordinary differential equation like this one cannot be solved easily in an analytical manner. Laplace transform can be applied like in solution ways of diffusion problems, but generally back transformation from Laplace transform

P. Gründler, *In-situ Thermoelectrochemistry*, Monographs in Electrochemistry,
DOI 10.1007/978-3-662-45818-1

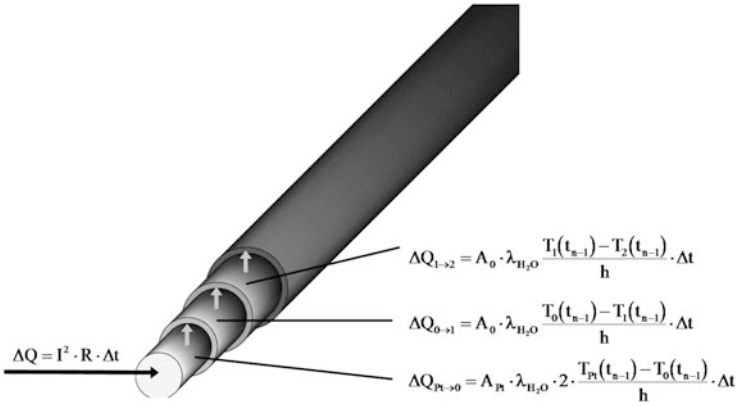

Fig. A1 Box model for digital simulation of temperature profile around a heated microwire electrode. From [1], with permission

makes problems. It is, however, quite simple to find a sufficient solution by digital simulation.

The digital calculation starts with the model depicted in Fig. A1. The heated wire with radius r_0 and the cylindric surface A_{Pt} (for platinum wire) is surrounded by cylindric solution shells with the thickness h. The model is a so-called box model, and the shells may be named "boxes". If we assume that the wire is heated by a constant AC current I_{heat}, and if we assume for a first approximation that the resistance R of the wire also is constant, then we can calculate easily the heat increment ΔQ, which is fed into the wire during the time interval Δt:

$$\Delta Q = I_{heat}^2 \cdot R \cdot \Delta t \tag{A2}$$

From this moment on, we consider all the following instants of time t_n, which are given by summing all intervals Δt. Every cylindric shell during the interval Δt is receiving a heat increment "Q_{in}" which flows into the considered shell from its neighbour with higher temperature (which is positioned closer to the heated wire), and simultaneously the considered shell gives away a second heat increment "Q_{out}" to the neighbouring shell with lower temperature (which is positioned more outside, towards solution side). In Fig. A1, more detailed formulas are given. As a result, during every time interval Δt, in the considered shell remains the heat increment

$$\Delta Q = \Delta Q_{in} - \Delta Q_{out} \tag{A3}$$

The increment ΔQ will heat up the considered shell to some degree. The new temperature can be calculated from solution data (heat capacity, length and thickness h).

The actual temperature of every cylindric shell is calculated by a spreadsheet, where every line means one shell, and every column means one instant of time.

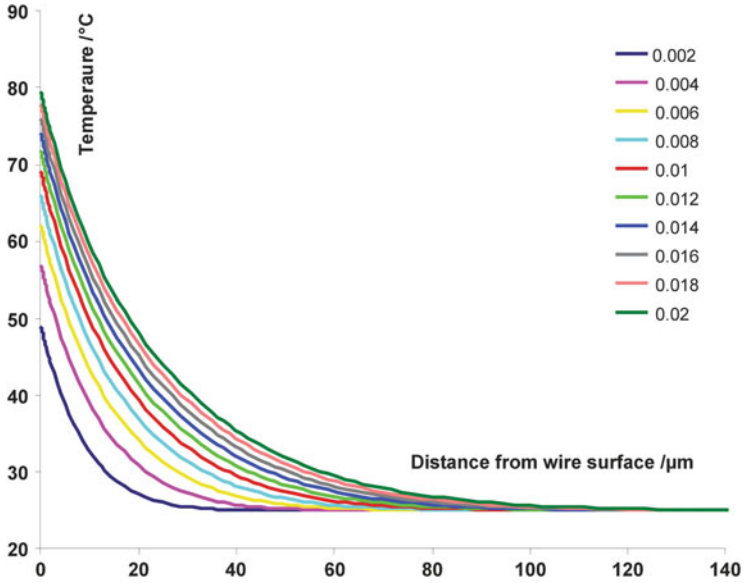

Fig. A2 Temperature profiles for a platinum wire 25 µm, heated with 725 mA in aqueous solution. Parameter: time of the recorded curve in seconds after start of heating

Arranging the calculated T columns with the column of radius r_n of the shells (the distance from wire surface) as abscissa, we get diagrams like that given in Fig. A2. Plotting the temperature values for a given radius versus time will give pictures like that in Fig. A3, where the T variation is calculated for $r = r_0$, i.e. for the electrode surface. Also, a three-dimensional plot is available with Excel (Fig. A4). Unfortunately, Excel does not provide reasonable tools to arrange results in scientific 3D diagrams; thereby it is preferable to utilize another program which will do the job more accurately.

The calculation does not reflect the real data for heating times more than ca. 50 ms, since the model does not account for the thermal stirring which is starting after the time mentioned. On the other hand, the calculated results agree very well with measured values for the start period where the solution remains stagnant due to the medium's inertia.

The calculation procedure can be tested by stepwise execution of an Excel table containing all the necessary parameters, e.g. using the table HEATNEW_eng.xls which can be obtained from the author. The procedure works this way: after having typed in all parameters at the head of Table 1, the table is reset by executing the macro "reset". Then the macro "*Kopschib*" is executed (see VBA listing given in Scheme A1). The crucial step of the calculation procedure consists in a copying act which initiates a column of formula to recalculate all values along the column. In worksheet HEATNEW_eng.xls, the column H11:H213 contains the "old" T values. Prior to start, in every line is written 25 °C (as an example). Right from this table is column I, where every line (each representing a "box", or cylindric shell) contains a

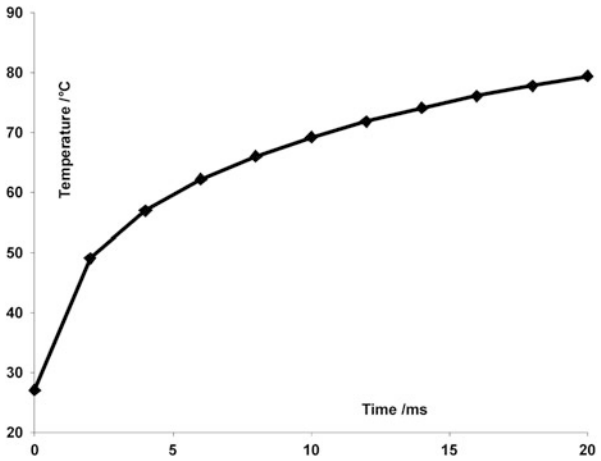

Fig. A3 Temperature variation of the electrode surface (i.e. for $r = r_0$) vs. time after heating start. Conditions as in Fig. A2

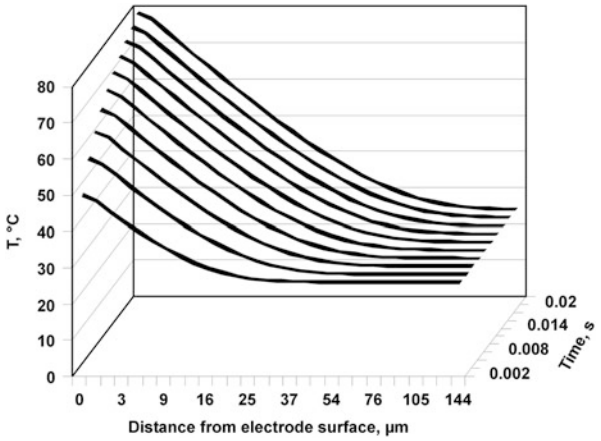

Fig. A4 Temperature profiles at a heated Pt wire for different times after start of heating. Conditions as in Fig. A2

formula which calculates a "new" T value by evaluating the difference between heat amounts *streaming in* and *streaming out* of the box, respectively. This way, in the worksheet we always find two columns, one with T values prior to the time step Δt (column H11:H213), and one with T values after the time step Δt has elapsed (column I11:I213). In the example given, the elementary time step Δt amounts to 10 µs. The macro *Kopschib* just copies the results written in column I and pastes them (as values, not as formulas) to the column H. Now, the column I is recalculated automatically, and we find very fast a column I with changed "new" values. In HEATNEW_eng.xls, this copying action is repeated 200 times, until a time of 2 ms is obtained. Then, *Kopschib* copies the column of results to the right, where now a first diagram $T = f(\Delta x)$ can be drawn. All the operations are done 10 times in the example, resulting in a diagram of 10 such curves. With the distance from electrode surface as the x-axis and temperature as the y-axis, a series of curves $T = f(\Delta x)$ like given in Figs. A2 and A4 is formed. It is worthwhile to mention that

```
Sub Kopschib()
For I = 1 To 10
   Application.ScreenUpdating = False
   For N = 1 To 200
      Range("I9:I98").Select
      Selection.Copy
      Range("H9").Select
      Selection.PasteSpecial Paste:=xlValues, Operation:=xlNone, _
      SkipBlanks:=False, Transpose:=False
   Next N
   Application.ScreenUpdating = True
   Range("H8:H98").Select
   Selection.Copy
   Range("I8").Select
   Selection.SpecialCells(xlNotes).Select
   ActiveCell.Offset(0, -1).Range("A1").Select
   ActiveSheet.Paste
   Range("I8").Select
   Selection.SpecialCells(xlNotes).Select
   Selection.Cut
   ActiveCell.Offset(0, 1).Range("A1").Select
   ActiveSheet.Paste
Next I
End Sub
```

Scheme A1 VBA macro *Kopschib* performing the calculation of 10 temperature profiles depicted in Figs. A1–A4. For description see text

the thickness of consecutive shells is not constant. In the example described here, the thickness is growing (from line to line) by 10 %. This way, the calculation was made much faster.

Reference

1. Gründler P (1998) Fresenius J Anal Chem 362:180–183 (Ref ID: 364)

Appendix B: A Home-Built Device for Temperature-Pulse Voltammetry

Commercial instruments are the easiest and the most reliable way but not the cheapest one to get experience in hot-wire electrochemistry. For home constructors among interested scientists who prefer to find a cheaper solution, in the following paragraphs a home-built apparatus will be presented. Capability of this device is on a par with commercial instruments. The inner structure of the arrangement is depicted schematically in Fig. B1. In Fig. B2, the apparatus is shown as it was used in the author's laboratory, i.e. in an experimental state.

The instrument described here should be considered as an example only. Some of the components used here will no longer be available, e.g. the microcontroller unit "SIOS". It can be substituted easily by modern microcontroller boards which are commercially available. An example is the widespread board "Arduino due" which has the additional advantage to be programmable much easier than the interface used in the present description. Consequently, the following description is restricted to more general principles, without details of programming.

What should a general purpose thermoelectrochemical instrument do?

1. The instrument should be capable of performing all the classic electrochemical methods such as *cyclic voltammetry*, *potentiometry*, *chronoamperometry*, *chronopotentiometry*, etc., and additionally modern thermoelectrochemical methods such as *temperature pulse voltammetry*.
2. The instrument should be subject to free programming, i.e. it should be open for technical experiments. It should allow to invent new methods additional to standard methods which are inbuilt "ready for use".

Clearly, the requirements given above can be fulfilled only by means of a digital instrument which is controlled by an ordinary PC. The techniques utilized in common digital electrochemical devices can be adopted. As an example, voltage ramps are simulated by a high-resolution voltage staircase. It is not very difficult to complete the corresponding digital sequences by additional pulsing series, which represent, e.g., the heat pulses applied in *temperature pulse voltammetry (TPV)*.

P. Gründler, *In-situ Thermoelectrochemistry*, Monographs in Electrochemistry,
DOI 10.1007/978-3-662-45818-1

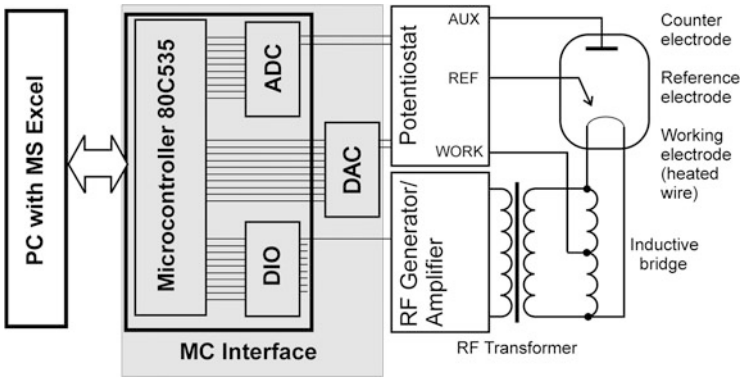

Fig. B1 Schematic representation of a hot-wire electrochemical instrument based on a microcontroller interface board (*center*, *shaded*) combined with PC as controlling computer (*left*), potentiostat, RF generator and transformer units (*right*). The heating current (AC, 100 kHz) is delivered to the electrode wire via an RF transformer. Connection between heated electrode and working electrode input of the potentiostat (WORK) is made by a bridge arrangement consisting of two inductive elements

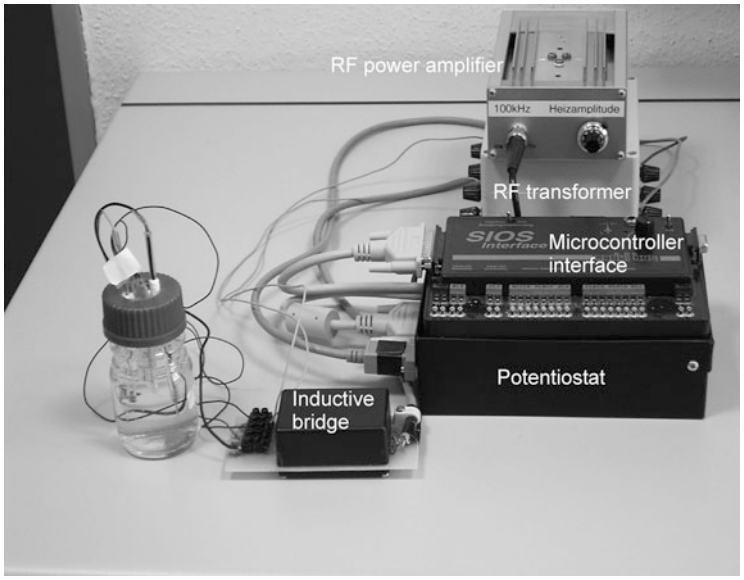

Fig. B2 "Hot-wire" instrument corresponding to the scheme given in Fig. B1 as an experimental set-up. Central part is the little commercial microcontroller interface SIOS shown in Fig. B3

The device presented here has some special characteristics. The idea was to avoid expansive parts and expansive software systems. Only easily available components were used. This requirement was one of the reasons to divide the software control into two levels. The *low-level program* was just a very short

Fig. B3 A commercial interface based on the microcontroller 80C535 (8051 family), equipped with ADC, DAC and UART

machine program which had to do nothing than to perform some command lines delivered by the *high-level program*. The latter consisted of a specialized Microsoft EXCEL® spreadsheet with a collection of macros written in Visual Basic for Applications (VGA). The software basis VGA is available without further cost to many persons utilizing routinely Microsoft Office. It can be used without special programming skills. The operator sees more or less an "animated Excel table", where the front panel of common instruments is simulated graphically (Fig. B7).

Modern operating systems like Microsoft Windows are not useful for directly controlling any instruments, since they perform many operations in background and precise time control of signal output would not be possible. Special instrumentation software systems like the widespread LabView® are capable of controlling instruments, but such systems are very expansive. Instead, the low-level–high-level principle used here allows a much cheaper solution.

The Analog Part

Up to now, any electrochemical instruments make use of an analog *potentiostat*. Its main function is to control and keep constant the voltage between the *working electrode* and the tip of a *reference electrode*. The arrangement used here is depicted in Fig. B4. Main part is a so-called non-inverting potentiostat circuit consisting of three operational amplifiers in the centre of the diagram (two AD708, one OP90). The counter electrode of the cell is connected at the AUX input and reference and working electrodes at REF and WORK, respectively. The lower AD708 acts as current follower and keeps the working electrode at virtual ground. Also, it generates at its output a voltage proportional to the flowing electrolysis current. The voltage between working and reference electrodes must be capable to attend changing polarity. The digital-to-analog converter (DAC) of the microcontroller interface, however, is of single polarity only. Thereby, the

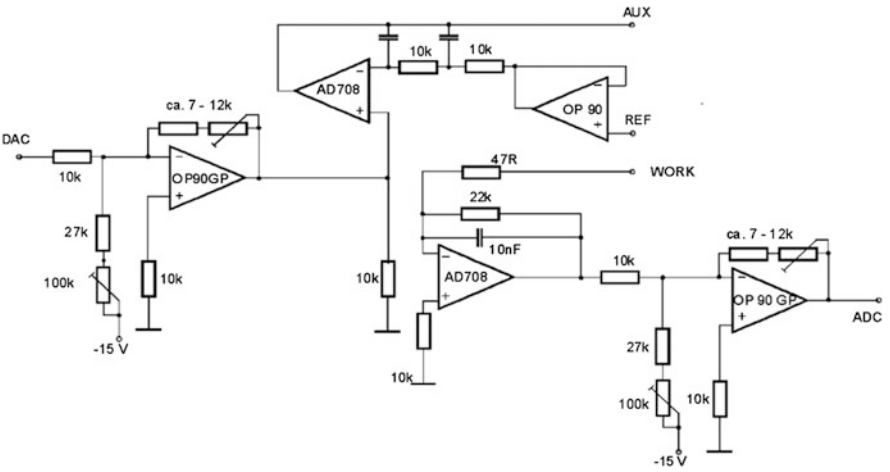

Fig. B4 Potentiostat circuit of non-inverting type with two "level shifters" connected to DAC, or ADC, respectively. For further explanations, see text

"level shifter" formed of the left amplifier OP90GP turns the voltage delivered (0 to +5 V) into symmetric voltage ±2.5 V. A second "level shifter" at the right of the diagram performs the opposite conversion from symmetric to asymmetric voltage to allow connection with the DAC of the microcontroller interface.

The "Lower-Level" Program

As mentioned, the machine code program to be executed by the microcontroller is simple. It has to execute a series of commands which are written in the form of a series of 4-byte binary numbers. The machine code is invariable, but the series of commands is specific for the actual electrochemical technique to be performed. At the start of a measurement, the controlling PC sends the command lines via serial interface to the microcontroller. Next, the PC sends the command to start execution. In the course of measurement, the microcontroller continuously is sending results via its serial interface to the PC. The results are stored intermediately in an UART register, so nothing is lost on the way to the input of the PC. The PC is busy with interrogating continuously the serial interface and plotting the results on the "animated spreadsheet" (see "high-level program") until its controlling macro is finished.

The machine code program in 8051 code has been written by means of an assembler [1]. Its structure is demonstrated by means of the structogram (Nassi–Shneiderman diagram) given in Fig. B5. The author asks for mercy since the diagram in the figure is labeled in German. There are alternative forms to illustrate the function of programs, but structograms proved very useful when software had to

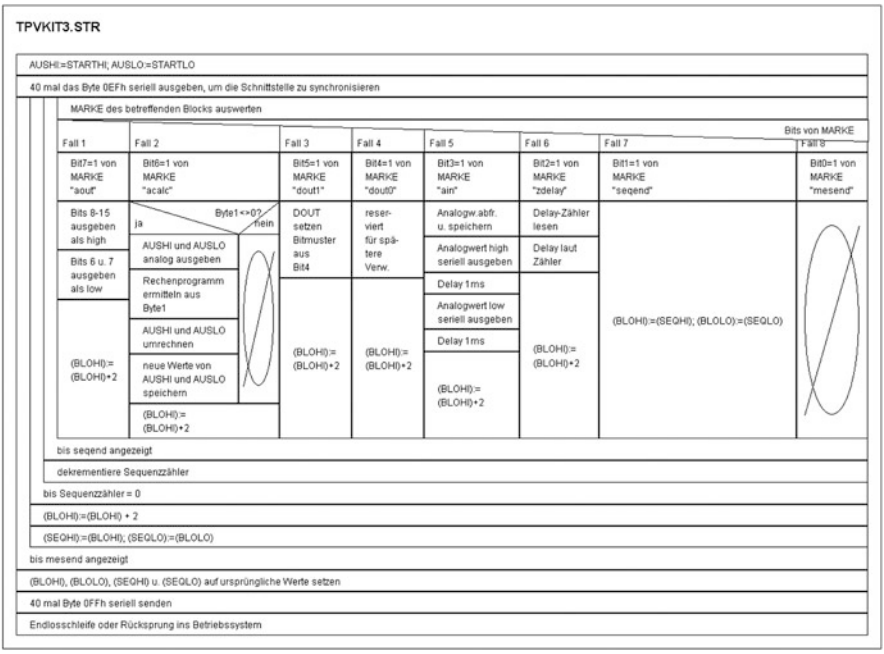

Fig. B5 Structogram (Nassi-Shneyderman diagram) of the 8051 machine code program performed by the microprocessor interface specified in Figs. B1 and B2

be developed. Essentially, the machine code program reads the command lines byte by byte, decides what to do, and performs either simple calculations or output–input operations. To understand the program's function, it is useful to look at the example of command series given in Fig. B6.

Each command line which is sent to the microcontroller corresponds to a specific operation. The lines are written at a specified area in the corresponding "animated spreadsheet" and can be manipulated easily by the operator sitting in front of the PC monitor prior to start of measurement. In the examples given in Fig. B6, we find, e.g., the command "dout1", which means that the digital output of the microcontroller says that the heating of the electrode has to be switched either "off" or "on". Byte 4 with a value 8 means off and value 9 means on. The current measuring range (i.e. the actual value of the negative feedback resistor in the current follower AD708 in Fig. B4) is defined by the byte 2 of "dout1". Another important command is "acalc". It means that the subprogram acalc is called with parameters specified in the bytes 1–4 of the line. This program calculates which potential value has to be output to the DAC in the next program step. This way, a potential staircase is formed by increasing or decreasing the actual voltage, normally in steps of 5 mV.

Sequences	Byte1	Byte2	Byte3	Byte4	Meaning of command words
dout1	0	32	0	8	send digital information "heating off", measuring range 3
seqend	0	2	0	1	execute this sequence once
acalc	1	64	0	64	calculate next (increased) potential value and send it to DAC
zdelay	0	4	1	99	wait for 99 milliseconds
ain	0	8	0	0	read information from ADC and send it to PC
seqend	0	2	0	120	execute this sequence 120 times
acalc	2	64	0	64	calculate next (decreased) potential value and send it to DAC
zdelay	0	4	1	99	wait for 99 milliseconds
ain	0	8	0	0	read information from ADC and send it to PC
seqend	0	2	0	120	execute this sequence 120 times
aout	0	128	111	0	send value for rest potential to DAC
seqend	0	2	0	1	execute this sequence once
dout1	0	32	0	8	send digital information "heating off", measuring range 3
seqend	0	2	0	1	execute this sequence once
mesend	0	1	0	0	send digital "end of measurement"
Sequence for CV1					

Sequences	Byte1	Byte2	Byte3	Byte4	Meaning of command words
acalc	2	64	0	64	calculate next potential value and send it to DAC
dout1	0	32	0	9	send digital information "heating on", measuring range 3
zdelay	0	4	1	39	wait for 40 milliseconds
ain	0	8	0	0	read information from ADC and send it to PC
dout1	0	32	0	8	send digital information "heating off", measuring range 3
zdelay	0	4	1	159	wait for 160 milliseconds
seqend	0	2	0	1	execute this sequence once
aout	0	128	127	192	send value for rest potential to DAC
seqend	0	2	0	1	execute this sequence once
mesend	0	1	0	0	send digital "end of measurement"
Test sequence for TPV					

Fig. B6 Series of commands written on a specific area of the actual spreadsheet in the form of a staple of 4-byte numbers. The series of numbers is sent by the "higher-level" program (Visual-Basic-macro) to the microcontroller prior to measurement start

The "Higher-Level" Program

It proved very useful to have a "two-level" software. The machine code program described above will be initiated by pressing a "start button" at the virtual control panel formed by the graphic facilities of Excel VBA. Examples of control panels are shown in the following pictures. Figure B7 is the front panel for ordinary cyclic voltammetry, whereas Fig. B8 is designed for the new method temperature pulse voltammetry (TPV). The front panels are the "face" of the "higher-level" program. They are designed to make the interface between an operator and the instrument. In both figures, we see at the right side three virtual potentiometers with sliders that can be shifted by means of mouse movements. They determine the potentials for polarizing the electrode, one for the inactive state (rest potential), and two for the start or end potentials in CV, respectively. Further fields and buttons allow choice of scan rate and current measuring range. There are minor differences between the presented front panels. The second one, dedicated to TPV, accounts for the stronger experimental character of the method. It contains additional buttons, which allow, e.g., to send new variations of the machine code to the microcontroller separately. Obviously, the development of the dedicated thermoelectrochemical methods is not completely finished yet. At the left side of the panels, long columns of numbers are seen. These are the results of actual measurement. As soon as the experiment has

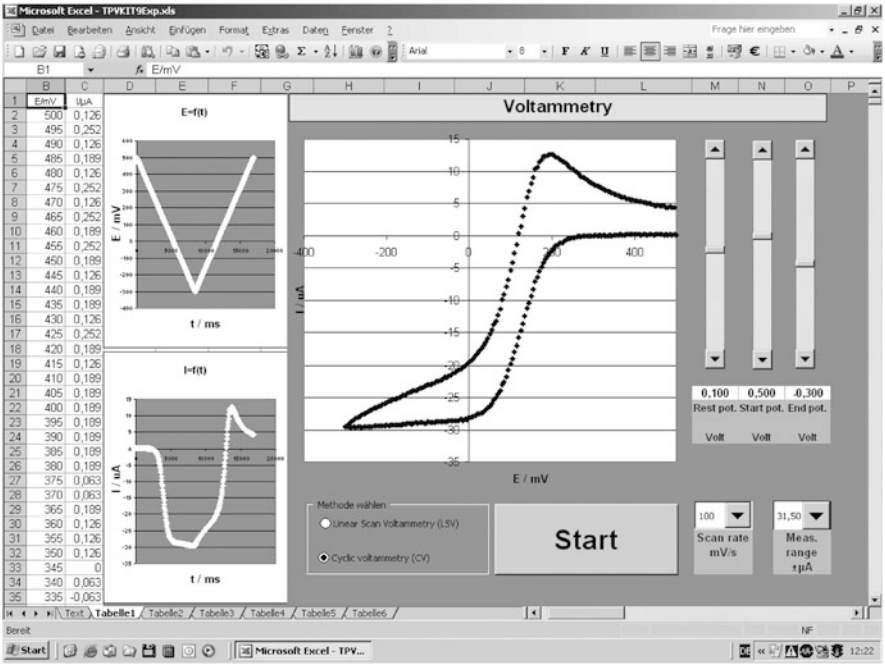

Fig. B7 Example of a virtual control panel made in an Excel sheet. The panel is made for classic voltammetry. Different buttons are designed to start VBA macros which allow to choose polarisation potentials, scan rate and measuring range or to start the experiment. After hitting the "start" button, the left-hand column is filling continuously with measured values, and the diagram is building up point by point

been started, the numbers appear, and the columns are filled continuously. Simultaneously, the results are plotted, and the diagram builds up point by point. Strictly speaking, there are three diagrams on the CV panel. On left, top, we see the voltammetric ramp formed by a high-resolution potential staircase. Below, the measured current samples are plotted versus time. Similar panels have been developed for other electrochemical techniques like *open circuit potentiometry* (OCP), *chronoamperometry* and *chronopotentiometry*. Also, for the electrochemical temperature determination mentioned further above, a specific panel has been made.

The "higher-level" program included in the "animated Excel sheet" presented here has not only the task to start the machine code. Prior to the virtual start, a VBA macro clears the columns of results and of exciting values, and prepares a new system of ordinates which will be filled later by results. All these operations require communication between PC and microcontroller. Just to activate the MC, special commands have to be sent via serial interface. Consequently, it is very important to have the correct DLL, i.e. the library which allows to communicate between "higher" and "lower" software systems. In the case discussed here, the necessary DLL has been provided by a CD which was attached to the book of Berndt and Kainka [1].

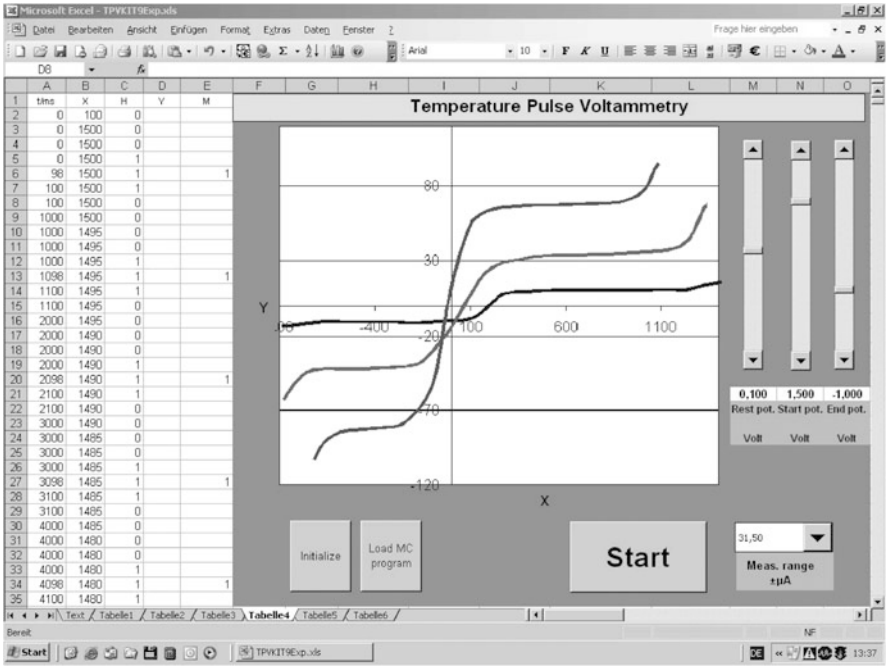

Fig. B8 Virtual control panel for temperature pulse voltammetry. The *curves* are composed of single current samples measured at the end of heating pulses. The three resulting temperature pulse voltammograms shown correspond to three different heating temperature values encountered during the current sampling period. Equimolar solution of 5 mM ferro- and ferricyanide in 0.1 M KCl. Pt wire electrode (diameter 25 µm). Temperature values (for *curves* with current in increasing order): 24 °C, 64 °C and 120 °C. Potential shift with temperature (-1.6 mV K^{-1}) as well as increase of diffusion coefficient with T is visible

The graphic facilities of Excel allowed to draw a descriptive diagram which is useful to understand better the function of the method TPV. In Fig. B9, such a diagram is shown. It is found in the Excel sheet containing the front panel. Scrolling down the sheet it can be seen. It is drawn as soon as the button "initialize" has been pressed. Then, the calculated ordinates are evaluated and used to make the picture which is useful to illustrate the mutual interference of potential staircase, heating pulses and measuring intervals.

The measuring technique utilizing an "animated Excel sheet" was an important step in the development of "hot-wire" electrochemical methods. Later, the system has been substituted by a combination of a home-built heating device with a commercial, freely programmable potentiostat. Till now, it is not determined yet which variant will predominate: either a dedicated instrument or a modified commercial device. Meanwhile, microcontroller boards became widespread and are easily available. Modern boards are much better programmable than the example presented here. The well-known *Arduino due* mentioned further above is an example only. It is equipped with ADC, DAC and UART, and it can be programmed

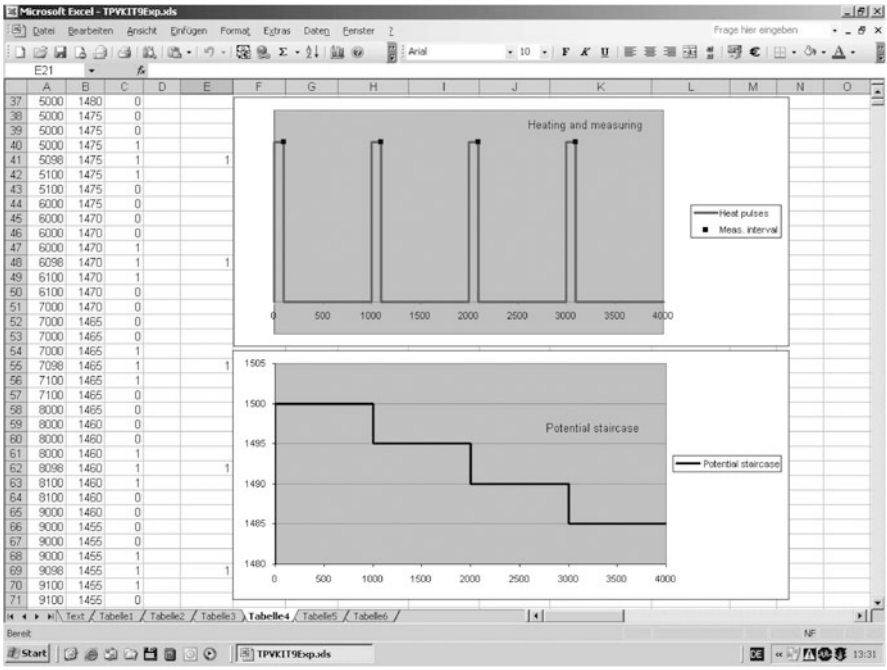

Fig. B9 Diagram as part of the TPV front panel sheet shown in Fig. B8. This diagram is designed to illustrate the temporary correlation of potential staircase, heating pulses and current sampling intervals. Diagrams of this kind are drawn by means of VBA macros evaluating the ordinate system which has been prepared prior to start of the virtual electrochemical experiment

easily since it has its own operating system based on the language C^{++}. Thus, the "lower-level" programming will not really be a problem.

Future hot-wire instruments could be constructed on the basis of a modern microcontroller board. However, till now it seems necessary to build individually two units, namely the potentiostat and the heating unit. Although potentiostat-ICs exist, traditional construction based on classical operational amplifiers can be fitted better to the necessities.

The system presented here has been published in short form [2]. Technical details and program code can be obtained from the author. Problems might arise since the MC interface "SIOS" has some unique features. In the system presented here, e.g., a higher resolution of the digital-to-analog converter has been achieved by combining two 8-bit DACs to form a 10-bit DAC.

References

1. Berndt HJ, Kainka B (2005) Messen, Steuern und Regeln mit Word & Excel. Franzis-Verlag GmbH, D-85586 Poing, Germany
2. Gründler P (2009) Electroanalysis 21:480–486

About the Author

Peter Gründler received his Diploma in Chemistry and his PhD from the University of Leipzig, Germany. He worked as a docent in Leipzig till 1988, when he became full Professor of Analytical Chemistry at the University of Rostock. After his retirement from the university in 2005, he worked as a guest scientist in the group of Professor Lothar Dunsch in Dresden till 2012.

He is author of approximately 100 scientific publications and of a textbook about chemical sensors which has been translated in several languages. During his active teaching period, he has been advisory board member of several scientific journals and also of research organisations.

His research interests were mostly connected with analytical application of electrochemistry, in the past mainly for precision analysis and later for electrochemical sensors of different kinds. In the years after 1990, he picked up an idea which he had since long and started working with heated microelectrodes. The resulting package of methods, named later "hot-wire electrochemistry", finally became the origin of a critical reconsideration of the scientific subject "thermoelectrochemistry" as a whole.

P. Gründler, *In-situ Thermoelectrochemistry*, Monographs in Electrochemistry,
DOI 10.1007/978-3-662-45818-1

About the Editor

Fritz Scholz is Professor at the University of Greifswald, Germany. Following studies of chemistry at Humboldt University, Berlin, he obtained a Dr. rer. nat. and a Dr. sc. nat. (habilitation) from that University. In 1987 and 1989, he worked with Alan Bond in Australia. His main interest is in electrochemistry and electroanalysis. He has published more than 300 scientific papers, and he is editor and co-author of the book "Electroanalytical Methods" (Springer, 2002, 2005, 2010, and Russian Edition: BINOM, 2006), coauthor of the book "Electrochemistry of Immobilized Particles and Droplets" (Springer 2005), co-editor of the "Electrochemical Dictionary" (Springer, 2008; 2nd ed. 2012) and co-editor of volumes 7a and 7b of the "Encyclopedia of Electrochemistry" (Wiley-VCH 2006). In 1997, he has founded the *Journal of Solid State Electrochemistry* (Springer). He serves as Editor-in-Chief since that time. In 2014, he has founded the journal *ChemTexts–The Textbook Journal* (Springer). He is the editor of the series "Monographs in Electrochemistry" (Springer) in which modern topics of electrochemistry are presented. Scholz introduced the technique "Voltammetry of Immobilized Microparticles" for studying the electrochemistry of solid compounds and materials, he introduced three-phase electrodes to determine the Gibbs energies of ion transfer between immiscible liquids, and currently he is studying the interaction of free oxygen radicals with metal surfaces, as well as the interaction of liposomes with the surface of mercury electrodes in order to assess membrane properties. In the last years, his research also comprises the interaction of electrode surfaces with free oxygen radicals.

P. Gründler, *In-situ Thermoelectrochemistry*, Monographs in Electrochemistry,
DOI 10.1007/978-3-662-45818-1

Index

P. Gründler, *In-situ Thermoelectrochemistry*, Monographs in Electrochemistry,
DOI 10.1007/978-3-662-45818-1